CHITOSAN COPOLYMERS FOR INTRANASAL DELIVERY OF INSULIN: SYNTHESIS, CHARACTERIZATION AND BIOLOGICAL PROPERTIES

Dissertation

Zur
Erlangung des Doktorgrades
der Naturwissenschaften
(Dr. rer. nat.)

dem
Fachbereich Pharmazie
der Philipps-Universität Marburg

vorgelegt von

Shirui Mao

aus Tianjin/China

Marburg/Lahn 2004

Vom Fachbereich Pharmazie der Philipps-Universität Marburg als Dissertation am 01.09.2004 angenommen.

Erstgutachter: Prof. Dr. Thomas Kissel
Zweitgutachter: Prof. Dr. Udo Bakowsky

Tag der mündlichen Prüfung: 06.10.2004

Die vorliegende Arbeit entstand auf Anregung und unter der Leitung von

Herrn Prof. Dr. Thomas Kissel

am Institut für Pharmazeutische Technologie und Biopharmazie

der Philipps-Universität Marburg

Acknowledgements

First of all, I would like to express my deep gratitude to my supervisor, Professor Dr. Thomas Kissel, for his invaluable comments, support and encouragement during the whole work with this dissertation. All of those were essential to the completion of this dissertation.

I would like to acknowledge German Academic Exchange Service (DAAD, Der Deutsche Akademische Austauschdienst) for the financial support during my doctoral study. Thanks to Professor Dianzhou Bi for his support and discussion during my study.

I will give a special thanks to Xintao Shuai for the guidance during the polymer synthesis and for the discussions. I appreciate Dr. Dagmar Fischer for the discussion and suggestions during the work and for reading the thesis.

I am very grateful to Professor Dr. Udo Bakowsky for the AFM images. Thanks to Oliver Germerhaus for the CLSM images and for the collaboration regarding the transfection efficiency of the polymers. Thanks to Klaus Keim for the excellent graphs.

The kind help of my other colleagues, namely: Jutta Fuchs, Michael Neu, Matthias Wittmar, Florian Unger, Oster Christine, Claudia Packhäuser, Sascha Maretschek, Nina Seidel, Julia Schnieders, Lea Ann Dailey, Ulrich Westedt, Thomas Merden, Elke Kleemann, Anchallee, Eva Mohr, Nicole Bamberger, are highly appreciated. I am also grateful to all of my colleagues for providing such a good working atmosphere here.

Last, but not least, I would like to thank my family members for their understanding and support during the past few years.

Table of Contents

Chapter 1

Introduction

In this chapter, an overview of intranasal delivery systems for proteins and peptides will be presented. The use of chitosan-based polymers in the pharmaceutical field will be summarized. Additionally, polyelectrolyte-protein complexes as a new drug delivery carrier will be discussed.

1.1 Intranasal delivery of proteins and peptides

Since oral absorption of proteins and peptides is severely hampered by the high metabolic activity and low permeability of intestinal epithelial membranes (1), several mucosal surfaces such as the nasal, pulmonary and peroral mucosae are being extensively investigated as alternative routes for the systemic administration of macromolecular drugs (2). The nasal mucosa is receiving particular attention due to the successful introduction of several nasal peptide drug formulations such as buserelin and desmopressin to the market (Table 1) (3,4). All of these peptides are inactive after oral administration and nasal delivery is regarded as an attractive alternative to chronic injection therapy.

Table 1. Nasal delivery of peptides and proteins (4)

Drug substances	Status
Calcitonin salmon (Miacalcin^{TM})	Marketed by Novartis
Desmopressin (DDAVP^{TM})	Marketed by Ferring and partners
Buserelin (Suprefact^{TM})	Marketed by Aventis
Nafarelin (Synarel^{TM})	Marketed by Searle
PTH (parathyroid hormone)	In clinical trials
Leuprolide	In clinical trials (utilize chitosan delivery system)
Insulin	In clinical trials
Interferon	In clinical trials
Influenza	In clinical trials
Diptheria & Tetanus	In clinical trials
Pertussis	Preclinical

The nasal passage, spanning from the nostril to the nasopharynx, has a length of approximately 12-14 cm (5). The total volume is 15 ml and total surface area is 150 cm^2. The nasal cavity itself is covered by 2 to 4 mm thick mucosa composed primarily of ciliated pseudostratified columnar epithelium covered by a layer of secreted mucus, which has a pH in the range of 5.5 to 6.5 in adults, and from 5.0 to 6.5 in children (6,7). Compared to other non-parenteral routes, such as buccal, peroral, rectal, transdermal and vaginal, intranasal administration has following advantages (8,9):

- ✧ Rapid absorption comparable to intramuscular injections due to highly vascularized mucosal surface.
- ✧ Comparatively high bioavailability.
- ✧ Bypass of first-pass hepatic metabolism.
- ✧ Patient compliance, particularly suitable for self-medication.
- ✧ Bypass of the blood brain barrier (BBB) and targeting of the central nervous system (CNS), reducing systemic exposure and thus systemic side effects.

Due to these pronounced advantages, both macromolecules and small molecules are extensively studied for nasal delivery, as listed in Table 2 (9). Recently, Illum reviewed the possibilities of nasal drug delivery and discussed the problems and solutions (4).

1.2 Insulin administration: current status

Insulin is a protein composed of 2 polypeptide chains, A-chain (21 amino acids) and B-chain (30 amino acids), which are covalently bound to one another by disulfide bonds between cysteine residues. Its molecular weight is about 6000. The primary structure of human insulin is shown in Figure 1. The charge of the insulin molecule depends upon pH. Below its isoelectronic point (pI, 5.3-5.35), insulin has a net positive charge and is soluble at pH < 4.5. Above the pI insulin has a net negative charge and is soluble at pH > 6.3. Insulin forms

high molecular weight aggregates, i.e., hexamers and octamers at pH values close to its isoelectric point.

Table 2. Small molecules and macromolecules currently being studied for nasal delivery (9)

	Small molecules	*Macro molecules*
Adreno corticosteroids		
Antibiotics	Gentamicin, Cephalosporin, Penicillins, Tyrothricin	Amino acids
Antimigraine drugs	Dihydroergotamine, Ergotamine tartrate	**Peptides**
Antiviral drug	Enviroxime	Calcitonin, Secretin,Thyrotropin-releasing
Cardiovascular drugs	Isosorbide dinitrate, Propranolol, Verapamil, Hydralazine, Nitroglycerin, Clofilium tosylate	hormone (TRH), Cerulein, Enkephalin analogs- Leucine enkephalin, Mekephamid
Central nervous system drugs		Pentagastrin, SS-6, Substance P, Kyotorphin,
a. Stimulants	Cocaine, Lidocaine	Cholecystokinin
b. Depressants	Diazepam, Lorazepam	
Autonomic nervous system drugs		
a. Sympathomimetics	Dopamine, Dobutamine, Ephedrine, Epinephrine, Phenyle phrine, Tramazoline, Xylometazoline	**Polypeptides and proteins**
b. Parasympathomimetics	Methacholine, Nicotine	a. Albumins
c. Parasympatholytics	Atropine, Prostaglandins, Ipratropium, Scopolamine	b. Anterior pituitary hormones - Adreno-corticotropic hormone, Gonadotropin-releasing hormone, Growth hormone
Diagnostic drugs	Dye T-1824, Phenolsulfonphthalein, Potassium ferrocyanide, Vital dyes	c. Biological products - Interferon, Vaccines
Histamine and antihistamines		d. Horseradish peroxidase
a. Histamine		e. Pancreatic hormones - Insulin, Glucagon
b. Antihistamines-	Meclizine	f. Posterior pituitary hormones - Oxytocin, Vasopressin
c. Mast cell stabilizers -	Disodium cromoglycate	
Narcotics and antagonists	Buprenorphine, Naloxone	
Sex Hormones	Estradiol, Progesterone, Norethindrone, Testosterone	
Inorganic compounds	Colloidal carbon, Colloidal gold, Inorganic salts, Lead carbonate P and Thorium B	
Vitamins	Folic acid, Cyanocobalamin	

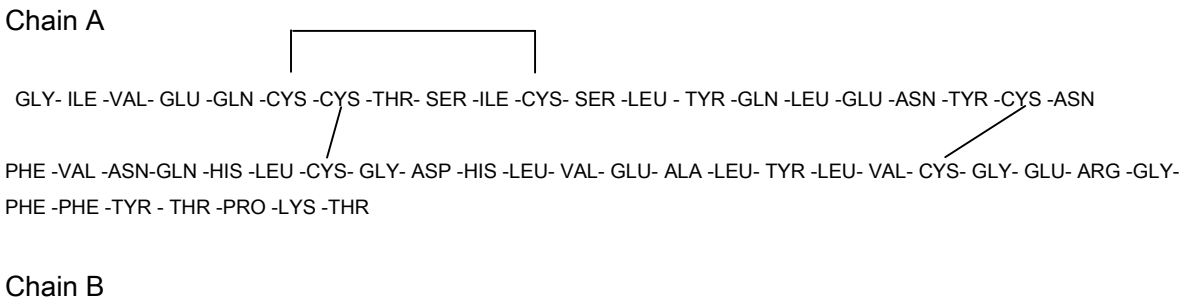

Figure 1. The primary structure of human insulin.

Administrating insulin orally results in limited biological activity due to gastrointestinal proteolytic degradation of the peptide. Therefore, insulin is

generally administrated by subcutaneous injection. Whilst this route is satisfactory in terms of efficacy, severe reactions may occur after subcutaneous injections and many patients are reluctant to accept a regimen of daily injections (10). Other drawbacks include the possibility of inducing hyperinsulinemia, variations in the absorption of the peptide (up to 60%), and difficulty in simulating the fast release of endogenous insulin at mealtimes (11). Due to these problems, other delivery routes have been investigated such as oral, buccal, rectal, transdermal, intranasal and pulmonary (2). Among them, intranasal and pulmonary routes are the most promising.

Interest in the nasal route has increased due to demonstrations that biologically active peptides show significant absorption across the nasal mucosa (Table 1). In fact, the nasal route has been recognized as an attractive alternative for the injection of insulin since 1922 (12). Additionally, intranasal administration of insulin potentially mimics the pulsatile endogenous secretion pattern of insulin (13). However, the efficacy of the nasal route for the absorption of insulin is low (14). Therefore, numerous attempts have been made to further improve the bioavailability of the intranasal administrated insulin. These include (15,16,17):

- ✧ Protecting the peptide from enzymatic degradation by using antiproteolytic agents.
- ✧ The use of a variety of different penetration enhancers.
- ✧ Chemical modification of the peptide to improve stability.
- ✧ Bioadhesive delivery systems to encourage prolonged contact between the drug and mucus membrane.
- ✧ Carrier systems such as microspheres and nanoparticles.

Amongst these, penetration enhancers appeared to have the most prominent effect. However, when they were used at appropriate concentrations for absorption, mucosal damage occured (18,19). Recently, chitosan was demonstrated to be an effective penetration enhancer without causing mucosal

damage. Additionally, it is mucoadhesive and nanoparticles can be obtained with this polymer. Therefore, it is anticipated that chitosan-based derivatives may considerably improve insulin absorption. The properties of chitosan and its potential application are described in the following section.

1.3 Chitosan: its use in the pharmaceutical field

Chitosan (poly[β -(1-4)-2-amino-2-deoxy-D-glucopyranose]) is a biodegradable cationic polysaccharide produced by partial deacetylation of chitin derived from naturally occurring crustacean shells. The molecular formula is $C_6H_{11}O_4N$ and its structure is shown in Figure 2. The polymer is comprised of copolymers of glucosamine and N-acetyl glucosamine. The term chitosan embraces a series of polymers that vary in molecular weight (from approximately 10,000 to 1 million Dalton) and degree of deacetylation (in the range of 50-95%). Since chitosan displays mucoadhesive properties, strong permeation enhancing capabilities for hydrophilic compounds and a safe toxicity profile (20), it has received considerable attention as a novel excipient in drug delivery system and has been included in the European Pharmacopoeia since 2002. Its applications are summarized in Table 3.

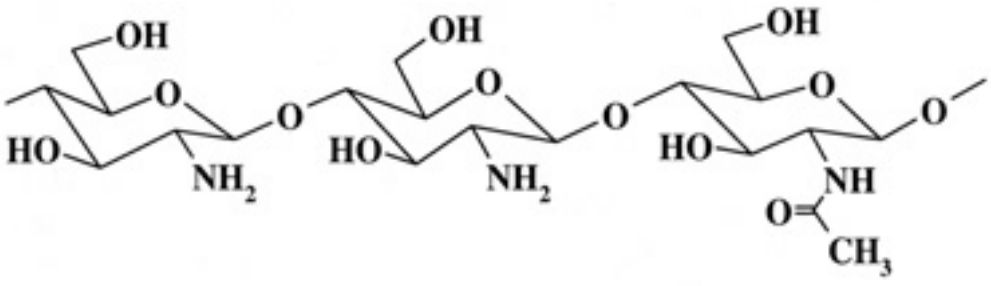

Figure 2. Structure of chitosan.

Despite its biocompatibility, the use of chitosan in biomedical fields are limited by its poor solubility in physiological media. Chitosan has an apparent

Table 3. Applications of chitosan in the pharmaceutical field

Conventional formulations	Novel applications
Direct compression tablets	Bioadhesion
Controlled release matrix tablets	Transmucosal drug transport
Wet graduation	Vaccine delivery
Gels	Non-viral DNA delivery
Films	
Emulsions	
Wetting agent	
Coating agent	
Microspheres and microcapsules	
Targeting	

pKa value between 5.5 and 6.5 and upon dissolution in acid media the amino groups of the polymer are protonated rendering the molecule positively charged. At neutral and alkaline pH, most chitosan molecules lose their charge and precipitate from solution. To improve the poor water-solubility of chitosan at physiological pH, several derivatives have been studied, For example, the modification of chitosan by quaternization of the amino groups (21, 22), N-carboxymethylation (23) and PEGylation (24, 25) have been reported. Additionally, other derivatizations of the amine functionalities of chitosan were performed to obtain polymers with a range of properties, as listed in Table 4. Moreover, chitosan was used to modify the surface of poly (D, L-lactic acid) (PDLLA) in order to enhance its cell affinity (37).

Absorption enhancer. Numerous studies have demonstrated that chitosan and their derivatives are effective and safe absorption enhancers to improve mucosa delivery of hydrophilic macromolecules such as peptides and protein drugs (41). The degree of deacetylation and molecular weight of

Table 4. Studies using chitosan based delivery systems for hydrophilic macromolecular drugs*

Polymers	Delivery system/purpose	Reference
Chitosan	Nanoparticle	[26,27]
	Microparticles	[28,29]
	DNA complex	[30]
N-Trimethyl chitosan	Absorption enhancer	[31,32]
Mono-N-carboxymethylated chitosan	Absorption enhancer	[33]
N-Alkylated chitosan	DNA complex	[34]
N-Acetylated chitosan	DNA complex	[35]
Galactosylated chitosan-graft-PEG	DNA complex	[36]
Deoxycholic acid-modified chitosan	DNA complex	[37]
Chitosan-EDTA conjugates	Peroral peptide delivery	[38,39]
Chitosan-coated liposomes	Insulin enteral absorption	[40]
PEG-g-chitosan	Increase solubility	[24,25]

* This is not a comprehensive list, but serves as an illustration of the broad scope of chitosan delivery systems.

chitosan determine their absorption enhancing and cytotoxic properties (42,43). Chitosans with a high degree of deacetylation (DD) (85 to 99%) promote drug absorption at both low and high molecular weights but also show clear dose-dependent toxicity. On the other hand, chitosans with DDs of 51 to 65% only increase the absorption of drugs with high molecular weights and display low toxicity. Chitosan-based formulations can greatly improve the absorption of drugs from the nasal cavity, and products for the treatment of migraine and cancer pain have reached Phase Ⅱ clinical evaluation (44). A Japanese patent reported that a nasal composition containing salmon calcitonin and chitosan (particle size 30-60 μm) was administered to normal human subjects to determine pharmacokinetics, and good bioavailability was obtained. A nasal solution formulation of chitosan greatly enhanced the absorption of insulin

across the nasal mucosa of rat and sheep (45). This effect was concentration dependent, with the optimal efficacy obtained for concentrations > 0.2% and 0.5% in rats and sheep, respectively (45).

Luessen et al. reported a plateau effect when chitosan glutamate was used as an absorption promoter (46). They reported that a maximum transport rate was reached at 0.4% (w/v). This observation was in agreement with results obtained with chitosan glutamate at pH values ranging between 4.9 and 6.0, where a plateau level in P_{app} (apparent permeability coefficient) was reached at polymer concentrations of 0.25 and 0.5% (w/v) (47). Such a plateau effect has also been found for nasal insulin absorption in sheep, where at a pH value of 4.4, chitosan glutamate in concentrations exceeding 0.4% (w/v) did not result in a stronger reduction of glucose levels (45). This is because, at an appropriate concentration of chitosan, the viscosity and the degree of mucoadhesion may have been sufficient to reach and maintain the required deposition characteristics in the nasal cavity (45).

It has also been demonstrated that the use of chitosan to promote the transport of drugs across the nasal membrane can be enhanced by employing chitosan powder formulations rather than solution formulations (48). Gamma scintigraphy demonstrated nasal clearance half times in the order of 25, 40 and 80 minutes for a control solution, a chitosan solution and a chitosan powder, respectively (49). This is due to the fact that a delivery device such as a nasal spray or a nasal insufflator (powder administration device) will normally deposit the formulation in the anterior part of the nasal cavity, a region largely devoid of ciliated cells. The formulation will then be cleared to the back of the throat by the mucociliary clearance mechanism. Therefore, a bioadhesive system that can slow down the process of mucociliary clearance, thereby allowing a prolonged period of contact between the formulation and the nasal tissues is advantageous. Soane et al. described the clearance characteristics of two bioadhesive nasal delivery systems in the form of chitosan microspheres

and chitosan solution from the nasal cavity of conscious sheep (50). The data showed the control was cleared rapidly from the sheep nasal cavity, with a half-time of approximately 15 min. The bioadhesive chitosan delivery systems were cleared at a slower rate, with half times of clearance of 43 min and 115 min, for the solution and microsphere formulations respectively. Consequently, chitosan delivery systems have the ability to increase the residence time of drug formulations in the nasal cavity, thereby providing the potential for improved systemic medication. Vila et al. coated PLGA nanoparticles with the mucoadhesive polymer chitosan and reported improved stability of the particles in the presence of lysozyme and enhanced nasal transport of the encapsulated tetanus toxoid; nanoparticles made solely of chitosan were also stable upon incubation with lysozyme and were particularly efficient in improving the nasal absorption of insulin (51).

Mechanism. The absorption promoting effect of chitosan has been found to be a combination of mucoadhesion and a transient opening of the tight junctions in the mucosal cell membrane, as shown in Figure 3. The mucoadhesive properties of chitosan are a consequence of an interaction between the positively charged chitosan and negatively charged sialic acid groups on the mucin. Such interactions encourage prolonged contact time between the drug substance and the absorptive surface, thereby permitting the absorption of drug molecules via the paracellular (Figure 3a, 1), transcellular pathway (Figure 3a, 3), or through endo- and transcytosis (Figure 3a, 2). Generally, only small, hydrophilic molecules with a molecular weight below 500 g/mol are able to penetrate via a paracellular pathway through the tight junction. Most compounds are absorbed via a transcellular pathway through the cell membrane of the epithelial cells due to the high surface area. Endo- and transcytosis is characterized by the engulfment of the extracellular material, followed by the pinching of the membrane vesicles from the plasma membrane (Figure 3a, 2). Adsorptive endocytosis of chitosan nanoparticles has previously

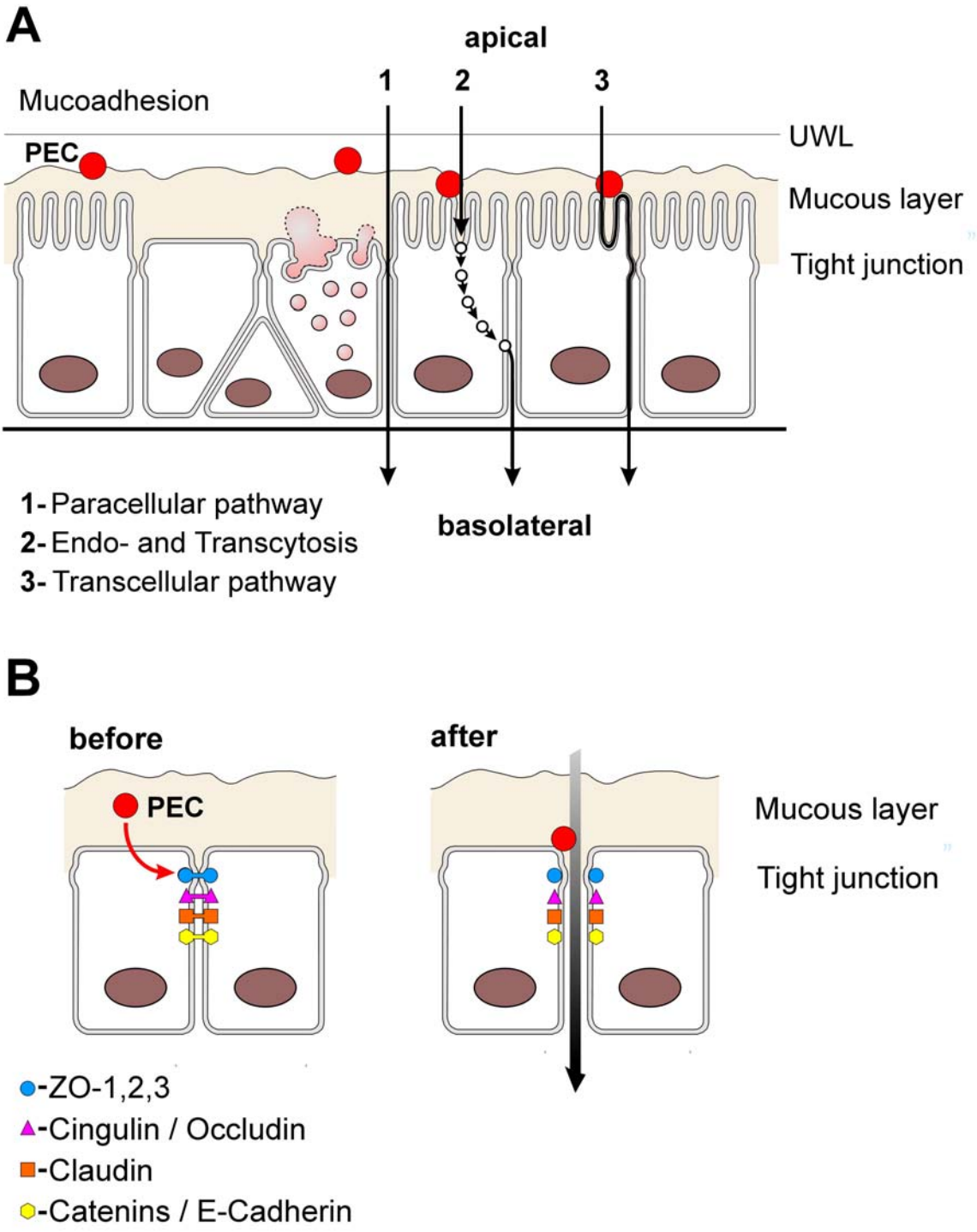

Figure 3. Schematic overview of the mechanism of chitosan as a permeation enhancer.

A. Mucoadhesion.

B. Opening the tight junction.

been demonstrated (52).

Tight junctions are located between apical and basolateral domains in epithelial cells, and appear as a continuous apical belt around the cell periphery. They regulate the passage of molecules across these natural barriers. Large molecular weight drugs need to pass through these tissue barriers in order to reach their targeted sites. As part of the body's normal activity, tight junctions selectively open and close in response to various signals both inside and outside the cells. This permits the passage of large molecules across the tight junction barrier. On a molecular level, tight junctions consist of proteins, for example, claudins, occludins and junctional adhesion molecules. Such molecules are anchored in the membranes of two adjacent cells and interact with one other to hold the cells together, preventing other molecules from passing between them. In intact tight junctions, these proteins are strongly associated with the plasma membrane (53). However under conditions precluding tight junction formation, these proteins appear to be relocated from the membrane into other cellular compartments (Figure 3B). It has been shown in both cell culture (Caco-2) and animal models that chitosan is able to induce a transient opening of tight junctions, thus increasing membrane permeability particularly to polar drugs, including peptides and proteins (53). The opening of the tight junctions has been demonstrated by a loss of ZO-1 proteins and occludins from the cytosolic and membrane fractions into the cytoskeletal fraction (42, 54).

Toxicity. Although a number of investigations have been performed to elucidate the cytotoxicity of chitosan, the results were controversial. A series of toxicity studies indicated that chitosan was toxic, with the extent of toxicity being dependent upon the molecular weight, degree of deacetylation and salt form (55,56). By contrast, other investigations have suggested that the toxicity of chitosan is negligible, with experiments investigating the effects on cilia beat frequency (CBF) in guinea pigs after 28 days application, effect on mucociliary clearance rates on human nasal tissue and effect on nasal membranes in rats

(57-59). A ten-day acute toxicity study in rabbits showed neither macroscopic nor microscopic effects on organs or tissues, and oral toxicity of chitosan was reported to be 16 g/kg body weight (LD_{50}) (49). The mucociliary clearance rate in man, measured by a saccharine clearance test, was found to be unaffected after daily nasal application of chitosan (49).

1.4 Complexation between polyelectrolytes and proteins.

In recent years, nanoparticles have increasingly been investigated as potential carriers for hydrophilic macromolecules such as proteins and vaccines. They are known to improve protein stability, and permit administration through non-parenteral routes (60-62). However, traditional methods for nanoparticle preparation require organic solvents or sonication, which may inactivate the proteins or cause the burst release effect. However, complexes formed by self-assembly between proteins and natural or synthetic polyelectrolytes do not require such harsh preparation methods, and have been the focus of many recent studies (63). In fact, protein-polyelectrolyte complexes (PEC) are not new, and have been used extensively in biology over many years for protein purification, immobilization and stabilization of enzymes (64). However, only recently has it been used as a drug carrier, especially for DNA condensation and complexation. Lee et al. reported that self-aggregated nanoparticles, prepared from hydrophobically modified chitosan, could find a potential application as a gene delivery vehicle due to the controlled complex formation with plasmid DNA (65). Chitosan and its derivatives are cationic polymers, and insulin was negatively charged at pH < pI, therefore complexes were formed at appropriate conditions and a new insulin carrier was obtained.

Until now, numerous techniques have been applied to the characterization of PEC, including turbidimetry, viscometry, analytical ultracentrifugation, size-exclusion chromatography, fluorescence spectroscopy, electrophoretic light scattering (ELS), static light scattering, electron-spin resonance, circular

dichroism, and dynamic light scattering (66). Parameters affecting the complex formation process have been described in detail in the literature (66).

Aim and Scope

In this dissertation, the potential of PEGylated trimethyl chitosan block copolymers as intranasal delivery carriers of insulin will be investigated systematically.

The successful application of chitosan as an absorption enhancer for macromolecules and as gene delivery vehicle is dependent on the molecular weight, therefore, in **Chapter 2**, factors affecting the oxidative depolymerization of chitosan were investigated, and physicochemical properties of the resulting polymer fractions including their cytotoxicity were characterized. However, as an absorption enhancer, chitosan is only effective at pH < 6.5. In order to improve its solubility at physiological pH, trimethyl chitosan (TMC) of varying molecular weights were synthesized using the chitosan fragments from chapter 2 as starting materials in order to investigate the effect of TMC molecular weight on its absorption ability. Unfortunately, using the MTT assay, it was shown that TMC was toxic and its cytotoxicity was MW and dose dependent. To improve the biocompatibility of TMC, PEGylated trimethyl chitosan block copolymers were synthesized and characterized by nuclear magnetic resonance and infrared spectroscopy (**Chapter 3**). Using the MTT assay and LDH assay, the cytotoxicity of PEGylated TMC copolymers was studied and compared with that of TMC in **Chapter 4.** PEGylation considerably decreased the cytotoxicity of TMC, and several copolymers were selected for further studies. It is well known that nanoparticles are a promising delivery system for peptides and proteins. To overcome the disadvantage of the traditional method for nanoparticle preparation, self-assembled insulin nanocomplexes were prepared with chitosan derivatives, the mechanism for complex formation was elucidated, and the process parameters were optimized

(**Chapter 5**). To investigate the potential of the polymer-insulin nanocomplexes as intranasal delivery carriers, uptake and transport studies of the complexes in Caco-2 monolayers were performed and the effect of polymer structure, polymer molecular weight, and charge density was evaluated. Moreover, the complex-uptake mechanism was investigated in detail and further demonstrated by confocal laser scanning microscopy (**Chapter 6**). A summary and prospects for further investigations is presented in the last chapter.

References

[1] A.N. Fischer, The effect of molecular size on the nasal absorption of water soluble compounds in the albino rat, J. Pharm. Pharmacol. 39 (1987) 357-362.

[2] D.R. Owens, B. Zinman, G. Bolli, Alterative routes of insulin delivery, Diabetic Medicine 20 (2003) 886-898.

[3] C.R. Behl, H.K. Pimplaskar, A.P. Sileno, W.J. Xia, J.C. Gries and V.D. Romeo, Optimization of systemic nasal drug delivery with pharmaceutical excipients, Adv. Drug Del. Rev. 29 (1998) 117-133.

[4] L. Illum, Nasal drug delivery-possibilities, problems and solutions, J. Controlled Rel. 87 (2003) 187-198.

[5] Y.V. Prasad, Intranasal drug delivery systems: an overview, Indian Journal of Pharmaceutical Science 58 (1996) 1-8.

[6] S.S. Hehar, J.D.T. Mason, A.B. Stephen, N. Washington, N.S. Jones, S.J. Jackson, Twenty four hour ambulatory nasal pH monitoring, Clin. Otolaryngol. 24 (1999) 24-25.

[7] A.E. Pontiroli, Intranasal drug delivery: potential advantages and limitations from a clinical pharmacokinetic perspective, Clinical Pharmacokinetics 17 (1989) 299-307.

[8] P. Edman, E. Björk and L. Rydén, Microspheres as a nasal delivery system for peptide drugs, J. Controlled Rel. 21 (1992) 165-172.

[9] S. Talegaonkar, P.R. Mishra, Intranasal delivery: an approach to bypass the blood brain barrier, Indian J. Pharmacol. 36 (2004) 140-147.

[10] A.E. Pontiroli, Insulin given intranasally induces hypoglycemia in normal and diabetic subjects, Br. Med. J. 284 (1982) 303-306.

[11] N.F. Farraj, Nasal administration of insulin using bioadhesive microspheres as a

delivery system, J. Controlled Rel. 13 (1990) 253-261.

[12] R.T. Woodyatt, The clinical use of insulin, J. Metab. Res. 2 (1922) 793.

[13] L. Illum and S. Davis, Intranasal insulin, Clinical pharmacokinetics 23 (1992) 30-41.

[14] A.E. Pontiroli, Intranasal administration of calcitonin and of other peptides: Studies with different promoters, J. Controlled Rel. 13 (1990) 247-251.

[15] F.W.H.M. Merkus, N.G. M Schipper, J.C. Verhoef, The influence of absorption enhancers on intranasal insulin absorption in normal and diabetic subjects, J. Controlled Rel. 41 (1996) 69-75.

[16] V.H.L. Lee, Protease inhibitors and penetration enhancers as approaches to modify peptide absorption, J. Controlled Rel. 13 (1990) 213-223.

[17] L. Rydén and P. Edman, Effect of polymers and microspheres on the nasal absorption of insulin in rats, Int. J. Pharm. 83 (1992) 1-10.

[18] L. Jian and A. Li Wan Po, Effects of insulin and nasal absorption enhancers on ciliary activity, Int. J. Pharm. 95 (1993) 101-104.

[19] N.G. M. Schipper, J. Verhoef, S.G. Romeijn and F.W.H.M. Merkus, Absorption enhancers in nasal insulin delivery and their influence on nasal ciliary functioning, J. Controlled Rel. 21 (1992) 173-186.

[20] A.K. Singla, M. Chawla, Chitosan: some pharmaceutical and biological aspects-an update, J. Pharm. Pharmacol. 53 (2001) 1047-1067.

[21] A.B. Sieval, M. Thanou, A.F. Kotze, J.C. Verhoef, J. Brussee, H.E. Junginger, Preparation and NMR characterization of highly substituted N-trimethyl chitosan chloride, Carbohydrate Polymers 36 (1998) 157-165.

[22] P. Le Dung, M. Milas, M. Rinando, J. Desbrieres, Water soluble derivatives obtained by controlled chemical modification of chitosans, Carbohydrate Polymers 24 (1994) 209-214.

[23] R.A.A. Muzzarelli, F. Tanfani, and M. Emanuelli, N- (carboxymethylidene) chitosans and N-(carboxymethyl) chitosans: novel chelating polyampholytes obtained from chitosan glyoxylate, Carbohydr. Res. 107 (1982) 199-214.

[24] H. Saito, X. Wu, J. Harris, A. Hoffman, Graft copolymers of poly (ethylene glycol)(PEG) and chitosan, Macromol. Rapid Commun. 18 (1997) 547-550.

[25] Y. Ohya, R. Cai, H. Nishizawa, K. Hara and T. Ouchi, Preparation of PEG-grafted chitosan nanoparticles as peptide drug carriers, S.T.P. Pharma. Science 10 (2000) 77-82.

[26] Y. Xu, Y. Du, Effect of molecular structure of chitosan on protein delivery properties

of chitosan nanoparticles, Int. J. Pharm. 250 (2003) 215-226.

[27] R. Fernández-Urrusuno, P. Calvo, C. Remuñán-López, J. L. Vila-Jato, M.J. Alonso, Enhancement of nasal absorption of insulin using chitosan nanoparticles, Pharm. Res. 16 (1999) 1576-1581.

[28] V.R. Sinha, A.K. Singla, S. Wadhawan, R. Kaushik, R. Kumria, K. Bansal, S. Dhawan, Chitosan microspheres as a potential carrier for drugs. Int. J. Pharm. 274 (2004) 1-33.

[29] S. Özbaş-Turan, J. Akbuğa, C. Aral, Controlled release of interleukin-2 from chitosan microspheres, J. Pharm. Sci. 91 (2002) 1245-1251.

[30] S. Gao, J. Chen, X. Xu, Z. Ding, Y. Yang, Z. Hua, J. Zhang, Galactosylated low molecular weight chitosan as DNA carrier for hepatocyte-targeting, Int. J. Pharm. 255 (2003) 57-68.

[31] A.R. Kotzé, H.L. Lueβen, B.J. de Leeuw, Bert G. de Boer, J.C. Verhoef, H.E. Junginger, N-Trimethyl chitosan chloride as a potential absorption enhancer across mucosal surfaces: In vitro evaluation in intestinal epithelial cells (Caco-2), Pharm. Res. 14 (1997) 1197-1202.

[32] J.H. Hamman, M. Stander, A.F. Kotzé, Effect of the degree of quaternisation of *N*-trimethyl chitosan chloride on absorption enhancement: in vivo evaluation in rat nasal epithelia, Int. J. Pharm. 232 (2002) 235-242.

[33] M. Thanou, M.T. Nihot, M. Jansen, J.C. Verhoef, H.E. Junginger, Mono-*N*-carboxymethyl chitosan (MCC), a polyampholytic chitosan derivative, enhances the intestinal absorption of low molecular weight heparin across intestinal epithelia *in vitro* and *in vivo,* J. Pharm. Sci. 90 (2001) 38-46.

[34] W. Liu, X. Zhang, S. Sun, G. Sun, K. De Yao, D. Liang, G. Guo, and J. Zhang, N-Alkylated chitosan as a potential nonviral vector for gene transfection, Bioconjugate Chem. 14 (2003) 782-789.

[35] E. Kai, T. Ochiya, A method for oral DNA delivery with N-Acetylated chitosan, Pharm. Res. 21 (2004) 838-843.

[36] I.K. Park, T.H. Kim, Y.H. Park, B.A. Shin, E.S. Choi, E.H. Chowdhury, T. Akaike, C.S. Cho, Galactosylated chitosan-*graft*-poly (ethylene glycol) as hepatocyte-targeting DNA carrier, J. Controlled Rel. 76 (2001) 349-362.

[37] K. Cai, K. Yao, Y. Cui, S. Lin, Z. Yang, X. Li, H. Xie, T. Qing, J. Luo, Surface modification of poly (D,L-lactic acid) with chitosan and its effects on the culture of osteoblasts in vitro, J. Biomed. Mater. Res. 60 (2002) 398-404.

[38] A. Bernkop-Schnürch, M.E. Krajicek, Mucoadhesive polymers as platforms for peroral peptide delivery and absorption: synthesis and evaluation of different chitosan–EDTA conjugates, J. Controlled Rel. 50 (1998) 215-223.

[39] A. Bernkop-Schnürch, A. Scerbe-Saiko, Synthesis and in vitro evaluation of chitosan-EDTA-protease-inhibitor conjugates which might be useful in oral delivery of peptides and proteins, Pharm. Res. 15 (1998) 263-269.

[40] H. Takeuchi, H. Yamamoto, T. Niwa, T. Hino, Y. Kawashima, Enteral absorption of insulin in rats from mucoadhesive chitosan-coated liposomes, Pharm. Res. 13 (1996) 896-901.

[41] M. Thanou, J.C. Verhoef, H.E. Junginger, Oral drug absorption enhancement by chitosan and its derivatives, Adv. Drug Deliv. Rev. 52 (2001) 117-26.

[42] N.G. M. Schipper, S. Olsson, J.A. Hoogstraate, A.G. deBoer, K.M. Vårum, Per Artursson, Chitosans as absorption enhancers for poorly absorbable drugs 2: Mechanism of absorption enhancement, Pharm. Res. 14 (1997) 923-929.

[43] N.G. M. Schipper, K.M. Vårum, Per Artursson, Chitosans as absorption enhancers for poorly absorbable drugs. 1: influence of molecular weight and degree of acetylation on drug transport across human intestinal epithelial (Caco-2) cells, Pharm. Res. 13 (1996) 1686-1692.

[44] L. Illum, I. Jabbal-Gill, M. Hinchcliffe, A.N. Fisher and S.S. Davis, Chitosan as a novel nasal delivery system for vaccines, Adv. Drug Delivery Rev. 51 (2001) 81-96.

[45] L. Illum, N.F. Farraj, S. S. Davis, Chitosan as a novel nasal delivery system for peptide drugs, Pharm. Res. 11 (1994) 1186-1189.

[46] H.L. Lueβen, C.O. Rentel, A.F. Kotzé, C.M. Lehr, A.G. de Boer, J.C. Verhoef, H.E. Junginger, Mucoadhesive polymers in peroral peptide drug delivery. IV. Polycarbophil and chitosan are potent enhancers of peptide transport across intestinal mucosae in vitro, J. Controlled Rel. 45 (1997) 15-23.

[47] P. Artursson, T. Lindmark, S. S. Davis, L. Illum, Effect of chitosan on the permeability of monolayers of intestinal epithelial cells (Caco-2), Pharm. Res. 11 (1994) 1358-1361.

[48] L. Illum, Chitosan and its use as a pharmaceutical excipient, Pharm. Res. 15 (1998) 1326-1331.

[49] R.J. Soane, M. Frier, A.C. Perkins, N.S. Jones, S.S. Davis, L. Illum, Evaluation of the clearance characteristics of bioadhesive systems in humans, Int. J. Pharm. 178 (1999) 55-65.

[50] R.J. Soane, M. Hinchcliffe, S.S. Davis, L. Illum, Clearance characteristics of chitosan based formulations in the sheep nasal cavity, Int. J. Pharm. 217 (2001) 183-91.

[51] A.Vila, A. Sánchez, M. Tobío, P. Calvo, M.J. Alonso, Design of biodegradable particles for protein delivery, J. Controlled Rel. 78 (2002) 15-24.

[52] M. Huang, Z. Ma, E. Khor, L. Lim, Uptake of FITC-chitosan nanoparticles by A549 cells, Pharm. Res. 19 (1999) 1488-1494.

[53] V. Dodane, M. Amin Khan, J. R. Merwin, Effect of chitosan on epithelial permeability and structure, Int. J. Pharm. 182 (1999) 21-32.

[54] J. Smith, E. Wood, M. Dornish, Effect of chitosan on epithelial cell tight junctions, Pharm. Res. 21 (2004) 43-49.

[55] D. Sgouras and R. Duncan, Methods for the evaluation of biocompatibility of soluble synthetic polymers which have potential for biomedical use. 1 Use of the tretazolium-based colorimetric assay (MTT) as a preliminary screen for evaluation of in vitro cytotoxicity, J. Mater. Sci. Mater. Med. 1 (1990) 61-68.

[56] B. Carreño-Gómez, R. Duncan, Evaluation of the biological properties of soluble chitosan and chitosan microspheres. Int. J. Pharm. 148 (1997) 231-240.

[57] T. Aspden, L. Illum and Φ. Skaugrud, Chitosan as a nasal delivery system: Evaluation of insulin absorption enhancement and effect on nasal membrane integrity using rat models, Eur. J. Pharm. Sci. 4 (1996) 23-31.

[58] T. Aspden, J.D.T. Mason, N.S. Jones, J. Lowe, Φ. Skaugrud, L. Illum, Chitosan as a nasal delivery system: The effect of chitosan solutions on in vitro and in vivo muco-ciliary transport rates in human turbinates and volunteers, J. Pharm. Sci. 86 (1997) 509-513.

[59] T. Aspden, L. Illum and Φ. Skaugrud, The effect of chronic nasal application of chitosan solution on cilia beat frequency in guinea pigs, Int. J. Pharm. 153 (1997) 137-146.

[60] M. Tobío, R. Gref, A. Sánchez, R. Langer, M. J. Alonso, Stealth PLA-PEG nanoparticles as protein carriers for nasal administration, Pharm. Res. 15 (1998) 270-275.

[61] Z. Cui, R.J. Mumper, Microparticles and nanoparticles as delivery systems for DNA vaccines, Crit. Rev. Ther. Drug Carrier Syst. 20 (2003) 103-137.

[62] S. Sakuma, M. Hayashi, M. Akashi, Design of nanoparticles composed of graft

copolymers for oral peptide delivery, Adv. Drug Deliv. Rev. 47 (2001) 21-37.

[63] H. Mao, K. Roy, Vu L. Troung-Le, K.A. Janes, K.Y. Lin, Y. Wang, J. T. August, K.W. Leong, Chitosan-DNA nanoparticles as gene carriers: synthesis, characterization and transfection efficiency, J. Controlled Rel. 70 (2001) 399-421.

[64] Y. Wen and P. L. Dubin, Potentiometric studies of the interaction of bovine serum albumin and poly (dimethyldiallylammonium chloride), Macromolecules 30 (1997) 7856-7861.

[65] K.Y. Lee, I.C. Kwon, Y.H. Kim, W.H. Jo, S.Y. Jeong, Preparation of chitosan self-aggregates as a gene delivery system, J. Controlled Rel. 51(1998) 213-220.

[66] P. Dubin, J. Bock, R. Davis, D.N. Schulz, C. Thies, Macromolecular complexes in chemistry and biology, Springer-Verlag Berlin Heidelberg (1994) 119-324.

Chapter 2

The depolymerization of chitosan: Effects on physicochemical and biological properties.

International Journal of Pharmaceutics 2004, 281(1-2), 45-54

Abstract

Chitosan has been extensively used as an absorption enhancer for macromolecules and as gene delivery vehicle. Both properties are molecular weight dependent. Here we investigate factors affecting the oxidative depolymerization of chitosan and physicochemical properties of the resulting polymer fractions including their cytotoxicity. The molecular weight of the depolymerized chitosan was influenced by the initial concentration and the source of chitosan. At constant initial concentrations, the molecular weight decreased linearly with the chitosan/$NaNO_2$ ratio and was a function of logarithm of the reaction time. Chitosan with larger molecular weight was more sensitive to depolymerization. No structural change was observed during the depolymerization process by infrared and proton nuclear magnetic resonance spectroscopy. In addition, thermal properties of chitosan fragments were studied by thermal gravimetric analysis and it was found that the decomposition temperature was molecular weight dependent. Furthermore, the solubility of different molecular weight chitosan was assayed as a function of pH and it increased with decreasing molecular weight. The cytotoxicity of chitosan was concentration dependent but almost molecular weight independent according to MTT assay using L929 cell line recommended by USP 26. In summary, low molecular weight fractions of chitosan may potentially useful for the design of drug delivery systems due to the improved solubility properties.

1. Introduction

Chitosan (poly[β -(1-4)-2-amino-2-deoxy-D-glucopyranose]) is a non-toxic and biocompatible cationic polysaccharide produced by partial deacetylation of chitin isolated from naturally occurring crustacean shells. Due to its specific properties, chitosan has found a number of applications in drug delivery including that of as an absorption enhancer of hydrophilic macromolecular drugs (Artursson et al., 1994; Illum et al., 1994; Lueßen et al.,

1996; Singla et al., 2001) and as gene delivery system (Erbacher et al., 1998; Richardson Simon et al., 1999).

The term chitosan embraces a series of polymers, which vary in molecular weight (MW) and degree of deacetylation (DD). Although a number of investigations have been performed to elucidate the relationship between MW and cytotoxicity, the results were controversial. A series of toxicity studies indicated that chitosan was toxic and the toxicity was dependent upon their molecular weight, degree of deacetylation and salt form (Sgouras et al., 1990; Heller et al., 1996; Carrecuno-Gomez et al., 1997). By contrast, other investigations suggested that the toxicity of chitosan was negligible (Aspden et al., 1995, 1996, 1997a, 1997b). Additionally, the transfection efficiency of chitosan with molecular weight >100 kDa was reduced compared to 15 and 52 kDa and chitosans of 10-50 kDa seem to be promising as gene transfer reagents (Sato et al., 2001). Lee et al. (2001) indicated that low molecular weight chitosan (molecular weight of 22 kDa) showed higher transfection efficiency than poly-L-lysine.

However, most commercially available chitosans possess quite large MWs. Due to promising properties of low molecular weight chitosans in the pharmaceutical field, it is essential to establish a reproducible and straightforward method for generating low MW chitosans. Generally, low molecular weight chitosans can be prepared from high molecular weight chitosan by depolymerization using enzymatic degradation (Chang et al., 1998), oxidative degradation (Li et al., 1999), acidic cleavage and ultrasonic degradation (Chen et al., 2000). The rate of molecular weight degradation was irregular during the time course of ultrasound treatment. Liu studied the depolymerization of chitosan using $NaNO_2$, H_2O_2, and HCl. They found that $NaNO_2$ showed the best performance (Liu et al., 1997). These results were recently confirmed, but no detailed experimental information was provided (Janes et al., 2003).

The purpose of this paper, therefore, is to study the factors affecting the depolymerization process of chitosan using sodium nitrite and to clarify the relationship between chitosan MW and cytotoxicity. Using intrinsic viscosity measurements, these factors were investigated systematically and the structure identification of chitosan during depolymerization was performed with IR and ^{1}H NMR methods. In addition, the solubility of different chitosans was characterized as a function of pH value. The cytotoxicity of chitosans was characterized by MTT assay using L929 fibroblast cell line.

2. Materials and methods

2.1 Materials

Three different commercially available chitosans F-LMW (150 kDa), F-MMW (400 kDa), F-HMW (600 kDa), with a nominal degree of deacetylation of 84.5%, 84.7%, and 85.0% respectively, were purchased from Fluka (Neu-Ulm, Germany). Acetic acid (HAc), sodium acetate (NaAc), sodium hydroxide (NaOH) and sodium nitrite ($NaNO_2$) were of analytical grade. Dulbecco's modified Eagle's medium (DMEM) was obtained from Gibco (Eggenstein, Germany). 3-(4, 5-dimethyl-thiazol-2-yl)-2, 5-diphenyl tetrazolium bromide (MTT) was purchased from Sigma (Deisenhofen, Germany), dimethylsulfoxide (DMSO) was from Merck (Darmstadt, Germany).

The chitosans selected for this study had similar degrees of deacetylation, but differed markedly in their molecular weights. The degrees of deacetylation, viscosity average molecular weights, and moisture contents of the commercial chitosans used in this study were determined experimentally and compared with the values reported by the supplier, as listed in Table 1.

2.2 Depolymerization of chitosan

The low molecular weight chitosans were prepared by oxidative degradation with $NaNO_2$ at room temperature. Briefly, 1% (W/W) chitosan was

dissolved in 1% acetic acid solution under magnetic stirring. When chitosan was completely dissolved, the appropriate amount of 0.1 M $NaNO_2$, as indicated below, was added dropwise and the reaction was performed at room temperature for 3 h unless indicated otherwise. The reaction mixture was subsequently neutralized with 1N NaOH to pH 8.0 to precipitate chitosan. The precipitated chitosan was recovered by centrifugation, washed several times with deionized water, and dried by lyophilisation.

Table 1. Characteristics of chitosans used in this study

Chitosan	Degree of deacetylation (%)		Molecular weight (kDa)		Moisture content (%)	
	Labeled[a]	Determined[b]	Labeled[a]	Determined[c]	Labeled[a]	Determined[d]
F-LMW	84.5	83.0	150	225	⩽10%	10.0
F-MMW	84.7	85.1	400	540	⩽10%	10.4
F-HMW	85.0	84.9	600	610	⩽10%	10.3

[a] Values supplied by the supplier.

[b] Determined by ^1H NMR.

[c] Calculated from the intrinsic viscosity using the classical Mark-Houwink equation $[\eta] = K (M_v)^a$, where the constants $K = 1.38*10^{-5}$ and $a = 0.85$.

[d] Calculated from TGA measurement.

2.3 Characterization of chitosan

Fourier Transformed Infrared Spectroscopy (FTIR) was conducted on a FT-IR 510P spectrometer (Nicolet) in the range between 4000 and 400 cm^{-1}, with a resolution of 2 cm^{-1}. All powder samples were compressed into KBr disks for the FTIR measurement.

Thermogravimetric Analysis (TGA) was performed on a thermogravimetric analyser TGA 7 with a thermal analysis controller TAC 7/DX from Perkin-Elmer using an approximately 5 mg polymer sample. The scanning rate was 20℃/min, and the thermograms were recorded within the temperature range 30-550℃. Analysis was performed under a nitrogen gas atmosphere in platinum crucibles.

2.4 Determination of intrinsic viscosity

Intrinsic viscosity of chitosans in 2% HAc/0.2M NaAc were measured using an automated Ubbelohde capillary viscometer (Model Schott AVS-360, Germany) in a constant-temperature water bath at 25±0.01℃ in triplicate. The capillary diameter used was 0.63 mm. Solution concentrations were adjusted based on the viscosity of the samples and the flow through time was kept in the range of 100-150 s. Six different concentrations were tested for each sample. The intrinsic viscosity was determined by the common intercept of both Huggins (η_{sp}/C~C) and Kraemer (η_{inh}~C) plots on the ordinate at C=0. As a representative example, the intrinsic viscosity calculation method of HMW chitosan was shown in Figure 1.

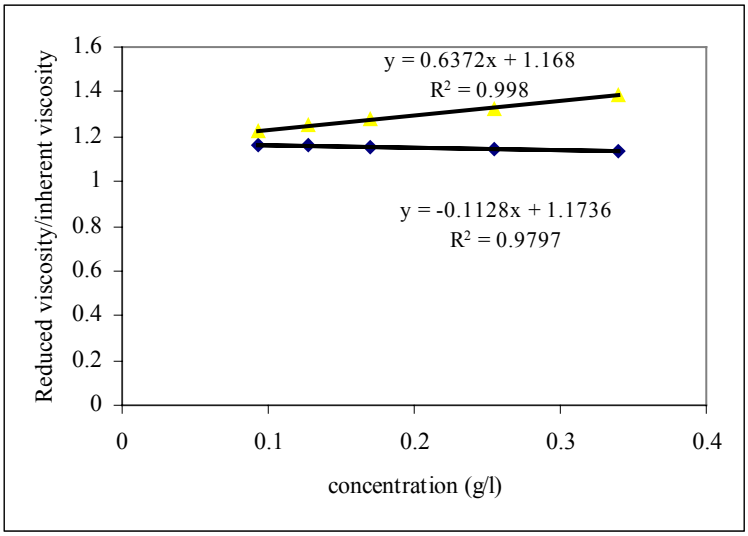

Figure 1. A representative plot for intrinsic viscosity calculation (HMW chitosan). Both η_{sp}/C and η_{inh} are plotted on the same graph and the common intercept of the plots on the ordinate at C=0 is the intrinsic viscosity.

While reduced viscosity of polymers is defined as:

$$\eta_{sp}/C = \frac{t - t_0}{t_0 \cdot C}$$

and inherent viscosity is defined as:

$$\eta_{inh} = \frac{\ln(t/t_0)}{C}$$

where t_0 is the flow time for solvent and t is the flow time for tested solution.

Both η_{sp}/C and η_{inh} are plotted on the same graph in Figure 1. The common intercept of the plots on the ordinate at C=0 gives:

$$[\eta] = (\eta_{sp}/C)_{c=0} = (\eta_{inh})_{c=0} = 1.168 \text{ L/g}$$

The viscosity average molecular weights of chitosans were calculated using the classical Mark-Houwink equation:

$$[\eta] = K (M_v)^a$$

where $[\eta]$ is the intrinsic viscosity of the depolymerized chitosan, K and a are constants for given solute-solvent system and temperature. For chitosan, they are influenced by the degree of deacetylation, pH, and ionic strength of the solvent (Kasaai et al., 2000). As to the chitosans with a DD value of 85%, the constants $K=1.38*10^{-5}$ and a=0.85 were reported (Gamzazade et al., 1985). The viscosity-average molecular weight of the HMW chitosan was therefore calculated as follows:

$$\overline{M_v} = (\frac{1.168}{1.38\times10^{-5}})^{1/0.85} \approx 610 \text{ kDa}$$

2.5 Determination of degree of deacetylation (DD)

In order to assess any structure modification occurred during the depolymerization process, the structure of original chitosans and the depolymerized chitosans were determined by ^{1}H NMR spectroscopy and infrared spectrum. ^{1}H NMR spectra were recorded on a FT-NMR spectrometer (AMX500, 500 MHz, Bruker) at 80℃ using D_2O containing 5% CD_3COOD as the solvent. The NMR experiment was performed at higher temperatures in order to shift the signal of HOD to a higher field, which allowed quantifying the H1 signals of glucosamine residues. The samples were dissolved at a concentration of 10 mg/ml. The DD was determined from the integral of the

CH_3 signal at 1.97 ppm compared with that of H-1 signals of glucosamine and N-acetylglucosamine (Varum et al., 1991).

2.6 Solubility testing

Solubility of various chitosans was measured at different pH values. Briefly, chitosans were dissolved in 0.25% HAC solution (2 mg/ml), the pH of the solution was adjusted by the addition of 1N NaOH solution and the transmittance of the solution at 600 nm as a function of pH value was recorded on a UV/Vis spectrophotometer (UV-160, Shimadzu) (Park et al., 2003). Cloud point pH values, which are defined as the pH when the transmittance was no less than 98%, were determined at the same time (Anderson et al., 2002) in triplicate.

2.7 Cytotoxicity testing (MTT assay)

A mouse connective tissue fibroblast cell line, L929 was selected to evaluate cytotoxicity as a direct contact test, as recommended by USP 26. The experiment was carried out according to the method described previously (Fischer et al., 1999). Briefly, L929 was cultured in DMEM supplemented with 10% fetal calf serum and 2 mM glutamine without antibiotics. The cells were cultivated in an incubator at 37℃, 95% RH and 10% CO_2. Chitosan was first dissolved in 0.5% HAC solution, and then diluted with equal volume of double DMEM medium. The pH of this stock solution was adjusted to 6.5 for all the chitosans tested. Thereafter, DMEM (pH 6.5) was used to prepare serial dilutions of the polymer. L929 cells were seeded into 96-well microtiter plates at a density of 8000 cells/well. 24 hour later, culture medium was replaced with 100 μl serial dilutions of chitosan (0.6-10 mg/ml) and cells were incubated for 24 h. Subsequently, 20 μl MTT (5 mg/ml) was added to each well. After 4 h, unreacted dye was aspirated and the formazon crystals were dissolved in 200 μl/well DMSO. Absorption was measured at 570 nm with a background

correction at 690 nm using a Titertek Plus MS 212 ELISA reader (ICN, Eschwege, Germany). The relative cell viability compared to control cells containing cell culture medium (pH 6.5) without polymer was calculated by $[A]_{test}/[A]_{control}$ (n = 7).

2.8 Calculations and statistics

Results are depicted as mean ± SD from at least three measurements. Significance between the mean values was calculated using ANOVA one-way analysis (Origin 7.0 SRO, Northampton, MA, USA). Probability values $P < 0.05$ were considered significant.

3. Results and discussion

3.1 Depolymerization of chitosan

The concentration of sodium nitrite could be expected to play a significant role in the depolymerization process. In order to facilitate the control of the molecular weight of chitosan fragment, keeping chitosan concentration at 1%, the depolymerization was carried out in a 1% acetic acid solution by varying chitosan / $NaNO_2$ molar ratio, using three types of chitosan as original material. The relationship between chitosan / $NaNO_2$ molar ratio and the MW of chitosan fragment is shown in Figure 2.

Regression analysis of chitosan/$NaNO_2$ molar ratio as a function of the molecular weight of chitosan fragment yielded an almost linear correlation with correlation coefficients of 0.98, 0.99 and 0.97 for chitosan LMW, MMW, HMW, respectively. Furthermore, from the slope of the profiles, one can conclude that HMW chitosan is more sensitive to $NaNO_2$ degradation compared to LMW chitosan. This may be explained by larger molecular dimensions of HMW chitosan in solution, which increases the contact area with $NaNO_2$.

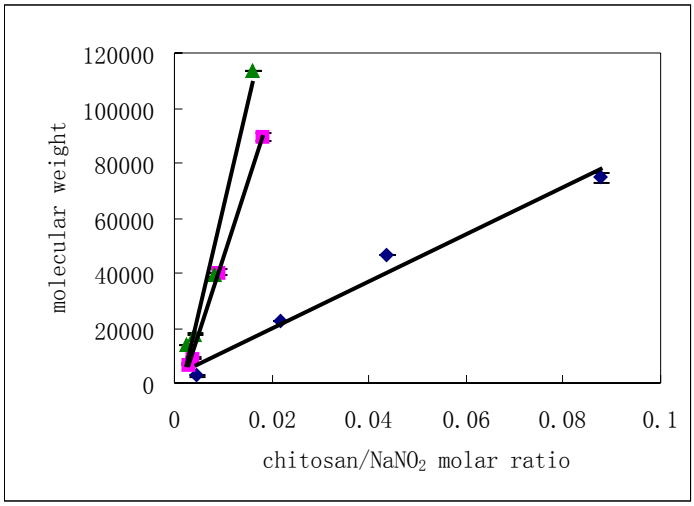

Figure 2. The relationship between chitosan/$NaNO_2$ molar ratio and chitosan molecular weight. (◆) chitosan 150 kDa; (■) chitosan 400 kDa; (▲) chitosan 600 kDa. The measurements were carried out in triplicate and the results are expressed as mean±SD. Different molecular weight chitosans (1%) were degraded by sodium nitrite in 1% acetic acid solution for 3 h at room temperature.

3.2 Effect of reaction time on the molecular weight of chitosan

In order to investigate the effect of reaction time, keeping chitosan /$NaNO_2$ molar ratio at 0.009, chitosan (1%) was degraded by $NaNO_2$ in 1% acetic acid solution and the reaction was stopped at 1, 2, 3 and 6 h respectively, and the corresponding samples were processed in the same way as that described before. LMW and MMW chitosan were used as starting materials. The intrinsic viscosities of the samples were determined and the molecular weights were calculated according to the MHS equation. The results are illustrated in Figure 3.

It was noted that the depolymerization occurred mainly in the first hour, and then slowed down significantly. This behavior was expected since the concentration of sodium nitrite decreased with the reaction time. Moreover, it could be deduced from the slope that MMW chitosan was more sensitive to $NaNO_2$ degradation compared with that of LMW chitosan. In addition, the molecular weight of depolymerized chitosans was plotted versus the logarithm

of the reaction time, and a linear relationship was observed with correlation coefficients 0.9991 and 0.9985 respectively for LMW and MMW chitosan, indicating that the degradation process belongs to first-order kinetics.

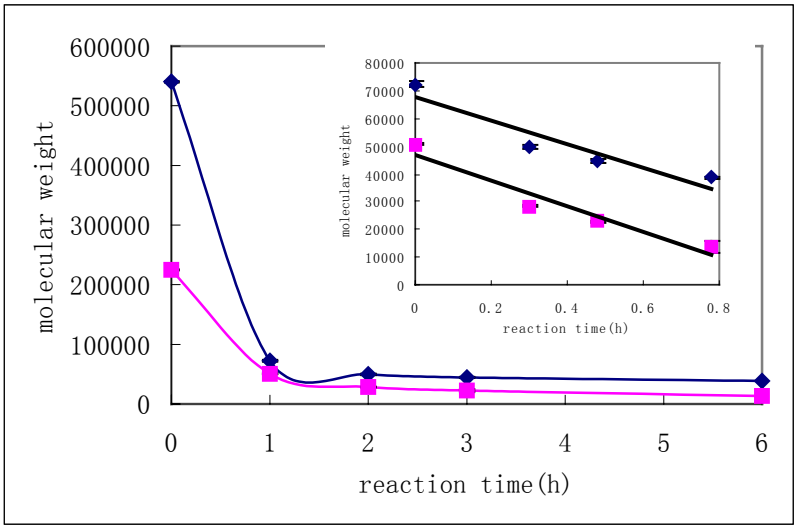

Figure 3. Effect of reaction time on the molecular weight of depolymerized chitosan. (■) low MW chitosan. (◆) medium MW chitosan. The measurements were carried out in triplicate and the results are expressed as mean±SD. Chitosan (1%) was degraded in 1% acetic acid solution with chitosan/$NaNO_2$ molar ratio 0.009.

3.3 Effect of chitosan initial concentration

In order to investigate whether chitosan/$NaNO_2$ molar ratio and reaction time were the only factors influencing the molecular weight of chitosan fragment, taking MMW chitosan as an example, the chitosan/$NaNO_2$ molar ratio was kept at 0.009 and reaction time 3 hours, two different chitosan initial concentrations, 0.5% and 1% respectively, were studied. The results are shown in Figure 4, with regression coefficients of 0.99 and 0.97 respectively for 1% and 0.5% initial concentrations of chitosan.

It seems that the depolymerization of chitosan was not only influenced by the ratio of chitosan/$NaNO_2$, but also by the initial concentration of chitosan. When the concentration was low, chitosan was more sensitive to depolymerization despite of the same chitosan/$NaNO_2$ ratio. This phenomenon

is related to the structure of chitosans in solution. Normally chitosans take the shape of an extended random coil in solution. When the concentration is high, due to the larger viscosity of the solution and strong intermolecular interactions, accessible chain segments can only stretch in a limited area, decreasing the contact probability with sodium nitrite, thus resulting in a lower degradation rate. In this case, low chitosan concentration would be preferred to yield very small molecular weight chitosan in a short time.

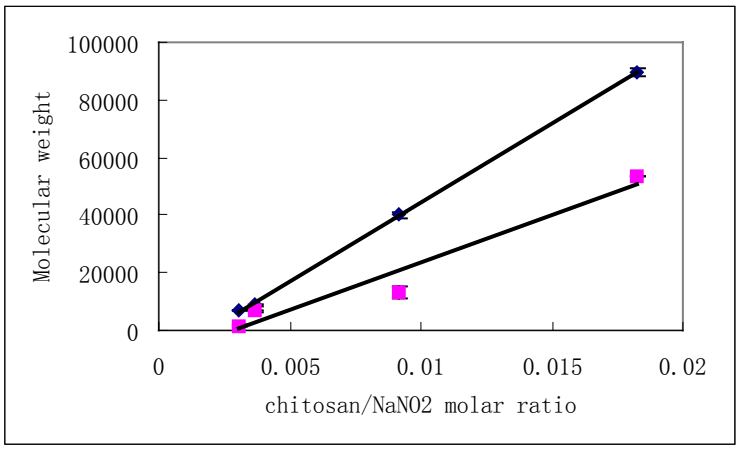

Figure 4. Effect of MMW chitosan initial concentration on the molecular weight of chitosan fragments. (■) 0.5% , (◆) 1.0%. The measurements were carried out in triplicate and the results are expressed as mean±SD. Medium molecular weight chitosans were degraded in 1% acetic acid solution with different chitosan/$NaNO_2$ ratios for 3 h at room temperature.

3.4 Investigation on the reproducibility of the degradation process

While the reproducibility of a method is of extremely importance, chitosan samples of LMW and MMW were degraded in triplicate to test the deviation of this oxidative degradation method. The chitosan/$NaNO_2$ molar ratio was adjusted based on the purposed molecular weight of chitosan. Briefly, 1% chitosan was degraded in 1% acetic acid solution for 3 h with chitosan/$NaNO_2$ molar ratio 0.004 and 0.009 respectively for LMW and MMW chitosans to get different molecular weight products. The resulting molecular weights were 2800

±200 and 49000±3600 respectively. Coefficients of variation for both samples were approximately 7% and no significant difference was indicated by t-test in the same array. Consequently, it could be concluded that this method has a good reproducibility and can be used to prepare chitosans with desired molecular weight.

3.5 Structure identification during the depolymerization process

In order to investigate any structural changes during the depolymerization process, IR spectra of the depolymerized chitosans were recorded, as shown in Figure 5.

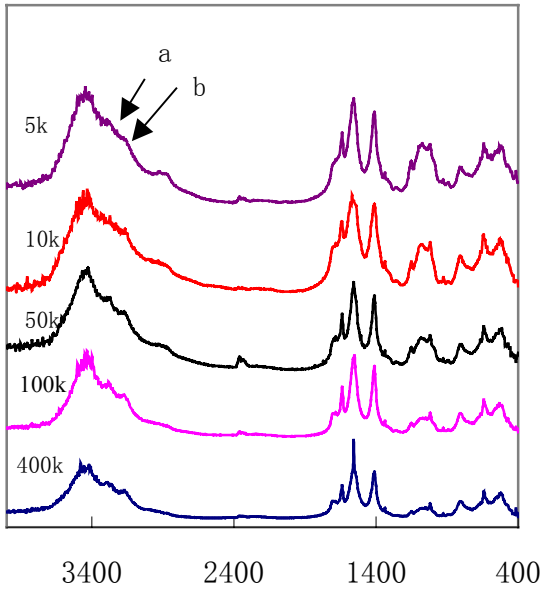

Figure 5. IR spectra of chitosan fragment with different molecular weights.

The IR spectrum clearly shows that the process has no significant influence on the structure. In case of great changes in the DD value, there should be some change in the absorption bands *a* (3253 cm^{-1}) and *b* (3143 cm^{-1}) which increase with decreasing DD. The decrease of peak *a* indicates the reduction of intermolecular C (2_1) NH---O=C (7_3) hydrogen bonds, and the decrease of peak *b* indicates the reduction of intermolecular C (6_1) OH---HOC (6_2) hydrogen

bonds (Cho et al., 2000). To quantify the absorption intensity as an indirect indicator for the change of DD, the absorption ratios at 3253 cm^{-1} and 3143 cm^{-1} compared with that of at 1551 cm^{-1} were calculated respectively and the results are shown in Table 2. Significance between different molecular weight samples was calculated using ANOVA one-way analysis (Origin 7.0 SRO, USA) and no statistically significant difference ($P > 0.05$) was indicated despite that the value was to some extent higher for chitosan 10 kDa and 50 kDa.

While IR is a coarse method for DD determination, the DD values were further measured by ^1H NMR and the results are listed in Table 2. It was consistent with the result from IR spectra and the DD values of different molecular weight samples had only a negligible difference.

Table 2 Characteristics of different molecular weight chitosans prepared from MMW chitosan

Mv (Da)	5000	10000	50000	100000	400000
A_{3143}/A_{1551}[a]	0.6713	0.7049	0.7195	0.5100	0.5295
A_{3259}/A_{1551}[a]	0.7946	0.8085	0.8456	0.6462	0.6928
DD(%)[b]	85.42	86.27	89.93	85.39	85.11

[a] Absorption ratios calculated by infrared spectroscopy.

[b] Degree of deacetylation calculated by ^1H NMR.

3.6 Thermoanalytical characterization of different molecular weight chitosans

The thermal properties of chitosan were further characterized by TGA. Molecular weight dependent degradation behaviour was observed, as illustrated in Figure 6. Chitosan with MW of 250~500 kDa showed a maximum degradation temperature at about 280℃, low MW chitosan degraded at lower temperature, at 220, 180℃ for MW 25~100 and 2.5~5 kDa respectively. A similar MW dependent degradation behaviour was observed for polyethylenimine and polyethylene glycol (Peterson et al., 2002).

3.7 Solubility of different molecular weight chitosans

The water solubility of chitosan was assayed as a function of pH. A good correlation between pH and transmittance at 600 nm was established for all the chitosans investigated. pH_{50}, which is defined as the pH value when the transmittance reached 50%, was calculated from the equation and was employed to express the solubility difference of different chitosans. pH_{50} and the cloud point pH of different molecular weight chitosans are shown in Figure 7.

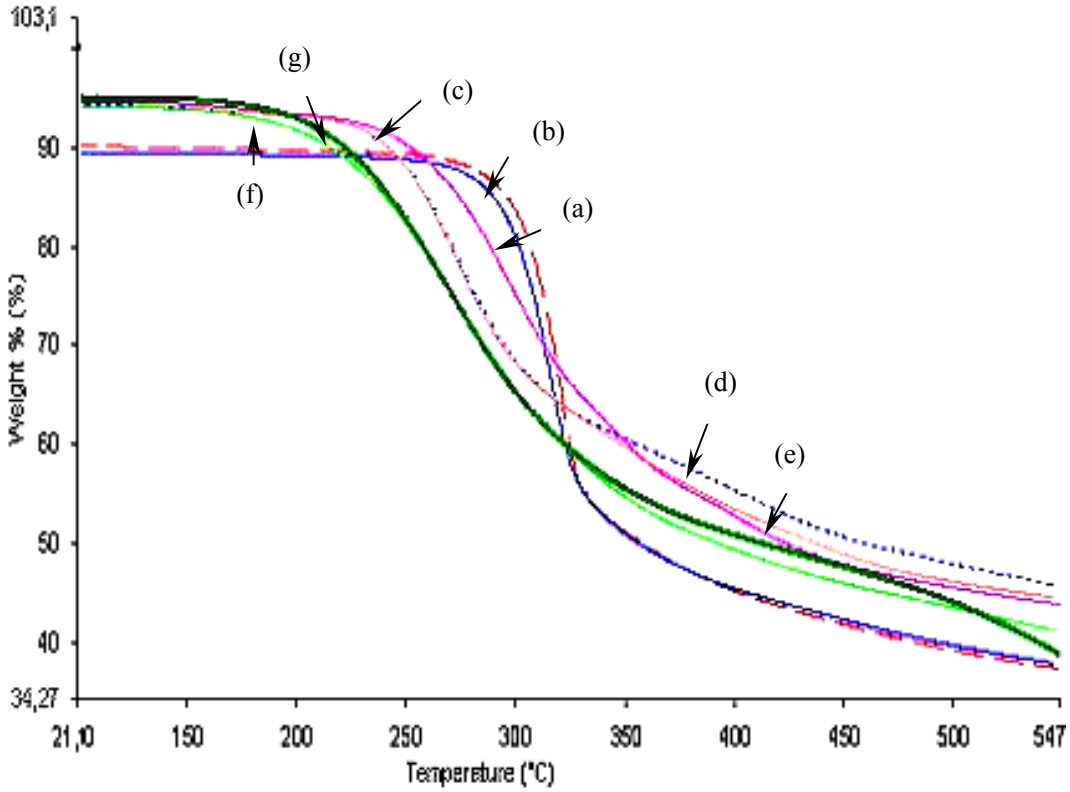

Figure 6. Degradation behavior of different molecular weight chitosans measured by thermal gravimetric analysis.
(a) MW 400 kDa; (b) MW 250 kDa; (c) MW 100 kDa; (d) MW 50 kDa; (e) MW 25 kDa; (f) MW 5 kDa; (g) MW 2.5 kDa. Molecular weight dependent degradation behaviour was observed.

We observed that pH_{50} and cloud point pH increased with decreasing

molecular weight. This was expected because, the presence of rigid crystalline domains, formed by intra- and/or intermolecular hydrogen bonding, was considered to be responsible for the poor solubility of chitosan in high pH solutions (Nishimura et al., 1991). The hydrogen bonding will be disturbed during the depolymerization process, resulting in the improved solubility. It should be noted that these tests were only carried out at one concentration and were simply used to verify that the solubility of chitosan could be improved by decreasing molecular weight.

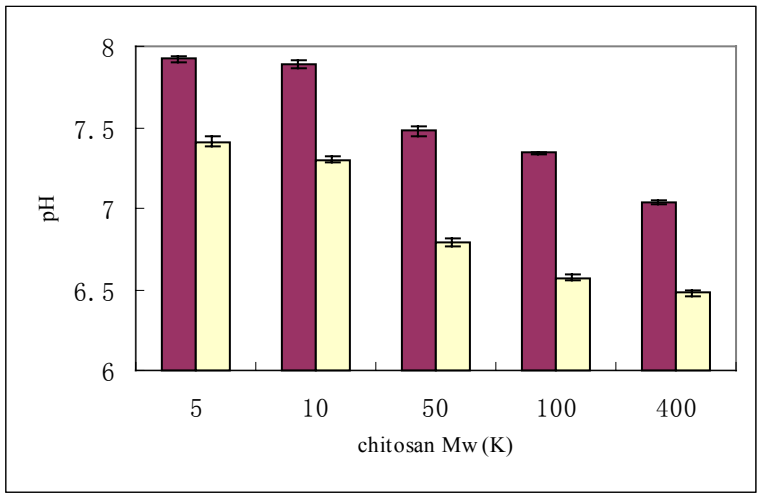

Figure 7. Solubility properties of different molecular weight chitosans. (■) pH_{50}, (□) critical pH. pH_{50} is defined as the pH value when the transmittance of the solution at 600 nm reached 50%. Cloud pH is defined as the pH when the transmittance at 600 nm was no less than 98%.

3.8 Biocompatibility studies

While chitosan is considered as a degradable polymer due to its susceptibility to various enzymes (Zhang et al., 2001), we performed in this work a cytotoxicity study to clarify the relationship between molecular weight and toxicity.

Generally, the determination of cell viability is an ordinary assay to evaluate the in vitro cytotoxicity of biomaterials. Common methods for determining cell viability depend upon membrane integrity (e.g. trypan blue

exclusion), or incorporation of nucleotides during cell proliferation (e.g. BrdU or 3H-thymidine). However, these methods are limited by the impracticality of processing large number of samples, or by the requirement for handling hazardous materials. The MTT Assay, in contrast, provides a rapid and versatile method for assessing cell viability (Mosmann, 1983**)**. This test is a quantitative colorimetric method to determine cell proliferation and it utilizes the yellow tetrazolium salt [3-(4, 5-Dimethylthiazol-2-yl)-2,5-diphenyltetrazolium-bromide] which is metabolized by mitochondrial succinic dehydrogenase activity of proliferating cells to yield a purple formazan reaction product which is largely impermeable to cell membranes, thus resulting in its accumulation within healthy cells. Solubilization of the cells results in the liberation of the product that can readily be detected using a simple colorimetric assay. The ability of cells to reduce MTT provides an indication of the mitochondrial integrity and activity, which, in turn, may be interpreted as a measure of viability and/or cell number. Comparison of results between control and test cultures provides an indication of the cytotoxic effect of test compounds.

The results are described in Figure 8. The cytotoxicity of chitosan was concentration dependent, as expected, but all the chitosans tested were relatively non-toxic at concentration up to 1 mg/ml. Chitosan 400 kDa showed an IC_{50} of 4200 μg/ml, whereas approximately 5000 μg/ml were found for chitosan 100-5 kDa. Taking the deviation of this method into account, it is reasonable to conclude that the cytotoxicity of chitosan was molecular weight independent although it was not in agreement with the result of Sgouras (Sgouras et al., 1990), who found a molecular weight dependence of the cytotoxicity. This difference can be attributed to different cell lines used in those experiments. The L929 fibroblast cell line used in our experiments is recommended by USP and several other pharmacopoeias as a standard method for cytotoxicity testing.

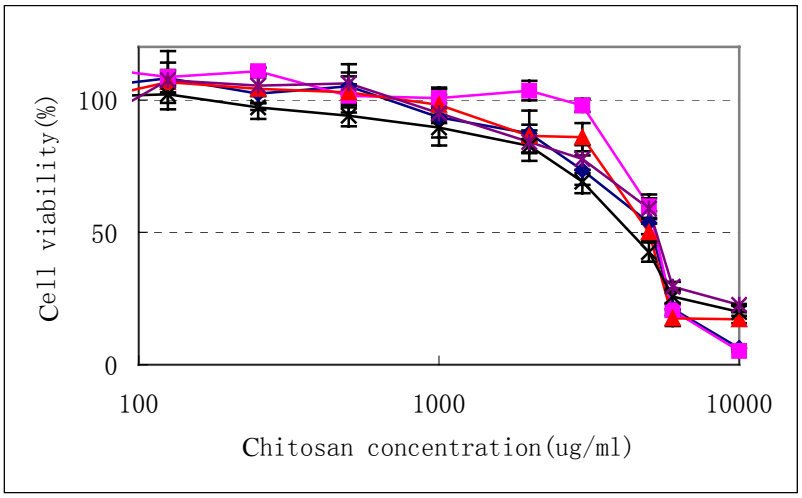

Figure 8. Cell viability upon incubation with increasing concentrations of chitosans for 24 h, as demonstrated by MTT assay with L929 cells. Values shown are mean±SD (n = 7). CH 400 kDa (◆); CH 100 kDa (■); CH 50 kDa (▲); CH 10 kDa (×); CH 5 kDa (*).

4. Conclusions

The depolymerization of chitosan could be carried out by oxidative degradation using sodium nitrite. A large series of chitosans with desired molecular weights could be obtained by changing chitosan/$NaNO_2$ molar ratio, chitosan initial concentration and reaction time. The molecular weight of the depolymerized chitosan was linear with chitosan/$NaNO_2$ ratio, and decreased as a function of the logarithm of reaction time. Chitosan with larger molecular weight was more sensitive to depolymerization. IR spectrum and ^1H NMR spectroscopy demonstrated that there was no structure change during depolymerization process. The reproducibility of this method was fairly good. The decomposition temperature of chitosan was molecular weight dependent and the solubility of chitosan increased with decreasing molecular weight. The cytotoxicity of chitosan was almost molecular weight independent according to MTT assay using L929 cell line. Chitosan was nontoxic when the concentration was as high as 1mg/ml.

In summary, using the oxidative depolymerization of chitosan, low

molecular weight fragments can be easily and reproducibly obtained.

References

Anderson, B.C., Mallapragada, S.K., 2002. Synthesis and characterization of injectable, water-soluble copolymers of tertiary amine methacrylates and poly (ethylene glycol) containing methacrylates. Biomaterials 23, 4345-4352.

Artursson, P., Lindmark, T., Davis, S.S., Illum, l., 1994. Effect of chitosan on the permeability of monolayers of intestinal epithelial cells (Caco-2). Pharm. Res. 11, 1358-1361.

Aspden, T., Adler, J., Davis, S.S., Skaugrud, Φ. and Illum, L., 1995. Chitosan as a nasal delivery system: Evaluation of the effect of chitosan on muco-ciliary clearance in the frog palate model. Int. J. Pharm. 122, 69-78.

Aspden, T., Illum, L. and Skaugrud, Φ., 1996. Chitosan as a nasal delivery system: Evaluation of insulin absorption enhancement and effect on nasal membrane integrity using rat models. Eur. J. Pharm. Sci. 4, 23-31.

Aspden, T.J., Mason, J.D.T., Jones, N.S., Lowe, J., Skaugrud, Φ., Illum, L., 1997a. Chitosan as a nasal delivery system: The effect of chitosan solutions on in vitro and in vivo muco-ciliary transport rates in human turbinates and volunteers. J. Pharm. Sci. 86(4), 509-513.

Aspden, T., Illum, L. and Skaugrud, Φ., 1997b. The effect of chronic nasal application of chitosan solution on cilia beat frequency in guinea pigs. Int. J. Pharm. 153, 137-146.

Carrecuno-Gomez, B., Duncan, R., 1997. Evaluation of the biological properties of soluble chitosan and chitosan microspheres. Int. J. Pharm. 148, 231-240.

Chang, C., Liao,Y., Li, S., 1998. Preparation of low molecular weight chitosan and chito-oligosaccharides by the enzymatic hydrolysis of chitosan. Adv. Chitin Sci. 3, 233-238.

Chen, R.H., Chen, J.S., 2000. Changes of polydispersity and limiting molecular weight of ultrasound-treated chitosan. Adv. Chitin Sci. 4, 361-366.

Cho, Y., Jong, J., Park, C.R. and Ko, S.W., 2000. Preparation and solubility in acid and water of partially deacetylated chitins. Biomacromolecules 1, 609-614.

Erbacher, P., 1998. Chitosan-based vector/DNA complexes for gene delivery:biophysical characterization and transfection ability. Pharm. Res. 15(9), 1332-1339.

Fischer, D., Bieber, T., Li, Y., Elsaesser, H., Kissel, T., 1999. A novel non-viral vector for DNA delivery based on low molecular weight, branched polyethylenimine. Effect of

molecular weight on transfection efficiency and cytotoxicity. Pharm. Res. 16(8), 1273-1279.

Gamzazade, A.I., Slimak, V.M., Skljar, A.M., 1985. Investigation of the hydrodynamic properties of chitosan solutions. Acta Polym. 36(8), 420-424.

Heller, J., Lium L., Ng, S., Duncan, R. and Richardson, S., 1996. Alginate/Chitosan microporous microspheres for the controlled release of proteins and antigens. Proc. Int. Symp. Control Release Bioact. Mater. 23, 269.

Illum, L., Farray, N.F., Davis, S.S., 1994. Chitosan as novel nasal delivery system for peptide drugs. Pharm. Res. 11, 1186-1189.

Janes, K.A., Calvo, P., Alonso, M.J., 2001. Polysaccharide colloidal particles as delivery systems for macromolecules. Adv. Drug Delivery Rev. 47, 83-97.

Janes, K.A., Alonso, M.J., 2003. Depolymerized chitosan nanoparticles for protein delivery: Preparation and characterization. J. Applied Poly. Sci. 88, 2769-2776.

Kasaai, M.R., Arul, J., Charlet, G., 2000. Intrinsic viscosity-Molecular weight relationship for chitosan. J. Polym. Sci. Part B: Polym. Phys. 38, 2591-2598.

Lee, M., Nah, J., Kwon, Y., Koh, J.J., Ko, K.S., Kim, S.W., 2001.Water-soluble and low molecular weight chitosan-based plasmid DNA delivery. Pharm. Res. 18(4), 427-431.

Li, B., Gao, S., Qiao, X., 1999. The preparation and analysis of low molecular weight chitosan. Zhongguo Shenghua Yaowu Zazhi 20(6), 292-294.

Liu, Y., Chen, S., Yu, P., 1997. Preparation of water-soluble low-molecular weight chitosan and its complex with calcium ions. Fujian Shifan Daxue Xuebao 13(3), 67-70.

Lueßen, H.L., De Leeuw, B.J., Langemeijer, M.W.E., de Boer, A.G., Verhoef, J.C., Junginger, H.E., 1996. Mucoadhesive polymers in peroral peptide drug delivery.VI. Carbomer and chitosan improve the intestinal absorption of the peptide drug buserelin in vivo. Pharm. Res. 13, 1666-1670.

Mosmann, T., 1983. Rapid colorimetric assay for cellular growth and survival: application to proliferation and cytotoxicity assays. J. Immunol Methods. 65(1-2), 55-63.

Nishimura, S.I., Kohgo, O., Kurita, K., Kuzuhara, H., 1991. Chemospecific manipulations of a rigid polysaccharide: syntheses of novel chitosan derivatives with excellent solubility in common organic solvents by regioselective chemical modifications**.** Macromolecules 24, 4745-4748.

Park, J.H., Cho, Y.W., Chung, H., Kwon, I.C., Jeong, S.Y., 2003. Synthesis and Characterization of Sugar-Bearing Chitosan Derivatives: Aqueous Solubility and Biodegradability. Biomacromolecules 4, 1087-1091.

Petersen, H., Fechner, P.M., Fischer, D. and Kissel, T., 2002. Synthesis, characterization and biocompatibility of polyethylenimine-graft-poly (ethylene glycol) block copolymers. Macromolecules 35, 6867-6874.

Richardson Simon, C.W., Kolbe Hanno, V.J., Duncan, R., 1999. Potential of low molecular mass chitosan as a DNA delivery system: biocompatibility, body distribution and ability to complex and protect DNA. Int. J. Pharm. 178, 231-243.

Sato, T., Ishii, T., Okahata, Y., 2001. In vitro gene delivery mediated by chitosan. Effect of pH, serum and molecular mass of chitosan on the transfection efficiency. Biomaterial 22, 2075-2089.

Sgouras, D and Duncan, R., 1990. Methods for the evaluation of biocompatibility of soluble synthetic polymers which have potential for biomedical use.1 Use of the tretazolium-based colorimetric assay (MTT) as a preliminary screen for evaluation of in vitro cytotoxicity. J. Mater. Sci. Mater. Med. 1, 61-68.

Singla, A.K., Chawla, M., 2001. Chitosan: Some pharmaceutical and biological aspects-an update. J. Pharm. Pharmacol. 53(8), 1047-1067.

Zhang, H., Neau, S.H., 2001. In vitro degradation of chitosan by a commercial enzyme preparation: effect of molecular weight and degree of deacetylation. Biomaterials 22, 1653-1658.

Varum, K.M., Anthonsen, M.W., Grasdalen, H., Smidsrod, O., 1991.Determination of the degree of N-acetylation and the distribution of N-acetyl groups in partially N-deacetylated chitins (chitosans) by high-field NMR spectroscopy**.** Carbohydr. Res. 211(1), 17-23.

Chapter 3

Poly (ethylene glycol)-graft-trimethyl chitosan block copolymers: synthesis, characterization and potential as water-soluble insulin carriers

Manuscript in preparation

ABSTRACT

PEGylated trimethyl chitosan copolymers were synthesized in an attempt to both increase the solubility of chitosan in water, and improve the biocompatibility of trimethyl chitosan (TMC). A series of copolymers with different degrees of substitution were obtained by grafting the activated PEG of different MW onto TMC via primary amino groups. Structure of the copolymers was characterized using FT-IR, ^{1}H and ^{13}C NMR spectroscopies. Solubility experiments demonstrated that PEG-g-TMC(400) copolymers were completely water-soluble over the entire pH range of 1-14 regardless of the PEG MW, even when the graft density was as low as 10%. Cytotoxicity of the copolymers and corresponding insulin complexes was studied using a MTT assay. We found that PEGylation with PEG 5 kDa and PEG 20 kDa significantly decreased the cytotoxicity of TMC 400 kDa, and complex formation with insulin led to further increases in $IC_{50.}$ Properties of PEG-g-TMC copolymer insulin complexes were further investigated to gain an insight into the effect of the copolymer composition on the complex properties. All complexes investigated had a particle size in the range of 150-300 nm and were positively charged, ξ –potentials were shown to decrease with increasing graft density. Association efficiency increased with PEG graft ratio, and extremely high association efficiency, that is, 96.22%, was obtained with $PEG(5k)_{679}$-g-TMC(400) copolymer. To conclude, the degree of PEGylation and the MW of PEG were found to strongly influence the biocompability of TMC 400 kDa and properties of the corresponding insulin complexes. These complexes merit further investigations in animal studies.

1. Introduction

Chitosan (poly(β -(1-4)-2-amino-2-deoxy-D-glucopyranose)), a non-toxic and biocompatible cationic polysaccharide, is produced by partial deacetylation

of chitin derived from naturally occurring crustacean shells. Due to its specific structure and properties, chitosan has found a number of applications in drug delivery including as an absorption enhancer for hydrophilic macromolecular drugs and as a gene delivery system [1]. The applications of chitosan in the biomedical field are limited, however, by its poor solubility in physiological media. Chitosan is only soluble in aqueous acidic solutions below pH 6.5, in which the primary amino groups of chitosan are protonated. To improve the poor water-solubility of chitosan, several derivatives have been proposed. For example, the modification of chitosan by quaternization of the amino groups [2,3], N-carboxymethylation [4] and PEGylation [5,6] have been reported.

However, these efforts were only partially successful in the case of PEG(5k)-g-chitosan, which was prepared via reacting chitosan (degree of deacetylation 70%, MW 70 kDa) with methoxy-PEG(5k)-g-nitrophenyl carbonate [6]. With a graft density of 78.5% (calculated as a weight ratio of PEG 5 kDa in the graft copolymer, the same below), PEG(5k)-g-chitosan copolymer solutions became cloudy at pH 6.8, which is suggestive of polymer precipitation. Even at graft densities as high as 92.7%, the copolymer solution became cloudy [5] and formed aggregates [6] when the pH was > 7.0. It is noteworthy that phase separation appeared at pH 6.5 or higher for unmodified chitosan, depending on the molecular weight [7]. This indicates that PEGylation can only marginally improve the solubility of chitosan in a very limited range (pH 6.5-7.0), even with high graft densities. Accordingly, the objective of the present study was to design chitosan derivatives with superior solubility and biocompatibility.

Another possible approach involves trimethyl chitosan (TMC). TMC is a permanently quaternized chitosan derivative, which has been proven to be highly soluble over a wide pH range (pH 1 to 9) up to 10% (w/v) concentration. Moreover, TMC is capable of opening tight junctions of intestinal epithelial cells at physiological pH values, thus increasing paracellular permeability of

intestinal epithelia [8], whereas chitosan itself is insoluble and thus ineffective in this role. Moreover, TMC seems to be an efficient gene delivery system [9]. However, in contrast to chitosan, TMC was shown to be cytotoxic in L929 mouse fibroblast cells as indicated by MTT assay in our laboratory (data shown below). Kotze et al. also indicated that reversibility of the effect of 0.5% concentrations of TMC with different degree of quaternization could not be demonstrated at pH 6.2 and 7.4 in Caco-2 cells [10]. Therefore, further improvement of the biocompatibility of TMC is desirable.

As a water soluble, biocompatible, non-toxic and non-immunogenic material, PEG can not only enhance biocompatibility but also favorably affect pharmacokinetics and tissue distribution. Conjugation of PEG to proteins is well known to enhance the in vivo half-life of the encapsulated drugs, assist penetration into the cell membrane, alter pharmacological properties and increase biocompatibility [11,12]. Therefore, PEGylated TMC copolymers could possibly provide further biological functionality, in addition to improving solubility and decreasing cytotoxicity. Here we described the synthesis and physico-chemical characterization of PEGylated trimethyl chitosan in an effort to improve both solubility and biocompatibility. Additionally, the feasibility of the copolymers as insulin carriers is investigated.

2. Materials and methods

2.1 Materials

Chitosan (MW~400 kDa, degree of deacetylation 84.7%) was purchased from Fluka (Steinheim, Germany). Methoxypoly (ethylene glycol) (M_n 550 and 5000 Da), water free toluene (99.9%), dichloromethane (99.9%), dimethyl sulfoxide (DMSO) (99.9%), diethyl ether (99.9%), maleic anhydride, N-hydroxysuccinimide (NHS) and dicyclohexylcarbodiimide (DCC) were obtained from Aldrich (Steinheim, Germany) and used as received. Human recombinant insulin powder (26.2 IU/mg) was purchased from Sigma

(Steinheim, Germany). All other chemicals and solvents were of analytical grade. Activated PEG 20 kDa (α -Methoxy- ω -NHS ester) was purchased from RAPP Polymer GmbH (Tuebingen, Germany).

2.2 Activation of mPEG

The monohydroxy-terminated PEGs were converted to a carboxyl-terminated intermediate by esterification with cyclic aliphatic anhydride according to the literature report [13]. Briefly, in a 50 ml round-bottomed flask equipped with a reflux condenser and an oil bubbler, 5 g (0.0091 mol) of pre-dried mPEG 550 Da was dissolved in 20 ml of water free toluene, 4.457 g maleic anhydride (0.04545 mol, 1:5 molar ratio *vs* PEG) was added under the protection of argon. The reaction mixture was stirred at 70℃ for 48 h under an argon atmosphere. After the esterification process, toluene and the excess maleic anhydride were eliminated by distillation and sublimation at 40℃ under vacuum.

Subsequently, the intermediate mentioned above (0.54 mmol) together with NHS (2.7 mmol) (1:5 in molar ratio) were dissolved in 20 ml dichloromethane (DCM) in a flask equipped with a magnetic stirring bar. The flask was then cooled in an ice-water bath and DCC (0.54 mmol) was added under argon. The reaction mixture was sealed under argon and stirred for 1 h at 0℃, and a further 24 h at room temperature. The precipitated 1, 3-dicyclohexylurea (DCU) was removed by filtration. The filtrate was added to diethyl ether (50 ml) and cooled at 4℃ for 2 h. The precipitated product was then redissolved in DCM and reprecipitated with diethyl ether. This procedure was repeated at least three times to completely remove excess NHS. Finally, the product was dried under vacuum and stored at room temperature under argon. mPEG 5 kDa was activated in the same manner.

2.3 Preparation of trimethyl chitosan (TMC)

TMC was prepared according to a two-step method previously described by Sieval et al. to obtain TMC with a quaternization degree of approximately 40% [2]. This degree of quaternization has been demonstrated to have improved permeation enhancing properties [14]. TMC 400 kDa used throughout this study was characterized by ^{1}H NMR and its composition is as follows: $N^{+}(CH_3)_3$ group 46.41%, $N(CH_3)_2$ group 12.44%, 3-OCH_3 group 6.14%, 6-OCH_3 8.04%, $NHCOCH_3$ 10.32%, free amino group 30.83%.

2.4 Coupling of activated mPEGs onto TMC

A predetermined quantity of TMC was dissolved in purified water at a concentration of 10 mg/ml. NHS-mPEG was dissolved in DMSO (50 mg/ml) solution. Subsequently, the TMC solution was added to the NHS-mPEG solution and the mixture was stirred at room temperature for 24 h. Weight ratios of TMC to NHS-mPEG were varied in order to achieve the optimal PEGylation level. After 24 h of stirring, the solution was purified by ultra filtration with an Amicon system equipped with a 10 000 MW cut-off membrane. The concentrated solution was diluted and ultrafiltrated again. This procedure was repeated at least 3 times and the dialyzed solution was finally freeze-dried. The graft ratio (wt %) of PEG was calculated from integral values of the characteristic peaks of PEG block at ~3.35 ppm (-OCH_3) and TMC blocks at ~ 3.0 ppm (-$N(CH_3)_2$) and ~ 3.3 ppm (-$N^{+}(CH_3)_3$) obtained in the ^{1}H NMR spectra, using the known molecular weight of mPEG. This method of comparing integration of ^{1}H NMR peaks has been widely implemented [13, 15].

PEGylated chitosans were prepared in the same manner for the purpose of comparison. However, due to its higher viscosity, concentration of chitosan 400 kDa was 0.2% instead of 1% for TMC 400 kDa.

2.5 Characterization of copolymers

Fourier Transformed Infrared (FTIR) spectral studies were conducted on a FT-IR 510 P spectrometer in the range of 4000 and 400 cm^{-1}, with a resolution of 2 cm^{-1}. All powder samples were compressed into KBr disks for the FTIR measurement.

Nuclear Magnetic Resonance Spectroscopy (NMR). ^{1}H NMR and ^{13}C NMR spectra were recorded on a JEOL GX 400 D spectrometer operating at 400 MHz at room temperature. Samples were dissolved in D_2O or $CDCl_3$.

Gel permeation chromatography (GPC) was carried out using a Supremamax 3000 column (Polymer Standard Service, Mainz, Germany) with 0.3 M acetic acid and 0.2 M sodium acetate as an eluent (1 ml/min). 40 µl samples were injected with a Merck Hitachi autosampler AS-2000A. The samples were analyzed with a differential refractive index (RI) detector RI-71 from Merck.

Differential Scanning Calorimetry (DSC). DSC measurements were performed on a Perkin-Elmer differential scanning calorimeter (DSC-7) at a heating rate of 20℃/min. The sample (approximately 5 mg) was first heated from –100℃ to 170 ℃. It was then quenched to -120℃ with liquid nitrogen, and heated again to 170 ℃. The melting temperature (T_m) was determined from the endothermic peak of the DSC curve recorded in the first heating scan.

Thermogravimetric Analysis (TGA) was carried out on a thermogravimetric analyser TGA 7 with a thermal analysis controller TAC 7/DX from Perkin-Elmer using a sample weighing approximately 5 mg. Thermograms were recorded within the temperature range of 30-550℃ at a scanning rate of 20℃/min. All experiments were performed under nitrogen in platinum crucibles.

2.6 Water Solubility Testing

Solubility of the various copolymers was measured at different pH values

at room temperature. Briefly, the copolymers were dissolved in a 0.25% acetic acid solution (2 mg/ml), the pH value of the solution was adjusted using 1N NaOH and transmittance of the solution at 600 nm as a function of pH was recorded on an UV/Vis spectrophotometer (UV-160, Shimadzu, Japan). The copolymers were considered insoluble when the transmittance was less than 90%, compared to that of distilled water.

2.7 Formation of copolymer-insulin complexes and characterization

The complexes were prepared via self-assembling process using the electrostatic interaction between the polymers and insulin, and the process parameters were optimised (chapter 5). Briefly, insulin (1 mg/ml) and appropriate quantity of copolymer (based on the ratio with insulin, as indicated in Table 3) were dissolved in 0.1 N Tris buffer solution pH 7.4. Complexes were prepared by mixing equal volumes of insulin and polymer solution under gentle magnetic stirring, and incubating for further 20 min at room temperature.

Dynamic light scattering determination (DLS). Complex size measurements were performed with a Zetasizer 3000 HS from Malvern Instruments, Herrenberg, Germany (10 mW HeNe laser, 633 nm). Scattering light was detected at a 90^{o} angle through a 400 micron pin hole at a temperature of 25℃. For data analysis, the viscosity (0.88 mPa•s) and the refractive index (1.33) of distilled water at 25℃ were used. The instrument was routinely checked using Standard Reference latex particles (AZ 55 Electrophoresis Standard Kit, Malvern Instruments). Measurements were analysed using the CONTIN algorithm. Values given are mean ± SD (n = 10).

Laser Doppler Anemometry (LDA). The ξ - potential measurements of the complexes were carried out in the standard capillary electrophoresis cell of the Zetasizer 3000 HS from Malvern Instruments at 25℃. Values given are mean ± SD (n = 10).

Insulin association efficiency of the complexes. The amount of insulin encapsulated in the complexes was calculated by measuring the difference between the total amount of insulin added and the quantity of non-associated insulin remaining in the aqueous medium after the self-aggregation process. For this purpose, prepared insulin complexes were centrifuged at 14000 rpm/min at room temperature for 30 min. The quantity of insulin in the supernatant was measured using a Merck HPLC system equipped with a fluorescence spectrophotometer (F-1050) and a LiChrospher 100 RP-18e column (5 μm, 4.6 ×250mm). A sample of 20 μl was injected on each occasion. The mobile phase comprised eluent A (ultrapure water with 0.1% trifluoroacetic acid (TFA)) and eluent B (acetonitril: water: TFA 89.9: 10: 0.1) 65: 35. The flow rate was 1.0 ml/min and an emission wavelength 600 nm together with an excitation wavelength 280 nm was employed. Insulin content was quantified by peak area measurement. The insulin association efficiency was then calculated using the following relationship:

$$Association\ efficiency = \frac{Total\ amount\ of\ insulin - Free\ insulin}{Total\ amount\ of\ insulin} \times 100\%$$

2.8 Cytotoxicity of the complexes

In vitro cytotoxicity of both the copolymers and the complexes was evaluated using a MTT assay with L929 fibroblast cell line, as described previously [16]. Briefly, L929 cells were seeded into 96-well microtiter plates at a density of 8000 cells/well. After 24 h, the culture medium was replaced with 100 μl serial dilutions of polymer/complex and cells were incubated for a further 24 h. Subsequently, 20 μl MTT (5 mg/ml) was added to each well. After 4 h incubation, unreacted dye was aspirated and the formazon crystals were dissolved in 200 μl/well DMSO. Absorption was measured at 570 nm with a background correction of 690 nm using a Titertek Plus MS 212 ELISA reader (ICN, Eschwege, Germany). The relative cell viability compared to control cells

containing cell culture medium (pH 6.5) without polymer was calculated by $[A]_{test}/[A]_{control}$.

3. Results and discussion

3.1 Copolymer preparation and characterization

Hydroxyl-terminated PEGs were converted to carboxyl-terminated intermediates by esterification with cyclic aliphatic anhydride. Maleic anhydride was chosen in the present study to activate PEG in preference to succinic anhydride [17] because it has been demonstrated to be more reactive to PEG hydroxyl group, and is straightforward to eliminate via sublimation after the esterification process [13]. After activation, PEGs were coupled to the amino groups of TMC, forming a graft copolymer, i.e., PEG-g-TMC. The synthetic route is shown in Scheme 1.

We investigated the influence of polymer solution pH on the final graft ratios, with no significant difference being observed at polymer pH 5.0, 7.0, 8.5 respectively. Therefore all copolymers were prepared at a constant polymer solution pH of 7.0. The effect of feed ratios was investigated and the graft ratios of the copolymers, calculated from ^{1}H NMR spectra based on the MW of the polymer provided by the supplier, are listed in Table 1. We used the following abbreviated nomenclature for the copolymers: PEG$(X)_n$ -g-TMC(400), where X denotes the MW of PEG in Da and the subscript *n* represents the average number of PEG chains per TMC 400 kDa macromolecule. The average number of free amino groups in the copolymer was measured using fluorescamine assay [18].

Obviously, the graft ratios increased with feed ratio and a good linear correlation between NHS-mPEG/polymer ratio and graft density was found (Table 1). It is generally assumed that the activity of PEG is molecular weight-dependent, for example, mPEG 550 Da should be more reactive than mPEG 5 kDa. This is the case for PEG-g-chitosan(400) copolymers, as shown in Table 1.

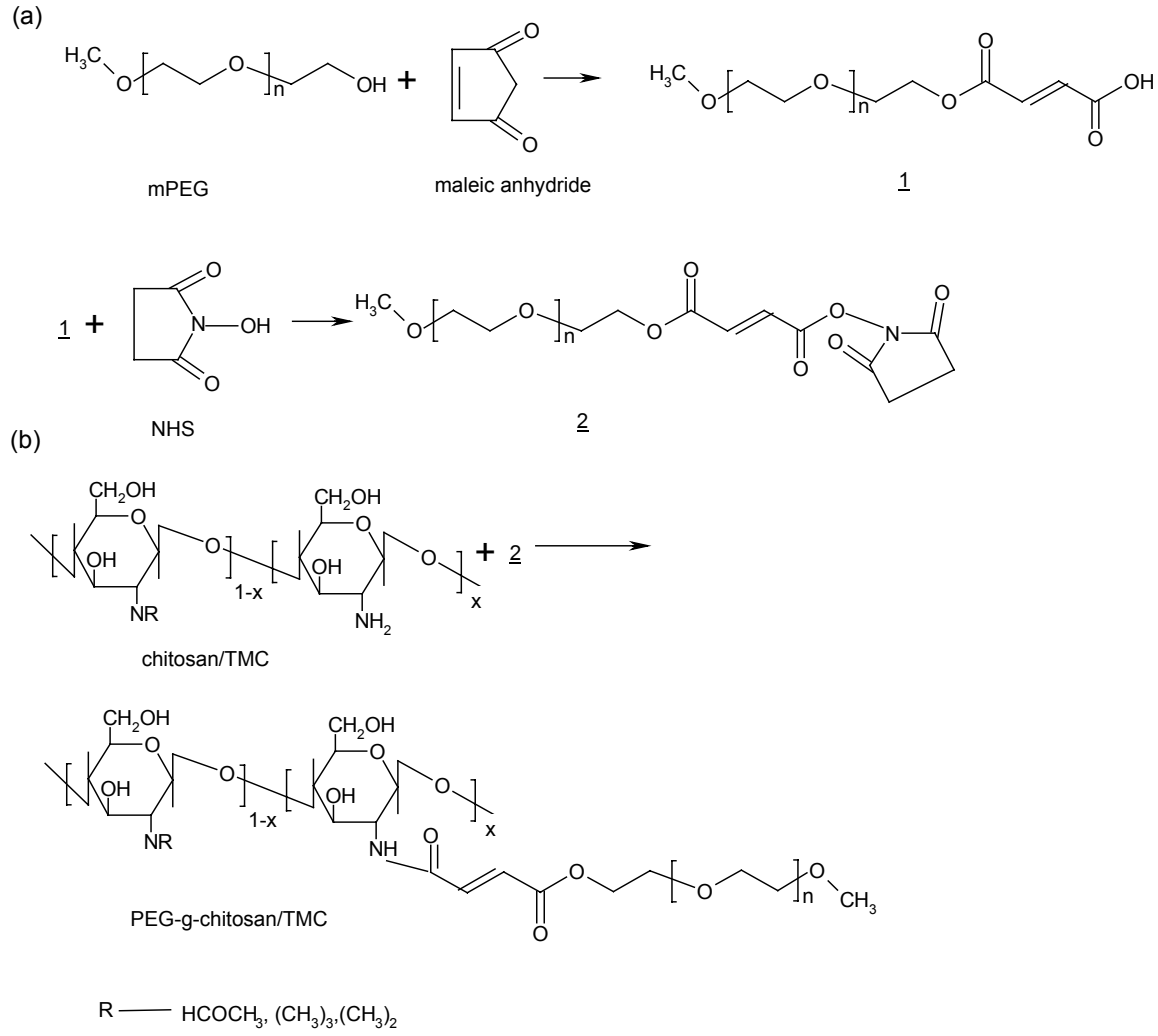

Scheme 1. Synthetic route of PEGylated chitosan derivatives.

However, the opposite is true for TMC 400 kDa, as indicated by the number of PEG chains per TMC molecule. For instance, when the NHS-mPEG/TMC 400 kDa feed ratio was 3:1, only 83 PEG 550 Da molecules were coupled to TMC molecule compared to 298 mPEG 5 kDa molecules at the same feed ratio and prepared under the same conditions. The results were reproducible with different batches of activated PEG, as annotated in Table 1. Furthermore, copolymers were prepared with TMC 100 kDa (with the same substitution ratio as that of TMC 400 kDa) in the same manner and were found that the graft ratios of PEG(550)-g-TMC(100) copolymers were similar to that of PEG (550)-g-chitosan(100) in the same feed ratio (data not shown). Steric effect

could not be a cause for the low graft ratio of PEG(550)-g-TMC(400), because at the same feed ratio even higher graft ratio was obtained with PEG(5k)-g-TMC(400) (75.44%) compared to PEG(5k)-g-TMC(100) (68.25%) due to relative high amount of primary amino groups. Possible explanations are competitive reactions of activated PEG 550 Da with water. PEG-NHS is moisture-sensitive and can lose its reactivity by interacting with water. The shorter the PEG chains, more sensitive with water. Though that short PEG-NHS possesses the highest reactivity to amino groups, it also possesses the highest reactivity to water. Principally, reactivity with -NH_2 is higher than with water. However, some substituted groups may shield part of -NH_2 groups of TMC and thus grafting will become slow, requiring the PEG-NHS to maintain reactive over a longer period.

Table 1. Properties of PEG-g-TMC(400) and PEG-g-chitosan(400) copolymers

Feeding ratio (PEG/polymer) (w/w)	PEG(550)-g-TMC(400)			PEG(5k)-g-TMC(400)			PEG(550)-g-chitosan(400)			PEG(5k)-g-chitosan (400)		
	graft%	PEG550[a]	free NH_2[b1]	graft%	PEG5k[a]	free NH_2[b1]	graft%[e]	PEG550[a]	free NH_2[b2]	graft%[e]	PEG5k[a]	free NH_2[b2]
3:1	10.3[c]	83	553	75.4[d]	298	250	43.7	564	1547	75.2	243	1868
4:1	16.1	139	524	88.9	641	233	49.4	710	1401	82.8	386	1725
5:1	17.1	148	341	89.4	679	168	55.1	892	1219	86.6	515	1596

[a] Number of PEG chains per TMC 400 kDa molecule, calculation based on ^{1}H NMR data.

[b1] Number of free amino groups per TMC 400 kDa molecule, calculation based on fluorescamine assay.

[b2] Number of free amino groups per chitosan 400 kDa molecule, calculation based on the substitution of chitosan 400 kDa and the graft density of PEG. Fluorescamine assay is not feasible due to the solubility limitation of the copolymers.

[C] Calculated as a weight ratio of PEG in the graft copolymer based on NMR analysis. Reproducibility of the copolymer preparation method with different batches of activated PEG 550 Da were investigated, the values were 8.93, 12.6, 10.3%, respectively, with SD of 1.85.

[d] Reproducibility of the copolymer preparation method with different batches of activated PEG 5 kDa were investigated, the values were 78.83, 77.72, 75.44%, respectively, with SD of 1.73.

[e] Calculated as a weight ratio of PEG in the graft copolymer.

FTIR spectroscopy, which is known to be a particularly relevant technique for the investigation of specific intermolecular interactions [19, 20], was

(A)

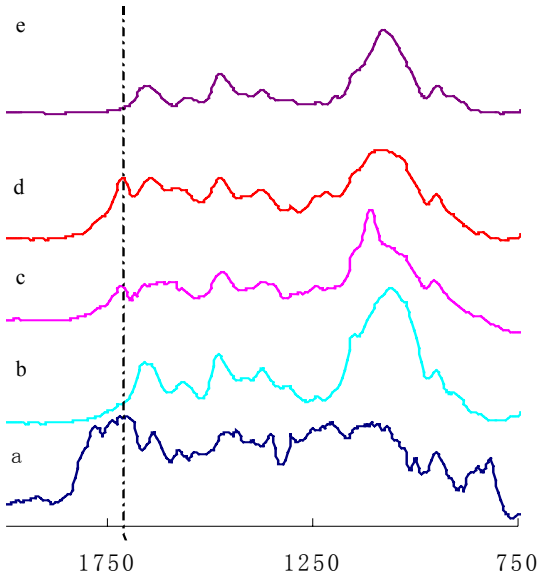

(B)

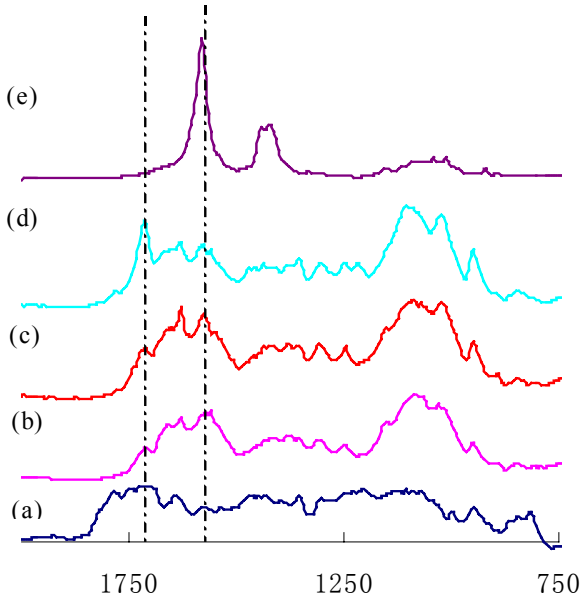

Figure 1. FTIR spectra of mPEG(550)-g-TMC(400) copolymers (A) and mPEG (550)-g-chitosan(400) copolymers (B).

(A). (a) mPEG(550)-NHS, (b) $PEG(550)_{21}$-g-TMC(400), (c) $PEG(550)_{83}$-g-TMC(400), (d) $PEG(550)_{139}$-g-TMC(400), (e) TMC 400 kDa.

(B). (a) mPEG(550)-NHS, (b) $PEG(550)_{564}$-g-chitosan(400), (c) $PEG(550)_{892}$-g-chitosan (400), (d) $PEG(550)_{1457}$-g-chitosan(400), (e) Chitosan 400 kDa.

employed to characterize the block copolymers. The FT-IR spectra of mPEG(550)-g-TMC(400) copolymers in the carbonyl vibration region are displayed in Figure 1 as a function of mPEG 550 Da composition. Another copolymer, $PEG(550)_{21}$-g-TMC(400), with a rather low graft density (2.9%) was utilized in this study to elucidate the signal evolution readily. For the mPEG(550)-g-TMC(400) copolymers studied here, the activated mPEG 550 Da contains a carboxyl group, yielding a $\upsilon_{c=o}$ stretching mode at ~1730 cm^{-1}, whereas TMC shows no absorption in the carbonyl vibration region ranging from 1650 cm^{-1} to 1800 cm^{-1}. Therefore, any change in the FTIR spectrum in this region can be directly attributed to a change in the carbonyl group environment, such as binding with other group. As shown in Figure 1(A), a new peak centered at ~1707 cm^{-1} appeared in the copolymer spectra and its intensity increased with PEG 550 Da content. A similar phenomenon was observed with PEG(550)-g-chitosan (Figure 1(B)). The amide band II at 1580 cm^{-1} decreased with increasing graft ratio.

^{1}H NMR spectra of a graft copolymer and corresponding intermediate prepolymers are shown in Figure 2A. ^{1}H NMR resonance signals are assigned accordingly. NHS-terminated mPEG 550 Da (Figure 2A(b)) showed two resonance absorptions at ~6.2 and 6.6 ppm (doublet, -C (=O) CH=CHC (=O)-), which are not present in the spectrum of HO-terminated mPEG containing no maleic moiety (Figure 2A(a)). Only a signal peak at ~6.0 (C=C) was observed in the graft copolymer (Figure 2A(c)), implying the environment of the double bond has changed, and likely the proton shielding effect of local chemical environment to the two methine groups became closer. Additionally, the graft copolymer showed strong absorption at ~3.0 ($N(CH_3)_2$) and ~3.3 ($N^{+}(CH_3)_3$) ppm, which are from the TMC. The structure of the copolymers was further investigated with ^{13}C NMR, as shown in Figure 2(B). These results are consistent with the expected chemical structure of the copolymer.

GPC measurements were also employed to verify the successful synthesis

A

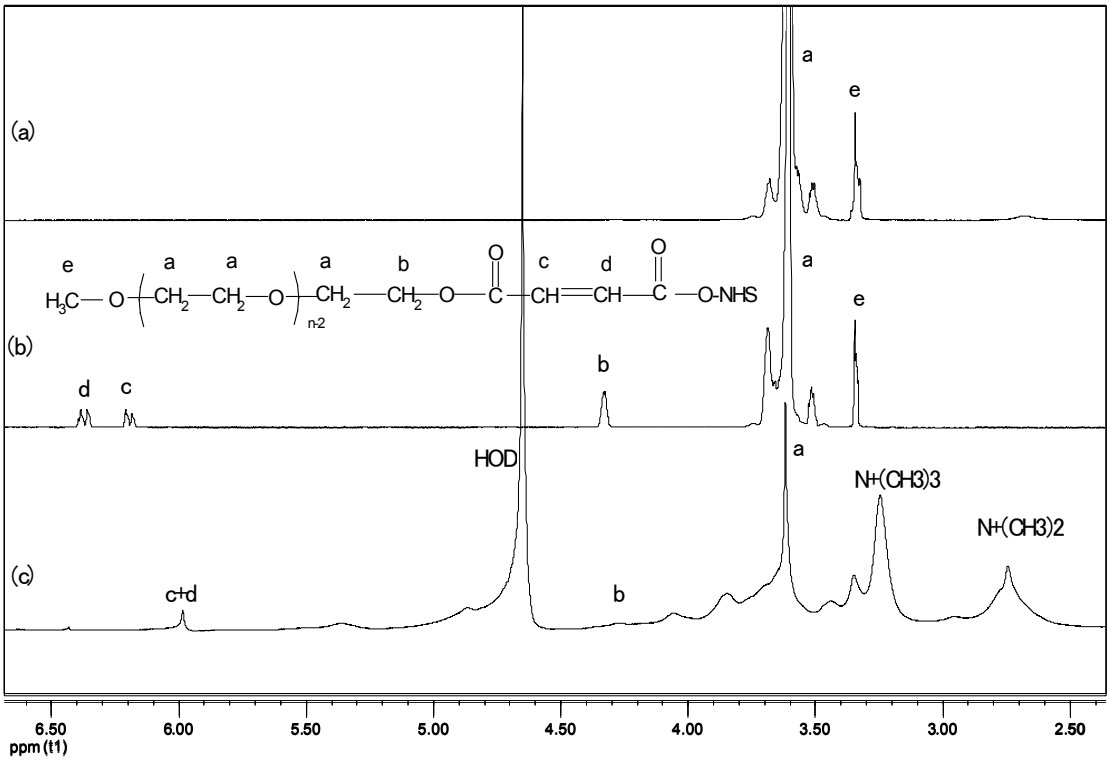

B

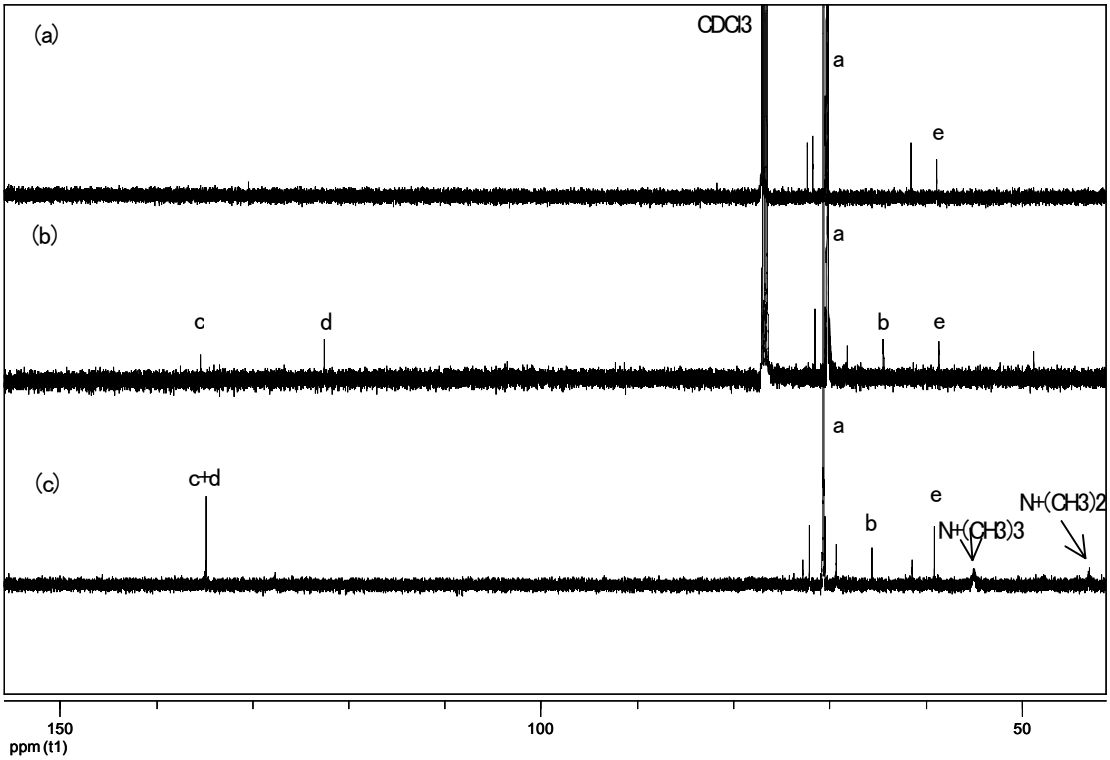

Figure 2. ^{1}H (A) and ^{13}C NMR (B) spectra of HO-terminated mPEG 550 Da (a), NHS-terminated mPEG 550 Da in $CDCl_3$ (b), and $PEG(5k)_{42}$-g-TMC(400) copolymerin D_2O (c).

of the graft copolymers. Copolymers showed unimodel molecular weight distribution in the GPC eluograms with increased molecular weight (data not shown), indicating that negligible PEG homopolymer was present in the copolymer products.

3.2 Thermal properties

The thermal properties of copolymers were studied with differential scanning calorimetry (DSC). DSC thermogram showed an endothermic peak at its melting temperature for PEG and a MW dependence was observed, T_m 14.6 ℃ and 63℃ for PEG 550 Da and PEG 5 kDa, respectively. However, no glass transition temperature was detected, probably because PEG crystallized too rapidly. Additionally, no T_g and T_m were observed for both chitosan 400 kDa and trimethyl chitosan 400 kDa.

The melting temperature of PEG 5 kDa decreased with increasing TMC content (Table 2). For instance, T_m of homo-PEG 5 kDa is 65.95℃ and only 55.48℃ in the copolymer with a graft ratio of 75.44%, a decrease about 10℃. This implies the crystallization of PEG 5 kDa was greatly affected by TMC 400 kDa. Considering that all the samples had the same thermal history, it is reasonable to conclude that PEG and TMC are at least partially miscible [21].

It is also noted that the decrease of T_m in PEG(5k)-g-chitosan(400) copolymers was larger than that in PEG(5k)-g-TMC(400) copolymers with similar PEG 5 kDa content (Table 2). The depression of T_m can be explained with the following equation [22]:

$$T_m = T_m^o(1-\frac{2\gamma_e}{\Delta H_f L})$$

where γ_e is the free energy of chain folding at the surface of the lamellae, ΔH_f is the heat of fusion of the lamellae, L is the thickness of the lamellae, and T_m^o is the melting point of a 100% perfect polymer crystal. As we can see, the

reduction of the lamellar thickness can lead to a melting point depression. The interactions between different blocks is expected to have a dominant effect on reducing L in the diblock copolymer, leading to a decreased T_m. Therefore, it is reasonable to assume that the interaction between PEG and chitosan is stronger than that of PEG and trimethyl chitosan. This result can be used to explain the solubility difference of the copolymers. On the other hand, decreased T_m indicated that those two components are miscible and compatible. As to the small MW mPEG 550 Da, the T_m change was not so obvious, as summarized in Table 2.

Table 2. Melting temperature of the copolymers

Polymer	Substitution %[a]	Graft ratio (%)[b]	T_m
mPEG 550 Da			14.6
mPEG 5000 Da			65.9
Chitosan 400 kDa			-[c]
TMC 400 kDa			-[c]
mPEG(550)-g-chitosan(400)	26.8	43.7	-[c]
	33.7	49.4	-[c]
	42.4	55.1	12.2
mPEG(550)-g-TMC(400)	3.9	10.3	13.6
	6.6	16.1	12.1
	7.0	17.1	13.2
mPEG(5k)-g-chitosan (400)	11.6	75.2	54.1
	18.4	82.8	53.1
	24.5	86.6	54.2
mPEG(5k)-g-TMC(400)	14.2	75.4	55.5
	30.5	88.9	60.0
	32.3	89.4	61.5

[a] Calculated based on the primary amino group content in chitosan 400 kDa, 84.7%.

[b] Calculated as a weight ratio of PEG in the graft copolymer.

[c] Not detected.

T_m of the pure mPEG 550 Da was observed at 14.63℃ and no T_m was observed in the PEG(550)-g-chitosan(400) copolymers when the content of mPEG 550

Da was less than 55.09%, implying that the crystallization of mPEG 550 Da was fully suppressed by chitosan 400 kDa, and a decreased T_m was identified only when PEG 550 Da content was above 60%. In contrast, a T_m decrease in all mPEG(550)-g-TMC(400) copolymers was found. This can probably be attributed to the stronger interaction between chitosan and PEG 550 Da, leading to improved miscibility.

TGA measurements were also performed to investigate the thermal decomposition temperatures (T_d) of mPEGs, chitosan, TMC and the copolymers. mPEG (M_n 550, 5000 Da) decomposed at 280-380℃, whilst chitosan 400 kDa decomposed at 280℃. As for the TMC 400 kDa, two distinct thermal decomposition transitions were identified at 200℃and 270℃. These are due to a special composition with a quaternization degree of 40%. TGA thermograms of graft copolymers based on mPEG 5 kDa and chitosan/TMC are shown in Figure 3.

Three-step T_d's are observed in the TGA thermograms of PEG-g-TMC copolymers, which we believe correspond to the T_d's of the TMC (two T_d's) and PEG segments, respectively. In all cases, chitosans/TMCs were degraded first, followed by PEG degradation at approximately 400℃, as demonstrated by the profiles of the homopolymers. However, it cannot be assumed that all of the chitosan/TMC is degraded when the first amount of PEG begins to degrade, as there is still 10% left in the end and PEG is known to be completely degradable at such a high temperature. In addition, it is noticed that only a single T_d was found for $PEG(5k)_{515}$-g-chitosan(400) copolymers. This can be explained by the miscibility enhancement observed in the block copolymer, leading to the identical component T_d [23,24]. Indeed, enhanced miscibility was additionally verified by DSC measurements, as described above.

(A)

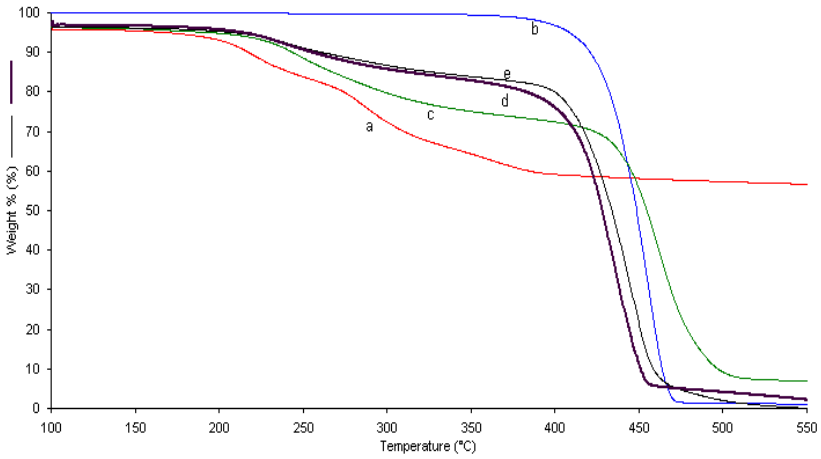

(B)

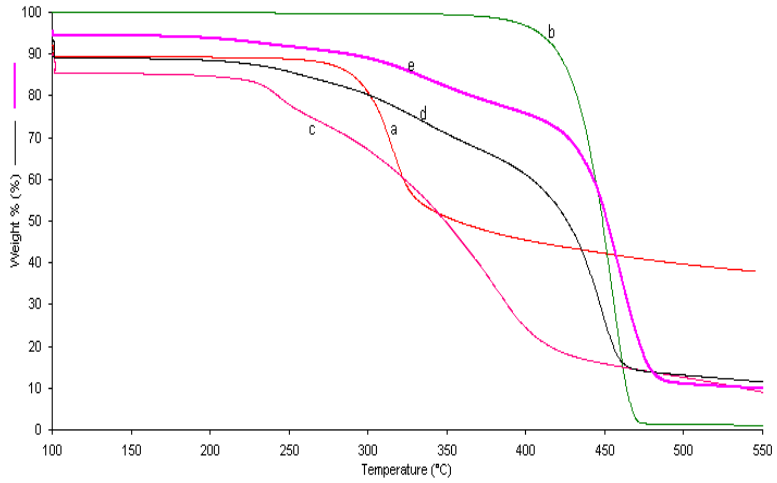

Figure 3. TGA thermograms of graft copolymers based on mPEG 5 kDa and chitosan/TMC

(A) PEG(5k)-*g*-TMC(400) copolymers.

(a) TMC 400 kDa, (b) PEG 5 kDa, (c) $PEG(5k)_{298}$-*g*-TMC(400), (d) $PEG(5k)_{641}$-*g*-TMC(400), (e) $PEG(5k)_{679}$-g-TMC(400).

(B) PEG(5k)-*g*-chitosan copolymers.

(a) Chitosan 400 kDa, (b) PEG 5 kDa, (c) $PEG(5k)_{243}$-*g*-chitosan(400), (d) $PEG(5k)_{386}$-*g*-chitosan(400), (e) $PEG(5k)_{515}$-*g*-chitosan(400).

3.3 Water Solubility of Copolymers

The primary aim of our present study is to improve the solubility of chitosan. As such, water solubility of the copolymers was evaluated under different pH conditions. Solutions of PEG-g-TMC copolymers remained transparent over the entire pH range irrespective of PEG MW even when the

graft density was as low as 10% and the concentration was as high as 50 mg/ml. The PEG moieties presented on the TMC chain increased the hydrophilicity of the copolymer, thus leading to improved solubility. In contrast, no clear solutions were observed with PEG grafted chitosan copolymers at pH 7, despite of high graft densities. This is due to the strong interaction between chitosan and PEG [5,6], as demonstrated by the significantly decreased T_m value in DSC experiments.

3.4 Biocompatibility and properties of the complexes

In addition to the solubility, biocompatibility is of particular importance when a polymer is to be used as a drug carrier. Generally, polycationic polymers are related to cytotoxicity as a consequence of their interaction with the negatively charged components on the cell membrane. Therefore, the cytotoxicity of these new synthesized copolymers was investigated, and the concentration of the copolymers resulting in 50% inhibition of cell growth, i.e. IC_{50} value, was calculated. Along with the increase of PEG 5 kDa substitution, the free amino groups on TMC 400 kDa chains decreased, which, together with the steric effect of PEG 5 kDa, led to considerably decreased cytotoxicity, as illustrated in Table 3.

Moreover, complex formation leads to further increase of $IC_{50.}$ This can probably be attributed to the electrostatic interaction between the copolymers and insulin, which decreased the charge density of the copolymers, as demonstrated by the decreased ξ –potentials (Table 3). Another possibility is that complex formation embeds part of the free amino groups, preventing them from direct contact with the cells. It was noticed that with PEG 5 kDa coupling, cytotoxicity of TMC 400 kDa could be decreased more than 30 fold. PEG(20k)-g-TMC(400) copolymers were prepared in the same manner to investigate the influence of PEG MW on the properties of the copolymer and corresponding insulin complexes. Despite the low substitution ratio,

cytotoxicity of the copolymer was decreased remarkably after PEG 20 kDa coupling, and further after complexation, which can probably be explained by the steric effect of the PEG 20 kDa molecules leading to subdued interaction with cell membrane. However, the ξ - potential of PEG $(20k)_{10}$-g-TMC(400) insulin complex decreased only marginally compared to that of TMC 400 kDa in 6 mM Tris buffer, 18.7±1.7 versus 20.9±1.4. A similar phenomenon was observed with PEI(25k)-g-$PEG(20k)_1$ compared to PEI 25 kDa [25].

Table 3. Properties of the PEG(5k)-g-TMC(400) copolymers and corresponding insulin complexes

Polymer	Substitution [b] (%)	Graft ratio[c] (%)	IC_{50}(μg/ml) (24 h)		Mass ratio[d]	Complex properties		
			Pure polymer	Complexes		Particle size (nm)	Zeta-potential (mV)	Association efficiency (%)
TMC 400 kDa	-	-	15	50	0.3:1	256.3±0.8	20.9±1.4	78.6±4.9
$PEG(5k)_{298}$-g-TMC(400)	38.9	75.4	40	100	0.7:1	171.7±1.9	11.2±0.9	81.3±1.1
$PEG(5k)_{640}$-g-TMC(400)	83.5	88.9	>500[a]	> 500[a]	1:1	181.8±2.1	2.3±0.3	87.0±6.3
$PEG(5k)_{680}$-g-TMC(400)	88.7	89.5	>500[a]	> 500[a]	1.5:1	245.6±2.9	1.7±1.0	96.2±2.1
$PEG(20k)_{10}$-g-TMC(400)	1.3	33.3	100	500	0.7:1	220.8±4.7	18.7±1.7	71.9 ±2.9
$PEG(20k)_{20}$-g-TMC(400)	2.6	50.0	>500[a]	> 500[a]	1:1	256.1±7.0	18.8±0.3	79.3 ±1.7

[a] The highest concentration investigated.

[b] Calculation based on the primary amino group content in TMC 400 kDa, 30.83%.

[c] Calculated as a weight ratio of PEG in the graft copolymer.

[d] Optimized polymer/insulin mass ratio for complex preparation.

PEG 5 kDa and PEG 20 kDa grafted TMC copolymer insulin complexes were also investigated to gain insight into the effect of copolymer composition. Based on the preliminary experimental procedure, soluble insulin complexes were prepared at optimal polymer/insulin mass ratios, as listed in Table 3. Particle size, ξ –potentials and the association efficiency (AE) of various

insulin complexes were also investigated. The particle size was in the range of 150-300 nm, and increased with graft ratio. No significant difference in particle size was observed for the two PEG(20k)-g-TMC(400) copolymer insulin complexes. All of the complexes investigated here were positively charged and ξ –potentials decreased with increasing graft density. This is consistent with the cytotoxicity results.

There have been reports that insulin binds to polymers via its negative charge, i.e. adhesion being facilitated by the interaction between the positively charged polymers and the negatively charged insulin. Based on this hypothesis, a decreased AE of PEGylated copolymers would be expected compared to non-modified polymers. Surprisingly, AE values increased with PEG 5 kDa graft ratio and extremely high association efficiency, that is, 96.22%, was achieved with $PEG(5k)_{679}$-g-TMC(400) copolymer. A similar result was found in PEG(2k)-g-chitosan DNA nanoparticles [26], and preferential partition of insulin into the PEG phase in PEG-dextran systems was also reported [27]. Previously, Prestwich et al. showed that insulin has a high affinity for PEG rich environement [28]. Furthermore, PEG chains have been shown to complex with protein and stabilize them [29,30]. Therefore it is reasonable to assume that a certain proportion of insulin was retained in the PEG moieties conjugated in the TMC matrix, resulting in a higher AE.

Taking all the above results into consideration, PEGylation with PEG 5 kDa is sufficient to increase the biocompatibility of TMC and the corresponding copolymers are promising insulin carriers.

4. Conclusions

PEGylated trimethyl chitosan 400 kDa copolymers with varying PEG molecular weight and graft ratios were successfully synthesized and demonstrated by FT-IR, ^{1}H NMR, ^{13}C NMR and GPC measurements. Decreased melting temperature of PEG in the copolymers indicated that the two blocks are

miscible and compatible. PEG-g-TMC(400) copolymers were completely water-soluble over the entire pH range, irrespective of PEG MW. Based on cytotoxicity results, the potential of PEG(5k)-g-TMC(400) and PEG(20k)-g-TMC(400) copolymers as insulin carriers was studied. The particle sizes were less than 300 nm and ξ-potential decreased with increasing graft density, which was consistent with the decreased toxicity. Insulin association efficiency was PEG graft density dependent, and the value could be as high as 96.22%. Based on the good solubility of the copolymers and the speciality of polyethylene glycol, we believe these copolymers could be used to enhance the therapeutic and biotechnological potentials of other macromolecules.

References

[1] Singla AK, Chawla M. Chitosan: some pharmaceutical and biological aspects-an update. J Pharm Pharmacol 2001; 53: 1047-1067.

[2] Sieval AB, Thanou M, Kotze AF, Verhoef JC, Brussee J, Junginger HE. Preparation and NMR characterization of highly substituted N-trimethyl chitosan chloride. Carbohydrate Polymers 1998; 36: 157-165.

[3] Le Dung P, Milas M, Rinando M, Desbrieres J. Water soluble derivatives obtained by controlled chemical modification of chitosans. Carbohydrate Polymers 1994; 24: 209-214.

[4] Muzzarelli RAA, Tanfani F and Emanuelli M. N-(carboxymethylidene) chitosans and N-(carboxymethyl) chitosans: novel chelating polyampholytes obtained from chitosan glyoxylate. Carbohydr Res 1982; 107:199-214.

[5] Saito H, Wu X, Harris J, Hoffman A. Graft copolymers of poly (ethylene glycol)(PEG) and chitosan. Macromol Rapid Commun 1997; 18: 547-550.

[6] Ohya Y, Cai R, Nishizawa H, Hara K and Ouchi T. Preparation of PEG-grafted chitosan nanoparticles as peptide drug carriers. STP Pharma Science 2000; 10: 77-82.

[7] Mao S, Shuai X, Unger, F, Simon M, Bi D, Kissel T. The depolymerization of chitosan: Effects on physicochemical and biological properties. Int J Pharm 2004; 281: 45-54.

[8] Thanou MM, Kotze AF, Scharringhausen T, Lussen HL, de Boer AG, Verhoef JC, Junginger, HE. Effect of degree of quaterization of N-trimethyl chitosan chloride for

enhanced transport of hydrophilic compounds across intestinal Caco-2 cell monolayers. J Controlled Rel 2000; 64: 15-25.

[9] Thanou M, Florea BI, Geldof M, Junginger HE, Borchard G. Quaternized chitosan oligomers as novel gene delivery vectors in epithelial cell lines. Biomaterials 2002; 23: 153-159.

[10] Kotzé AF, Thanou MM, Lueben HL, De Boer AG, Verhoef JC, Junginger HE. Enhancement of paracellular drug transport with highly quaternized *N*-trimethyl chitosan chloride in neutral environments: In vitro evaluation in intestinal epithelial cells (Caco-2). J Pharm Sci 1999; 88: 253-257.

[11] Ogris M, Brunner S, Schüller S, Kircheis R, Wagner E. PEGylated DNA/transferring-PEI complexes: reduced interaction with blood components, extended circulation in blood and potential for systemic gene delivery. Gene Therapy 1999; 6: 595-605.

[12] Veronese FM. Peptide and protein PEGylation: a review of problems and solutions. Biomaterials 2001; 22: 405-417.

[13] Shuai X, Jedlinski Z, Luo Q, Farhod N. Synthesis of novel block copolymers of poly (3-hydroxybutyric acid) with poly (ethylene glycol) through anionic polymerisation. Chinese J Polym Sci 2000; 18: 19-23.

[14] Hamman JH, Schultz CM, Kotze AF. N-trimethyl chitosan chloride: optimum degree of quaternization for drug absorption enhancement across epithelial cells. Drug Dev Ind Pharm 2003; 29: 161-172.

[15] Petersen H, Martin AL, Stolnik S, Roberts CJ, Davies MC, Kissel T. The macrostopper route: A new synthesis concept leading exclusively to diblock copolymers with enhanced DNA condensation potential. Macromolecules 2002; 35: 9854-9856.

[16] Fischer D, Bieber T, Li Y, Elsaesser H, Kissel T. A novel non-viral vector for DNA delivery based on low molecular weight, branched polyethylenimine. Effect of molecular weight on transfection efficiency and cytotoxicity. Pharm Res 1999; 16: 1273-1279.

[17] Hermanson GT. Bioconjugate Techniques. Academic press, 1996.

[18] Read ML, Etrych T, Ulbrich K, Seymour LW. Characterisation of the binding interaction between poly (L-lysine) and DNA using the fluorescamine assay in the preparation of non-viral gene delivery vectors. FEBS Lett 1999; 461: 96-100.

[19] Shuai X, Merdan T, Unger F, Wittmar M, Kissel T. Novel Biodegradable ternary copolymers hy-PEI-g-PCL-b-PEG: Synthesis, characterization and potential as

efficient nonviral gene delivery vectors. Macromolecules 2003; 36: 5751-5759.

[20] He Y, Asakawa, N, Inoue Y. Biodegradable blends of high molecular weight poly (ethylene oxide) with poly (3-hydroxypropionic acid) and poly (3-hydroxybutyric acid): a misbility study by DSC, DMTA and NMR spectroscopy. Polym Int 2000; 49: 609-617.

[21] Zhang L, Goh SH, Lee SY. Miscibility and crystallization behaviour of poly (L-lactide)/poly (p-vinylphenol)blends. Polymer 1998; 39: 4841-4847.

[22] Wei M, Shuai X, Tonelli AE. Melting and crystallization behaviors of biodegradable polymers enzymatically coalesced from their cyclodextrin inclusion complexes. Biomacromolecules 2003; 4: 783-792.

[23] Shuai X, Porbeni FE, Wei M, Bullions T, Tonelli AE. Formation of inclusion complexes of poly (3-hydroxybutyrate)s with cyclodextrins. 1. Immobilization of atactic poly(*R*, *S*-3-hydroxybutyrate) and miscibility enhancement between poly(*R*, *S*-3-hydroxybutyrate) and poly (ε-caprolactone). Macromolecules 2002; 35: 3126-3133.

[24] Wei M, Tonelli AE. Compatiblization of polymers via coalescence from their common cyclodextrin inclusion compounds. Macromolecules 2001; 34: 4061-4065.

[25] Petersen H, Fechner PM, Martin AL, Kunath K, Stolnik S, Roberts CJ, Fischer D, Davies MC, Kissel T. Polyethylenimine-graft-poly (ethylene glycol) copolymers: influence of copolymer block structure on DNA complexation and biological activities as gene delivery system. Bioconjug Chem 2002; 13: 845-854.

[26] Mao H, Roy K, Troung-Le VL, Janes KA, Lin KY, Wang Y, August JT, Leong KW. Chitosan-DNA nanoparticles as gene carriers: synthesis, characterization and transfection efficiency. J Controlled Rel 2001; 70: 399-421.

[27] Moriyama K, Yui N. Regulated insulin release from biodegradable dextran hydrogels containing poly (ethylene glycol). J Controlled Rel 1996; 42: 237-248.

[28] Prestwich G, Luo Y, Kirker K. Crosslinked hyaluronic acid hydrogel films: new biomaterials for drug delivery. J Controlled Rel 2000; 69:169-184.

[29] Iwanaga K, Ono S, Narioka K, Morimoto K, Masawo K, Yamashita S, Nange M, Oku N. Oral delivery of insulin by using surface coating liposomes: Improvement of stability of insulin in GI tract. Int J Pharm 1997; 157: 73-80.

[30] Yeh M. The stability of insulin in biodegradable microspheres based on blends of lactide polymers and poly (ethylene glycol). J Microencapsul 2000; 17: 743-756.

Chapter 4

In vitro cytotoxicity of biodegradable poly (ethylene glycol)-grafted trimethyl chitosan copolymers

Manuscript in preparation

Abstract

The purpose of this study was to evaluate the in vitro cytotoxicity of trimethyl chitosan (TMC) and PEGylated TMC copolymers. Using the methyl tetrazolium (MTT) assay, the effect of TMC molecular weight, PEGylation ratio, PEG and TMC molecular weight in the copolymers, and complexation with insulin on the cytotoxicity of TMC was examined, and IC_{50} values were calculated with L929 cell line. All polymers exhibited a time- and dose-dependent cytotoxic response that increased with molecular weight. PEGylation can decrease the cytotoxicity of TMC, to a great extent in the case of low molecular weight TMCs. According to the cytotoxicity results, PEG 5 kDa is superior for PEGylation when compared to PEG 550 Da at similar graft ratios. Complexation with insulin further increased cell viability. In addition, LDH (Lactate dehydrogenase) assays were performed to quantify the membrane-damaging effects of the copolymers. These results indicated that after 3 h of incubation with 1 mg/ml copolymer solutions, less than 6% LDH release were measured for $PEG(5k)_{40}$-g-TMC(100), $PEG(5k)_{19}$-g-TMC(50) and $PEG(550)_{228}$-g-TMC(100) copolymers, compared to approximately 50% for TMC 100 kDa, which is in line with the conclusion drawn from MTT assay. Moreover, the safety of the copolymers was corroborated by observing the morphological change of the cells with inverted phase contrast microscopy.

1. Introduction

Chitosan is a non-toxic and biocompatible cationic polysaccharide produced by partial deacetylation of chitin derived from naturally occurring crustacean shells. Due to its specific structure and properties, chitosan has found a number of applications in drug delivery including as an absorption enhancer for hydrophilic macromolecular drugs and as a gene delivery system [1]. The applications of chitosan in the biomedical field are limited, however, by its poor solubility in physiological media. Chitosan is only soluble in aqueous acidic

solutions below pH 6.5, at which the primary amino groups of chitosan are protonated. To overcome the poor solubility displayed by chitosan in physiologically-relevant environments, N-trimethyl chitosan chloride (TMC), a partially quaternized chitosan derivative, has been synthesized and proven to be soluble over a wide pH range (pH 1 to 9) up to 10% (w/v) concentration, even at very low degree of quaternization [2]. Moreover, TMC is capable of opening tight junctions of intestinal epithelial cells at physiological pH values, and highly quaternized TMC has been proven to be a potent absorption enhancer, especially at neutral pH [3], whereas chitosan itself is insoluble and therefore ineffective. Moreover, TMC seems to be an efficient gene delivery system [4].

However, the biocompatibility of TMC needs to be taken into consideration, and the absence of cytotoxicity is of vital importance. Whilst Kotze et al. suggested that TMC was non-toxic using a number of techniques including trypan blue exclusion technique [2,3], nuclear staining in Caco-2 cell monolayers and ciliary beat frequency assay [5], the reversibility of transepithelial electrical resistance (TEER) of 0.5% TMC solutions with different degrees of quaternization could not be demonstrated at pH 6.2 and 7.4 in Caco-2 cells [3]. TMC, like most cationic macromolecules such as protamine and polylysine, probably interacts with anionic components (sialic acid) of the glycoproteins on the surface of epithelial cells, causing cytotoxic effects. Changes in cell morphology have already been observed with 1.0 μg/ml polylysine [6].

Recently, a number of different molecular weight (MW) TMCs were synthesized in our laboratory. Unfortunately, we found that TMC was cytotoxic in L929 mouse fibroblast cells by MTT (methyl tetrazolium) assay (data shown below), a cell line recommended by USP 26 and several other pharmacopoeias as a standard method for cytotoxicity testing [7].

From a safety point of view, it must be guaranteed that polymers used as drug carriers are biocompatible and non-toxic. The cytotoxicity of various MW

chitosans has been systematically investigated in our lab, and they were proven to be non-toxic [8]. However, no such work has been performed with TMC and its derivatives so far, despite their promising applications in the field of drug delivery. In general, polycations are considered to be cytotoxic [9], with the mechanism of cytotoxicity being mediated by interactions of polycations with cell membranes [10]. As TMCs exhibit a high positive charge density, such an investigation is essential. To our knowledge, no study has systematically explored the influence of TMC MW on the physico-chemical and biological properties. Additionally, in order to further improve the biocompatibility of TMC, PEG-g-TMC copolymers were synthesized [11]. Conjugation of PEG (polyethylene glycol) to proteins is well known to enhance the in vivo half-life of the encapsulated drugs, assist penetration into the cell membrane, alter pharmacological properties and increase biocompatibility [12,13]. Since these polymers are positively charged, self-assembled insulin complexes were readily obtained at optimal conditions. The influence of complexation on cytotoxicity was further investigated in order to elucidate the correlation between polymer MW, polymer structure, complexation and cytotoxicity, providing experimental support for the development of drug carriers from such materials.

2. Materials and methods

2.1 Materials

Chitosan (~ 400 kDa) was purchased from Fluka (Steinheim, Germany) with a degree of deacetylation (DD) value of 84.7% and depolymerized according to the method described previously [8] to obtain chitosans of different molecular weights. Human recombinant insulin powder (26.2 IU/mg) was a gift from Aventis Pharma AG (Germany). Dulbecco's modified Eagle's medium (DMEM) was obtained from PAA (Coelbe, Germany). MTT (3-(4, 5-dimethyl-thiazol-2-yl)-2, 5-diphenyl tetrazolium bromide) was purchased from Sigma (Deisenhofen, Germany). Lactate dehydrogenase assay kit (Product

No. LK 100) was obtained from Sigma (Taufkirchen, Germany). Dimethylsulfoxide (DMSO) analytical grade was from Merck (Darmstadt, Germany).

2.2 Synthesis of TMC with different MW

Different MW TMCs were prepared according to a two-step method described previously using depolymerized chitosans of appropriate MW as starting materials and were subsequently characterized by ^{1}H NMR [14]. Throughout, we used the abbreviation TMC 400 kDa to denote the polymer prepared from chitosan 400 kDa, and the same for the other polymers. Since the degree of quaternization of TMC plays an important role in opening the tight junctions and a higher degree of substitution had improved permeation enhancement [4,15], TMCs with a 40% degree of substitution were prepared.

2.3 Copolymer preparation and characterization

PEGylated TMC copolymers were synthesized as described elsewhere in detail [11]. The products were purified by ultrafiltration and lyophilized. The graft ratio (wt%) of PEG was calculated from integral values of the characteristic peaks of PEG block at ~3.35 ppm ($-OCH_3$) and TMC block at ~3.0 ppm ($-N(CH_3)_2$) and ~3.3 ppm ($-N^+(CH_3)_3$) obtained in the ^{1}H NMR spectra, using the known molecular weight of mPEG.

The following nomenclature for the copolymers was adopted: $PEG(X)_n$-g-TMC(Y), where X denotes the MW of PEG in Da, Y denotes the MW of TMC in kDa, and the subscript *n* represents the average number of PEG chains per TMC macromolecule of Y kDa.

2.4 Preparation and characterization of insulin complexes

The complexes were prepared via self-aggregation using the electrostatic interaction between polymers and insulin. The process parameters were

optimized as described in chapter 5. Briefly, an appropriate quantity of copolymer and insulin (1 mg/ml) were dissolved in 0.1 N Tris buffer pH 7.4. Complexes were prepared by mixing equal volumes of insulin and polymer solution under gentle magnetic stirring, and incubating for a further 20 min at room temperature. The complexes were characterized by dynamic light scattering and laser doppler anemometry (LDA) measurements. Complex size measurements were carried out with a Zetasizer 3000 HS from Malvern Instruments, Herrenberg, Germany (10 mW HeNe laser, 633 nm). Scattering light was detected at 90^{o} angle through a 400 micron pin hole at a temperature of 25℃. For data analysis, the viscosity (0.88 mPa•s) and the refractive index (1.33) of distilled water at 25℃ were used. Measurements were analysed using the CONTIN algorithm. The zeta potential measurements of the complexes were carried out in the standard capillary electrophoresis cell of the Zetasizer 3000 HS from Malvern Instruments at 25℃ in 6 mM Tris buffer pH 7.4. Values given are mean ± SD (n =10).

2.5 MTT assay

A mouse connective tissue fibroblast cell line, L929, was selected to evaluate cytotoxicity as a direct contact test, as recommended by USP 26. The experiment was carried out according to the method described previously [7,16]. The relative cell viability compared to control cells containing cell culture medium without polymer was calculated by $[A]_{test}$ / $[A]_{control}$. Polyethylene 600 (1 mg/ml) and polyethylenimine (10 mg/ml) were used as positive and negative controls of the method, respectively.

2.6 LDH assay

50 000 L929 cells/well were seeded in 12-well cell culture plates. After 24 h incubation, cells were washed with PBS (phosphate buffered solution) and

were then incubated with selected polymers (1 mg/ml) in 2 ml PBS. 100 μl /well samples were collected at predetermined points. The LDH content in these samples was assayed utilizing a commercial kit according to the manufacturer's protocol, which spectrophotometrically determined the amount of reduced nicotinamide adenine dinucleotide (NAD) at 492 nm in the presence of lactate and LDH. Control experiments were performed with 0.1% (w/v) Triton X-100 and set as 100% cytotoxicity. LDH release was calculated by the following equation:

$$LDH(\%) = \frac{[A]_{sample} - [A]_{medium}}{[A]_{100\%} - [A]_{medium}} \times 100$$

where $[A]_{sample}$, $[A]_{medium}$, $[A]_{100\%}$ denote the absorbance of the sample, medium control and Triton X-100 control, respectively. All experiments were run in triplicate.

2.7 Calculations and Statistics

Results are depicted as mean ± SD from at least three separate measurements. Significance between the mean values was calculated using ANOVA one-way analysis (Origin 7.0 SRO, Northampton, MA, USA). Probability values $P < 0.05$ were considered significant.

3. Results

3.1 Characterization of TMCs

The compositions of TMCs after undergoing a two-step synthesis are listed in Table 1. No significant difference in the degree of quaternization was observed with different MW TMCs ($P > 0.05$).

Characteristics of the intermediates of TMC 50 kDa, TMC 25 kDa, and TMC 5 kDa after undergoing a one-step reaction are described in Table 2. Comparing Table 1 and 2, it is evident that the degree of substitution of trimethylated amino groups was only about 20% after the one step reaction. However, the substitution degrees of dimethylated amino group were high.

Table 1. Degrees of substitution of different trimethyl chitosans after second step reaction

%*	TMC 400 kDa	TMC100 kDa	TMC 50 kDa	TMC 25 kDa	TMC 5 kDa
$N^+(CH_3)_3$	42.4	39.2	39.6	40.4	38.8
$N(CH_3)_2$	12.4	13.0	12.7	7.2	0.6
3-OCH_3	6.1	5.4	7.8	12.0	12.0
6-OCH_3	8.0	6.7	11.9	14.7	14.8
$NHCOCH_3$	10.3	10.7	7.4	8.7	5.9
NH_2 free	30.8	37.0	40.3	43.6	54.7

* Calculation based on ^{1}H NMR analysis.

Table 2. Characteristics of trimethyl chitosan intermediates after first step reaction

%*	TMC 50 kDa	TMC 25 kDa	TMC 5 kDa
$N^+(CH_3)_3$	17.2	18.2	20.0
$N(CH_3)_2$	35.8	32.8	21.5
$NHCOCH_3$	12.1	16.8	10.9
NH_2 free	34.9	43.6	47.5

* Calculation based on ^{1}H NMR analysis.

Therefore, the two-step synthesis was essential to the preparation of TMC with a higher $N^+(CH_3)_3$ substitution degree. Additionally, when the molecular weight of chitosan was < 50 kDa, it was easier to convert the intermediate $N(CH_3)_2$ to the $N^+(CH_3)_3$ form in a second step, as indicated by the significantly decreased degree of $N(CH_3)_2$ substitution. However, it also resulted in O-methylation in the 3- and 6-position, and the degree of 3-OCH_3 and 6-OCH_3 substitutions increased considerably with TMC 25 kDa and TMC 5 kDa, which can be explained by the decreased steric hindrance of the low molecular weight polymers. On the other hand, the degree of deacetylation of chitosan decreased slightly due to the sodium hydroxide used in the process, and chitosans with

molecular weight < 50 kDa were more sensitive compared with the larger molecular weight polymers.

FT-infrared spectroscopy was used to investigate the change in structure after substitution, as depicted in Figure 1.

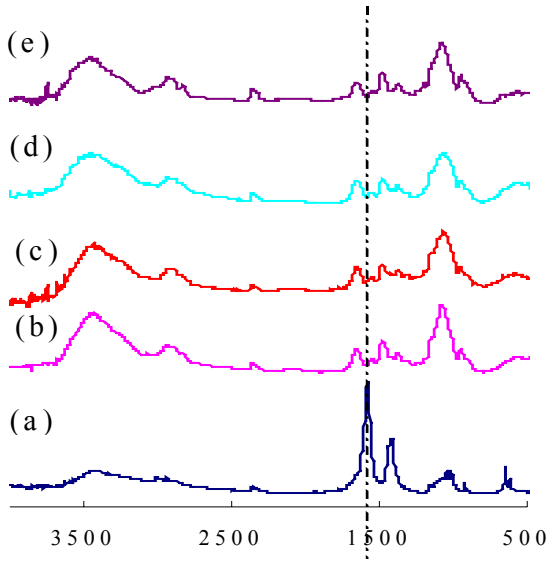

Figure 1. IR spectra comparing of chitosan with trimethyl chitosan. (a) Chitosan 400 kDa, (b) TMC 400 kDa, (c) TMC 100 kDa, (d) TMC 50 kDa, (e) TMC 5 kDa.

Pure chitosan 400 kDa shows a distinct amide Ⅱ band at 1580 cm^{-1}(s, δ_{NH}) and amide linkage at 1406 cm^{-1}(υ_{C-N}) [17], the area between 1000 and 1150 cm^{-1} was saturated, maybe due to the presence of three distinct modes of C-O-C, C-OH, and C-C ring vibrations. N-H stretching and O-H stretching vibrations can be characterized by the broad signals in the region of 3200-3500 cm^{-1}. After preparation of TMC, the absorption at 1580 cm^{-1}(δ_{NH}) decreased significantly. Normally there should be no absorption in this area for pure tertiary amine. However, the TMC prepared with this method is a mixture of primary amine, secondary amine and trimethyl amine, hence a small signal remains at this wavelength. Comparing the spectra of TMCs with that of chitosan, the signals at 1453 cm^{-1}(δ^{as}_{CH3}) and 1337 cm^{-1}(δ^{s}_{CH3}) became

stronger due to the formation of $N^{+}(CH_{3)3}$ group. This is in good agreement with the structure of TMC.

3.2 Effect of TMC MW on cytotoxicity

MTT assays were performed to test the effects of polymer structure on the metabolic activity of cells. All the polymers showed a dose and MW dependent effect on cytotoxicity. Cell viabilities of different MW TMCs versus concentration were investigated, and the IC_{50} values, which represent concentration of the copolymers resulting in 50% inhibition of cell growth, were calculated. The results are summarized in Table 3.

Table 3. Properties and IC_{50} values of TMC and its derivatives (Mean±SD). Cell viability was quantified by MTT assay (n = 7).

Polymer (kDa)	Degree of substitution (%)[a]	TMC content [%(w/w)]	Theoretical MW (g/mol)	Dalton/ charge[b]	IC_{50} of pure polymers (μg /ml)		Complexes Particle size (nm)	Zeta potential (mv)
					3 h	24 h		
TMC 400	-	100	400000	189.4	30	15	256.6±0.8	19.6±2.3
TMC 100	-	100	100000	189.4	70	22	273.3±4.6	22.7±2.5
TMC 50	-	100	50000	189.4	90	37	236.6±1.3	21.7±1.9
TMC 25	-	100	25000	189.4	270	125		
TMC 5	-	100	5000	189.4	>1000	>1000		
$PEG(5k)_{298}$-g-TMC(400)	12.0	22.7±1.7	1890000	1042	220	40		
$PEG(5k)_{640}$-g-TMC(400)	25.7	11.1±2.1	3600000	2446	370	>500		
$PEG(5k)_{680}$-g-TMC(400)	27.4	10.6±2.5	3800000	2655	380	>500		
$PEG(5k)_{40}$-g-TMC(100)	6.44	32.8±1.0	300000	640	>500	>500		
$PEG(5k)_{19}$-g-TMC(50)	6.13	34.2±0.9	145000	590	>500	>500		
$PEG(550)_{228}$-g-TMC(100)	36.7	41.5±1.5	225000	750	>500	270		
$PEG(550)_{116}$-g-TMC(50)	37.4	40.8±3.4	120000	930	>500	460		

[a] Calculated by ^{1}H NMR measurement.

[b] Denoted as Dalton per charge.

With similar charge ratios, the cytotoxicity of TMCs increased with

increasing MW. TMC 400 kDa was especially toxic with an IC_{50} of 15 μg/ml. However, TMC 5 kDa was shown to be completely nontoxic with an IC_{50} > 1 mg/ml. An exponential relationship between TMC MW and IC_{50} after 3 h incubation was established, as presented in Figure 2, which can be used to predict the cytotoxicy of different MW TMC.

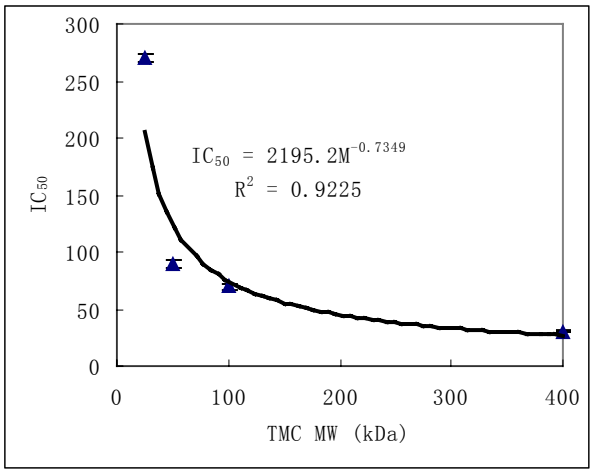

Figure 2. Relationship between TMC MW and IC_{50} values.

3.3 Cytotoxicity of PEG(5k)-g-TMC copolymers

Taking the extremely toxic TMC 400 kDa as a model, the effect of PEGylation on cytotoxicity was assessed with MTT assay. The theoretical molecular weights and compositions were calculated from the degree of substitution based on ^1H NMR spectra and listed in Table 3. Cell viabilities of the copolymers are also shown in Figure 3.

Compared to the unmodified TMC, PEGylation decreased cytotoxicity significantly (P > 0.05) despite of the increased MW of the copolymers. The cytotoxicity decreased with an increase in PEG substitution degree. A linear correlation between substitution degree and IC_{50} value after 3 h incubation was found (Figure 3C). When the substitution degree reached 25%, the resulting decrease in toxicity slowed. Moreover, it was noted that for the copolymers with a substitution degree above 25%, the cell viabilities at 24 h were even higher than at 3 h, but no statistical difference (P > 0.05).

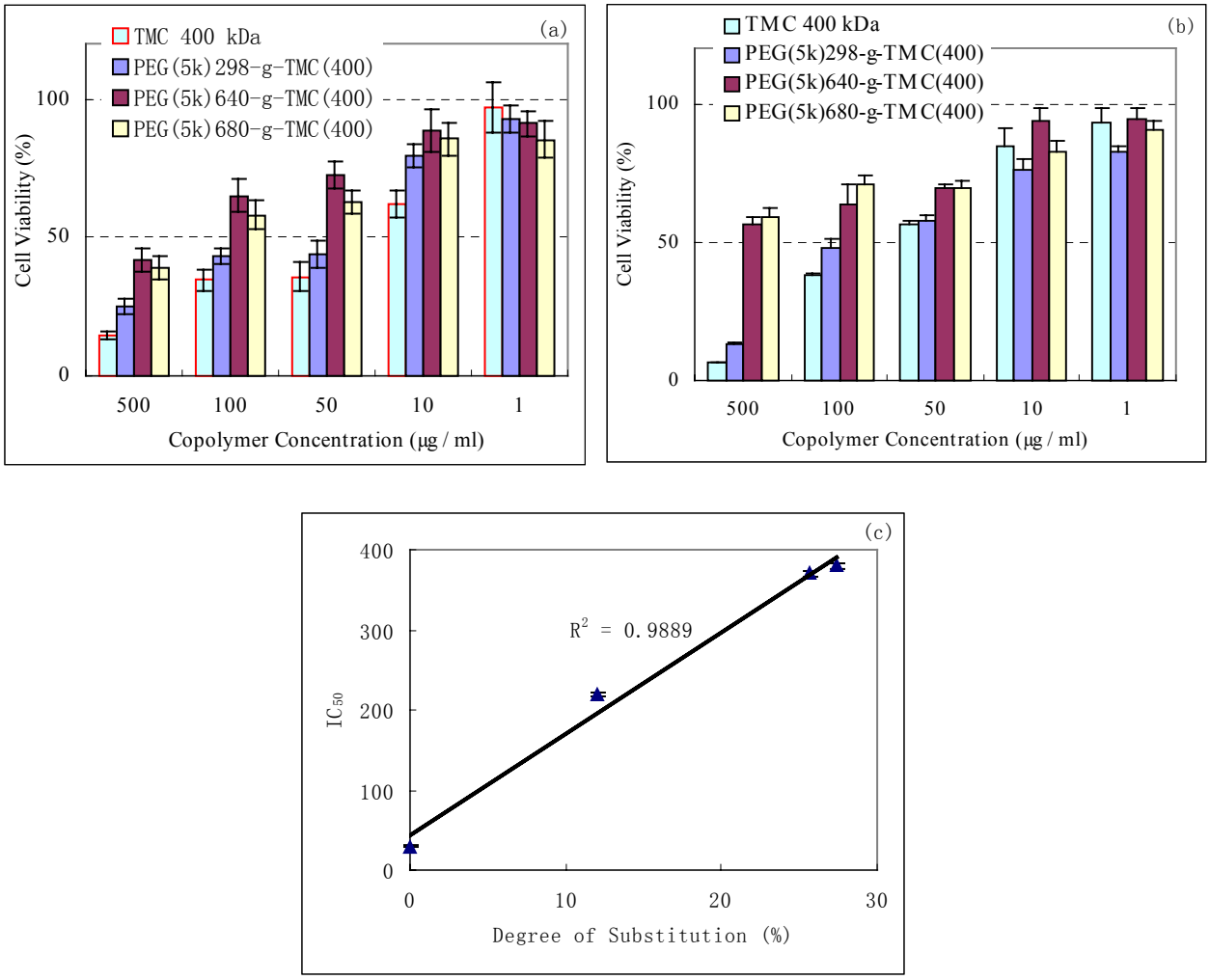

Figure 3. Cytotoxicity of PEG(5k)-g-TMC(400) copolymers measured by MTT assay with L929 cells. Each point represents the mean ± SD of seven experiments.

(a) 3 h incubation.

(b) 24 h incubation.

(c) Correlation between degree of substitution of TMC and IC_{50} values after 3 h incubation with the L929 cells.

3.4 Effect of TMC MW in PEG(5k)-g-TMC copolymers

As demonstrated, cytotoxicity of TMC was MW dependent. However, whether PEGylation has the same influence with different MW TMCs remains unclear. Therefore, PEG(5k)-g-TMC copolymers were prepared with similar graft ratio but different TMC MW (TMC 400 kDa, 100 kDa and 50 kDa, respectively), and the cytotoxicity was evaluated. Results are shown in Figure 4.

Cytotoxic dependency on TMC MW was more obvious in the copolymers. The cytotoxicity of TMC 100 kDa and TMC 50 kDa was decreased more than 10 fold after PEGylation with a substitution degree of approximately 6%, with more than 80% of the cells still viable after 24 h incubation with a 500 μg/ml polymer solution, which was considerably higher than the concentration applied in practice. In contrast, PEG(5k)$_{298}$-g-TMC(400) was more toxic compared to PEG(5k)$_{40}$-g-TMC(100) and PEG(5k)$_{19}$-g-TMC(50) copolymers, despite its higher substitution degree (12.0% versus 6%) and lower TMC content. Additionally, for the copolymers PEG(5k)$_{40}$-g-TMC(100) and PEG(5k)$_{19}$-g-TMC(50), no apparent time and dose dependent cytotoxicity was observed, implying that they were non-toxic.

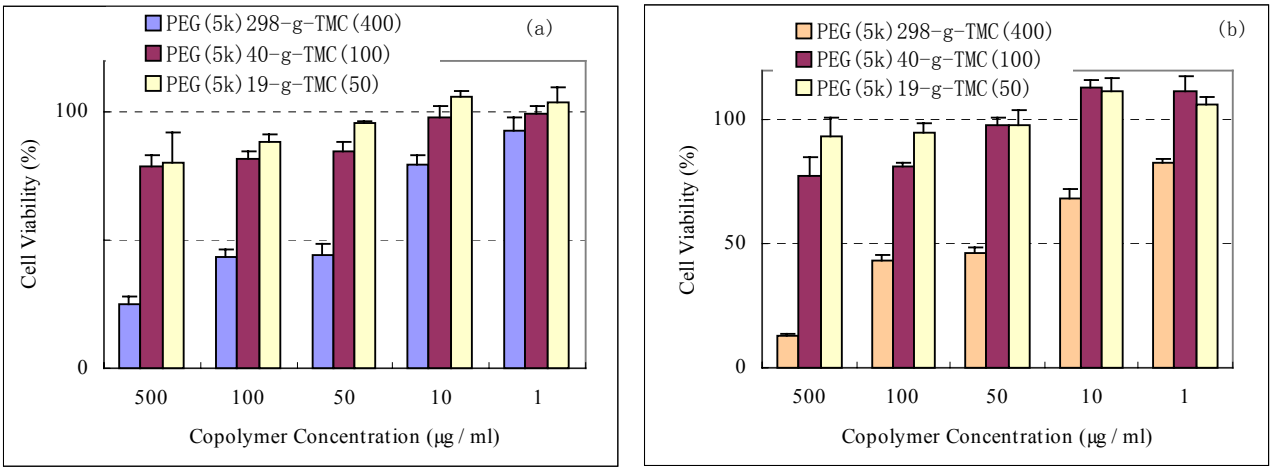

Figure 4. Effect of TMC MW on the cytotoxicity of PEG(5k)-g-TMC copolymers measured by MTT assay after (a) 3 h and (b) 24 h incubation with L929 cells. Each point represents the mean±SD of seven experiments.

3.5 Effect of PEG MW in the copolymers

It is believed that PEG MW in the copolymers will influence the cytotoxicity to some extent. Therefore, taking TMC100 kDa as an example, PEG(5k)$_{40}$-g-TMC(100) and PEG(550)$_{228}$-g-TMC(100) copolymers, which have similar graft ratios, were synthesized and the cell viabilities were investigated with MTT assay. Results are shown in Figure 5.

After 3 h of incubation, no significant difference in cell viability was observed between the two copolymers according to two sample paired t-test ($P > 0.05$). However, the difference was significant in the concentration range of 10-500 μg/ml after 24 h of incubation ($P < 0.05$). Higher cell viability, especially at concentrations of 500 μg/ml, was observed for PEG(5k)$_{40}$-g-TMC(100) compared to that of PEG(550)$_{228}$-g-TMC(100), despite the higher substitution degree of PEG(550)$_{228}$-g-TMC(100) (36.7% versus 6.4%).

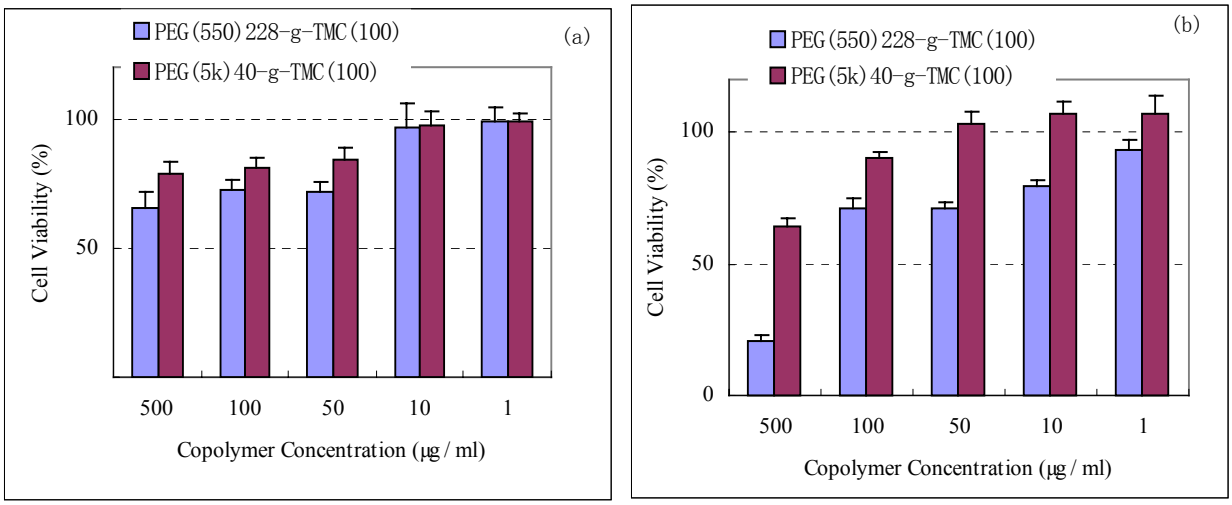

Figure 5. Effect of PEG MW on the cytotoxicity of PEG-g-TMC copolymers measured by MTT assay after (a) 3 h and (b) 24 h incubation with L929 cells. Each point represents the mean ± SD of seven experiments.

3.6 Effect of complexation with insulin

Based on the assumption that complexation may decrease the cytotoxicity of the polymers, the relatively toxic polymers TMC 400 kDa, 100 kDa, 50 kDa were used as examples. Polymer concentration was kept constant at 0.1 mg/ml. Complexes were prepared at optimized polymer/insulin mass ratio 0.3:1. All of the complexes are comparable in size and carry a positive charge (Table 3). Effects of complexation on cell viability are shown in Figure 6. After 3 h of incubation, the effect of complexation was only apparent with TMC 400 kDa. No significant differences were found with TMC 100 kDa and 50 kDa ($P >$

0.05). However, after 24 h incubation cell viabilities increased approximately two fold with the complexes for all TMCs investigated.

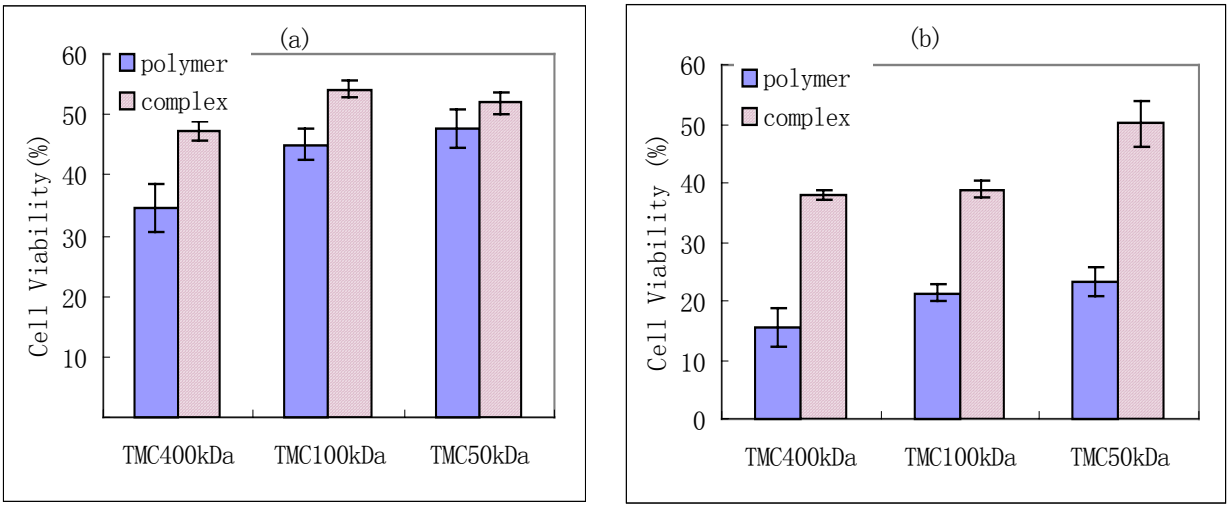

Figure 6. Effect of complexation with insulin on the cytotoxicity of TMC (100 μg /ml) measured by MTT assay after (a) 3 h and (b) 24 h incubation with L929 cells. Each point represents the mean ± SD of seven experiments. The complexes were prepared at polymer/insulin mass ratio 0.3:1.

3.7 LDH assay

Lactate dehydrogenase (LDH) is a stable cytosolic enzyme present in the cytosol that is released upon cell lysis. This assay permits the investigation of chemicals that may induce alternations in cell integrity. It was performed to measure the membrane-damaging effects of the copolymers via the quantity of LDH in the culture media at different time points.

Based on MTT assay, PEG(5k)$_{40}$-g-TMC(100), PEG(5k)$_{19}$-g-TMC(50), and PEG(550)$_{228}$-g-TMC(100) copolymers were parctically nontoxic, with IC_{50} > 500 μg /ml after 24 h of incubation. In order to elucidate any membrane-damaging effect caused by the copolymers, their influence on LDH release was investigated using TMC 100 kDa as a positive control, as shown in Figure 7. After 3 h of incubation, the LDH released was less than 6% for the three copolymers investigated, compared to 50.5±3.1% for TMC100 kDa,

which is in agreement with the results of the MTT assay.

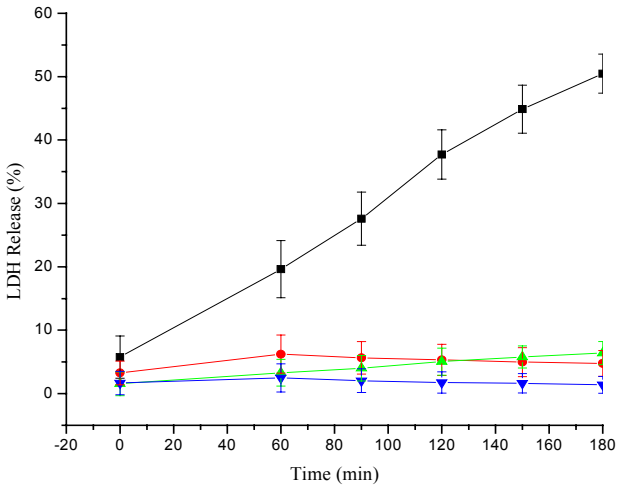

Figure 7. Cytotoxicity of the TMC and its derivatives by LDH assay. Each point represents the mean ± SD of three experiments. (■)TMC 100 kDa, (●) PEG(5k)$_{40}$-g-TMC(100), (▲)PEG(550)$_{228}$-g-TMC(100), (▼)PEG(5k)$_{19}$-g-TMC(50).

3.8 Microscopic observations

After performing the LDH assay, changes in cell morphology were observed using a Nikon inverse phase contrast microscope (Nikon TMS, Nikon, Japan) equipped with an objective (Plan 10/0.30Dl/Ph1, Nikon, Japan) of 100× magnification. Figure 8 shows a selection of phase contrast microscopy images obtained after 3 h of incubation with 1 mg/ml polymer solutions, and compared with medium control (PBS solution). In general, L929 mouse fibroblasts are large, spindle-shaped, adherent cells that grow as a confluent monolayer (Figure 8a). Complete cell death was observed using 0.1% Triton X-100 in PBS as a positive control (Figure 8b). The cells were grainy and lacked normal cytoplasma space, the open area between cells indicated cell lysis had occurred. In contrast, the fibroblast L929 cells incubated with copolymers PEG(5k)$_{40}$-g-TMC(100), PEG(5k)$_{19}$-g-TMC(50), and PEG(550)$_{228}$-g-TMC(100) maintained a polygonal shape with stretched filapodia (Figure 8d, 8e, 8f), no

cell debris, no detachment from dish bottom was observed, which was comparable to that of the medium control. As a contrast, the boundary of the cells became blurry after incubation with TMC 100 kDa and spindle shape was lost (Figure 8c). These morphological observations were consistent with the results obtained from both the MTT and LDH assays.

4. Discussion

In vitro cytotoxicity of TMC and PEGylated TMC copolymers were studied with the MTT and LDH assay in the current work. All the polymers exhibited a time- and dose-dependent cytotoxic response that increased with MW. PEGylation decreased the cytotoxicity and was substitution degree dependent. Complexation with insulin decreased the cytotoxicity after 24 h incubation.

Using the ninhydrin complexation reaction, Sabnis et al. found that the reactivity of chitosan was inversely proportional to its MW [18]. However, in our study, degree of quaternization of different MW TMC was similar, implying that the activity of primary amino groups was chitosan MW independent. Our result is consistent with Flory' s theory, which suggests the intrinsic activity of all functional groups on a polymer remains the same [19].

Generally, the determination of cell viability is an assay to evaluate the in vitro cytotoxicity of biomaterials. The predicative value of in vitro cytotoxicity tests is based on the concept that toxic chemicals affect the basic functions of cells. Such functions are common to all cells, and hence the toxicity can be measured by assessing cellular damage. MTT and LDH assays are two methods commonly used for this purpose. Normally an early indication of cellular damage is a reduction in metabolic activity and this is the principle of MTT assay [16]. It utilizes the yellow tetrazolium salt [3-(4, 5-Dimethylthiazol-2-yl)-2, 5-diphenyltetrazolium-bromide], which is metabolized by mitochondrial succinic dehydrogenase activity of proliferating

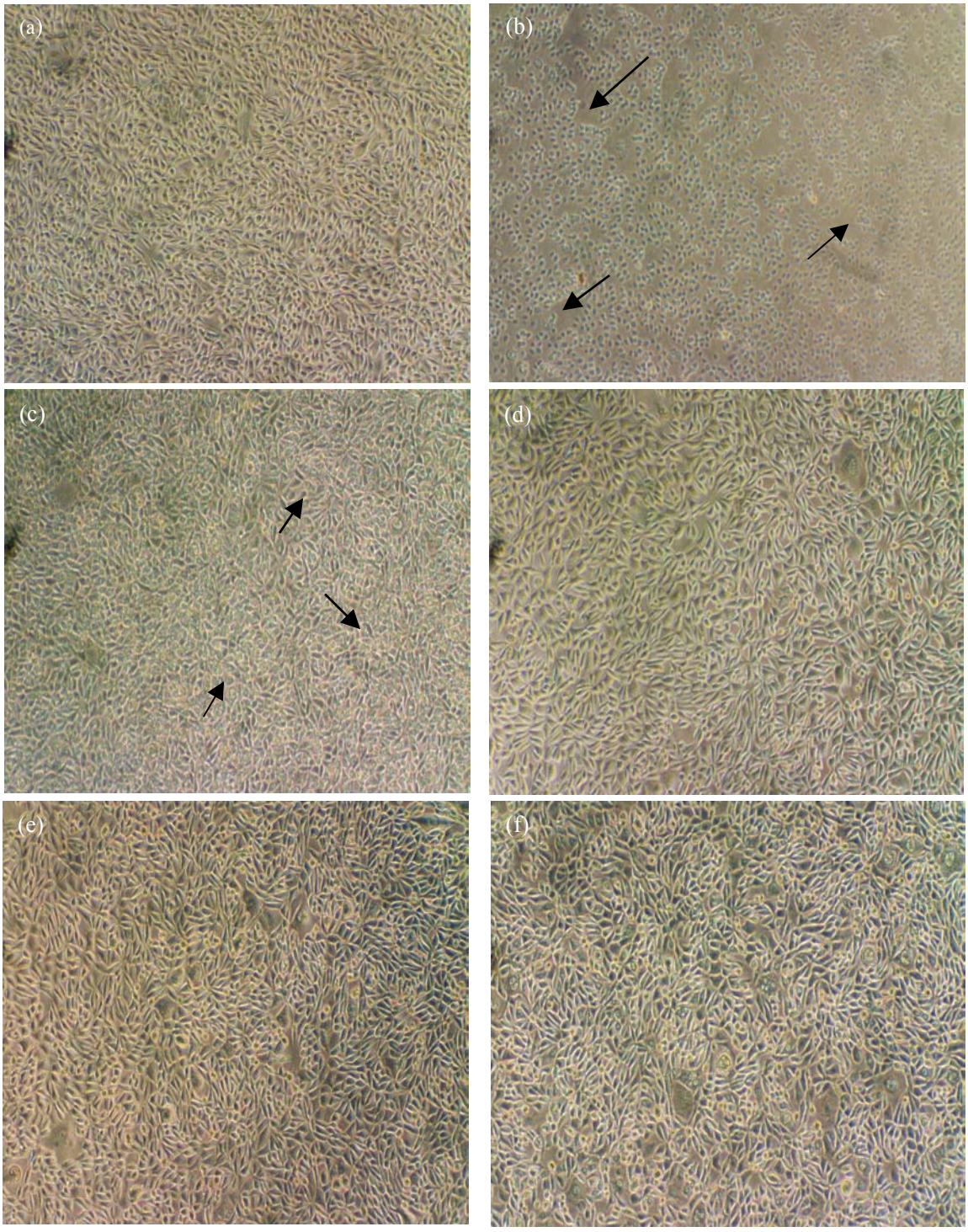

Figure 8. Phase contrast microscopy images of L929 cells after incubation with different polymers (1 mg/ml) for 3 h. (a) Medium control, (b) 100% cytotoxic control, (c) TMC 100 kDa, (d) PEG(5k)$_{40}$-g-TMC(100), (e) PEG(5k)$_{19}$-g-TMC(50), (f) PEG(550)$_{228}$-g-TMC(100). All figures are of the same magnification (100×).

cells to yield a purple formazan reaction product which is largely impermeable

to cell membranes, thus resulting in its accumulation within healthy cells. Solubilization of the cells results in the liberation of the product that can readily be detected using a simple colorimetric assay. The ability of cells to reduce MTT provides an indication of the mitochondrial integrity and activity, which, in turn, may be interpreted as a measure of viability and/or cell number. In contrast, LDH reflects the damage /leakage of plasma membranes. It has been shown that changes in metabolic activity are superior indicators of early cell injury, and effects on membrane integrity are indicative of more serious damage, leading to cell death [20]. Therefore, in this study, MTT assay was employed first to evaluate the correlation between polymer structure and toxicity, and LDH assay was used for corroboration. As indicated, MTT and LDH assay gave similar results. PEG(5k)$_{40}$-g-TMC(100), PEG(5k)$_{19}$-g-TMC(50), and PEG(550)$_{228}$-g-TMC(100) copolymers did not induce a significant decrease in metabolic activity after 3 h incubation. Additionally, no considerable LDH release was measured. In contrast, a remarkable LDH release was observed with TMC 100 kDa, a toxic polymer indicated by MTT assay. However, using trypan blue exclusion assay, a direct measurement of cell number, Kotze et al. suggested that TMC was almost nontoxic [2,3]. This discrepancy could probably be attributed to the different method employed. Generally, trypan blue exclusion assay is a direct measurement of cell number, since dead cells normally detach from a culture plate, and are washed away from the medium, therefore, it cannot quantifiably differentiate between dead cells that may have been damaged.

Generally, biocompatibility is influenced by different properties of the polymers such as MW, charge density and type of the cationic functionalities, structure and sequence (block, linear, branched), and conformational flexibility [7]. TMC 400 kDa was found to display the highest cytotoxicity, whilst TMC 25 kDa and TMC 5 kDa were almost nontoxic. An increase in cytotoxicity as a function of MW, which was observed for TMC in this study, was also reported

for other polycations, such as DEAE-dextran [7] and PEI (polyethylenimine) [21]. Whilst it has been found that chitosan was nontoxic irrespective of the MW [8], the cytotoxicity of TMC can probably attributed to the positive charge carried by the polymer even in neutral environment, which can subsequently interact with the negatively charged cell membrane, resulting in membrane damage. PEGylation decreased the cytotoxicity of TMC considerably, the extent of which was substitution degree, TMC MW and PEG MW dependent. The effect of PEG can be explained by steric effects, which acts to shield a proportion of the positive charges present on TMC. This was particular relevant in the case of small MW TMC. However, since parts of the primary amino groups in TMCs were substituted by PEG , positive charge density decreased overall.

High cytotoxicity of the PEG(5k)$_{298}$-g-TMC(400) copolymer was observed, despite the high degree of substitution. This effect was probably related to the polymers high MW. Hence, a higher substitution degree is essential to decrease the cytotoxicity of TMC 400 kDa and 25% substitution was demonstrated to be sufficient. It should be noted here that a degree of substitution of > 40% is impossible to attain, since only primary amino function groups can participate in the reaction (Table 1). When considering the cytotoxicity, PEG 5 kDa is preferable to PEG 550 Da for PEGylation as its comparatively long chain structure probably shields the positive charges of TMC more efficiently.

Complexation with insulin decreased the cytotoxicity of TMC after 24 h of incubation with cells. This phenomenon can be ascribed to the electrostatic interaction between TMC and insulin, which, decreased the interaction of the positively charged amino groups of TMC with the anionic components of the glycoproteins on the cell membrane, leading to higher cell viability. Kunath et al. reported similar results with PEI and galactosylated PEI [22].

Based on studies with modified PLL (poly-l-lysine), Ferruti et al. noted

that macromolecules with tertiary amine groups exhibit a lower toxicity than those with primary and secondary residues [23]. Dekie et al. found that the presence of primary amines had a significant toxic effect on red blood cells with poly l-glutamic acid derivatives [24]. However, TMC is toxic despite of its high tertiary amino group content (approximately 40%) and low primary amine groups (approximately 40%) compared to chitosan. In contrast, chitosan, despite its high primary amine group content, was biocompatible. Therefore, it is clear that both the type of amine groups and nature of the polymer influence the cytotoxicity.

In summary, different MW TMCs have been synthesized and characterized. Cytotoxicity of TMC and its derivatives was investigated with the MTT and LDH assays, which allow the quantification of the cell metabolic activity and membrane integrity, respectively. Similar results were obtained with the two methods, which were in turn in agreement with observations from inverted phase contrast microscope images. MW dependent cytotoxicity was observed for TMC, and PEGylation led to increased biocompatibility. PEG 5 kDa is preferable to PEG 550 Da for efficacious PEGylation. Complexation with insulin decreased the toxicity of TMCs after 24 h incubation. These insights could be particular helpful due to the promising application of TMC as drug delivery vehicles.

References

[1] Singla AK, Chawla M. Chitosan: some pharmaceutical and biological aspects-an update. J Pharm Pharmacol 2001; 53: 1047-1067.

[2] Kotzé AF, Lueßen HL, de Leeuw BJ, de Boer BG, Coos Verhoef J, Junginger HE. Comparison of the effect of different chitosan salts and *N*-trimethyl chitosan chloride on the permeability of intestinal epithelial cells (Caco-2). J Controlled Rel 1998; 51: 35-46.

[3] Kotzé AF, Thanou M, Lueben HL, De Boer AG, Verhoef JC, Junginger HE. Enhancement of paracellular drug transport with highly quaternized *N*-trimethyl chitosan chloride in neutral environments: In vitro evaluation in intestinal epithelial cells

(Caco-2). J Pharm Sci 1999; 88: 253-257.

[4] Thanou MM, Florea BI, Geldof M, Junginger HE, Borchard G. Quaternized chitosan oligomers as novel gene delivery vectors in epithelial cell lines. Biomaterials 2002; 23: 153-159.

[5] Thanou MM, Verhoef JC, Romeijn SG, Nagelkerke JF, Merkus F, Junginger HE. Effects of *N*-trimethyl chitosan chloride, a novel absorption enhancer, on Caco-2 intestinal epithelia and the ciliary beat frequency of chicken embryo trachea. Int J Pharm 1999; 185: 73-82.

[6] Quinton, PM, Phillpot, CW. A role for anionic sites in epithelial architecture. Effect of cationic polymers on cell membrane structure. J Cell Biol 1973; 56: 787-796.

[7] Fischer D, Li Y, Ahlemeyer B, Krieglstein J, Kissel T. In vitro cytotoxicity testing of polycations: influence of polymer structure on cell viability and hemolysis. Biomaterials 2003; 24: 1121-1131.

[8] Mao S, Shuai X, Unger F, Simon M, Bi D, Kissel T. The depolymerization of chitosan: Effects on physicochemical and biological properties. Int J Pharm 2004; 281: 45-54.

[9] Morgan DM, Larvin VL, Pearson JL. Biochemical characterization of polycation-induced cytotoxicity to human vascular endothelial cells. J Cell Sci 1989; 94:553-559.

[10] Morgan DM, Clover J, Pearson JL. Effects of synthetic polycations on leucine incorporation, lactate dehydrogenase release, and morphology of human umbilical vein endothelial cells. J Cell Sci 1988; 91: 231-238.

[11] Mao S, Shuai X, Wittmar M and Kissel T. Poly (ethylene glycol)-graft-trimethyl chitosan block copolymers: synthesis, characterization and potential as water-soluble insulin carriers. (In preparation)

[12] Ogris M, Brunner S, Schüller S, Kircheis R, Wagner E. PEGylated DNA/transferring-PEI complexes: reduced interaction with blood components, extended circulation in blood and potential for systemic gene delivery. Gene Therapy 1999; 6: 595-605.

[13] Veronese FM. Peptide and protein PEGylation: a review of problems and solutions. Biomaterials 2001; 22: 405-417.

[14] Sieval AB, Thanou M, Kotze AF, Verhoef JC, Brussee J, Junginger HE. Preparation and NMR characterization of highly substituted N-trimethyl chitosan chloride. Carbohydrate Polymers 1998; 36: 157-165.

[15] Thanou MM, Kotze AF, Scharringhausen T, Luessen HL, de Boer AG, Verhoef JC,

Junginger HE. Effect of degree of quaternization of N-trimethyl chitosan chloride for enhanced transport of hydrophilic compounds across intestinal Caco-2 cell monolayers. J Controlled Rel 2000; 64: 15-25.

[16] Mosmann T. Rapid colorimetric assays for cellular growth and survival: application to proliferation and cytotoxicity assays. J Immunol Methods 1983; 65: 55-63.

[17] Kolhe P and Kannan RM. Improvement in ductility of chitosan through blending and copolymerization with PEG: FTIR investigation of molecular interactions. Biomacromolecules 2003; 4: 173-180.

[18] Sabnis S, Block LH. Chitosan as an enabling excipient for drug delivery systems I. Molecular modifications. International Journal of Biological Macromolecules 2000; 27:181-186.

[19] Florian PJ. Principles of polymer chemistry. New York: Cornell University Press, 1953. P. 69.

[20] Davila JC, Reddy CG, Davis PJ and Acosta D. Toxicity assessment of papaverine hydrochloride and papaverine-derived metabolites in primary cultures of rat hepatocytes. In Vitro Cell Dev Biol 1990; 26: 515-524.

[21] Fischer D, Bieber T, Li Y, Elsaesser HP, Kissel T. A novel non-viral vector for DNA delivery based on low molecular weight, branched polyethylenimine: effect of molecular weight on transfection efficiency and cytotoxicity. Pharm Res 1999; 19: 1273-1279.

[22] Kunath K, von Harpe A, Fischer D, Kissel T. Galactose-PEI–DNA complexes for targeted gene delivery: degree of substitution affects complex size and transfection efficiency. J Controlled Rel 2003; 88: 159-172.

[23] Ferruti P, Knobloch S, Ranucci E, Gianasi E, Duncan R. A novel chemical modification of poly-l-lysine reducing toxicity while preserving cationic properties. Proc Int Symp Control Rel Bioact Mater 1997; 24: 45-46.

[24] Dekie L, Toncheva V, Dubruel P, Schacht EH, Barrett L, Seymour LW. Polyl-glutamic acid derivatives as vectors for gene therapy. J Controlled Rel 2000; 65: 187-202.

Chapter 5

Nanocomplex formation between chitosan derivatives and insulin: The effect of system pH, polymer structure and molecular weight

Manuscript in preparation

Abstract

Polyelectrolyte complexes (PEC) formed from chitosan derivatives and insulin were prepared and parameters influencing complex formation were characterized. Turbidimetric titration, in combination with dynamic light scattering (DLS) and laser doppler anemometry (LDA), were used to study the complexation process. The morphology of the PECs were determined using atomic force microscopy (AFM). PEC formation was predominantly pH dependent. Complexation with insulin occurred only above critical pH value (pHc) of 6.0 for all the chitosan derivatives investigated. Soluble PECs in the size range of 200-500 nm with spherical or sub-spherical morphology and smooth surface structure were obtained at optimized polymer/insulin charge ratios. Optimal conditions were obtained when the pH of PECs was in the range of 6.5-8.0, depending on polymer structure. The stability of PECs was influenced by polymer chain length. Only when the MW of the polymers was $\geqslant$25 kDa PEC precipitation could be avoided. Increasing the ionic strength of the medium accelerated complex dissociation. Conversely, high temperatures facilitated PEC formation and compaction. Chitosan trimethylation and PEGylation significantly improved the stability of PECs. All of the complexes could be lyophilized without influencing the properties. On the basis of our results, we suggest that interactions involved in PEC formation were predominantly electrostatic in nature, involving the positively charged amino groups of chitosan and the negatively charged insulin above its isoelectric point.

1. Introduction

Recently, nanoparticles have increasingly been investigated as carriers for hydrophilic macromolecular drugs such as peptides, proteins, vaccines and DNA to improve stability and permit administration through non-parenteral routes (1). Although a wide variety of techniques are available for producing

nanoparticles including solvent evaporation (2), interfacial polymerization (3) and emulsion polymerization methods (4), most of these approaches involve the use of organic solvents, heat or vigorous agitation, procedures which are potentially harmful to sensitive biomolecules. In recent years, self-assembly of proteins with natural or synthetic polyelectrolytes to form complexes (poly-electrolyte-complexes, PEC) with drug candidates has drawn increasing attention (5). PEC formation leads to particles with dimensions on a colloidal level, generating optically homogeneous and stable nano-dispersions. Additionally, such methods have the advantage of not necessitating sonication and organic solvents during preparation, therefore minimizing possible damage to drug candidates during PEC formation.

Chitosan is a non-toxic and biocompatible cationic polysaccharide produced by partial deacetylation of chitin that is isolated from naturally occurring crustacean shells. Due to its specific properties, chitosan has found a number of applications in drug delivery including that of an absorption enhancer of hydrophilic macromolecular drugs (6,7) and as gene delivery system (8,9). Additionally, it has been included in the European Pharmacopoeia 2002 as an excipient. Moreover, enhancement of nasal absorption of insulin in rabbits and sheep was reported (10,11). In 1997, Calvo et al. prepared chitosan nanoparticles by ionotropic gelation of chitosan with tripolyphosphate counterions (12). Since this time, almost all chitosan nanoparticles have been prepared in this manner. Chitosan is positively charged at pH < 6.5 due to the protonation of the amino groups, and insulin is negatively charged at pH above its isoelectric point (apparent pI 6.4). Consequently, electrostatic interactions between both entities can be used as a driving force for PEC formation.

The purpose of this investigation is to evaluate the feasibility of PEC formation between insulin and various chitosan derivatives by self-assembly through the electrostatic interaction in the absence of TPP. Although Dyer et al. mentioned this approach (13), this work has yet to be investigated

systematically to the best of our knowledge. In this paper, using turbidimetric titration and dynamic light scattering, the properties of soluble PECs between insulin and chitosan derivatives have been characterized, and various factors influencing the process were investigated in detail.

2. Materials and methods

2.1 Materials

Chitosan (400 kDa) was purchased from Fluka (Steinheim, Germany) with a degree of deacetylation (DD) of 84.7%. Depolymerization was carried out as described previously to obtain chitosans of different molecular weights (14). Trimethyl chitosan (TMC) derivatives were synthesized in a two-step synthesis (15). Grafting of TMC with poly (ethylene glycol), PEG 5 kDa and PEG 550 Da was achieved to yield copolymers: $PEG(5k)_{40}$-g-TMC(100) and $PEG(550)_{228}$-g-TMC(100) as described elsewhere (16). The following nomenclature was adopted for the copolymers: $PEG(X)_n$-g-TMC(100), where X denotes the MW of PEG in Da and the subscript *n* represents the average number of PEG chains per TMC macromolecule of 100 kDa. Human recombinant insulin powder (26.2 IU /mg) was a gift from Aventis Pharma AG (Germany).

2.2 Preparation of insulin nanocomplexes

Chitosan-insulin PEC can be obtained when both molecules oppositely charges. To facilitate this, the pH of chitosan solutions was adjusted to 5.5 (in this case, more than 90% of the amine groups are protonated), and pH of insulin solution was adjusted as required. Polymer solutions of appropriate concentration (as indicated below) were prepared by dissolving the dry polymer powder in 0.25% acetic acid solution under stirring and adjusting the pH to 5.5 with 1 N NaOH. Insulin solution (1 mg/ml) was prepared by dissolving insulin powder in 87% (v/v) 0.01 N HCl. Subsequently, 13% (v/v) 0.1 N Tris

(hydroxymethyl) aminomethane solution was added, resulting in a clear insulin solution in Tris buffer at pH 7.4. The pH was further adjusted with 1 N HCl or 1N NaOH as required. Due to the poor solubility of chitosan at neutral pH conditions, PECs were prepared by adding 1 ml polymer solution to an equal volume of insulin solution in a glass vial under gentle magnetic stirring, and incubating for a further 20 min at room temperature. All experiments were performed in triplicate at ambient temperature. Freshly prepared solutions were used in each experiment.

2.3 Characterization of polymer-insulin complexes

Dynamic Light Scattering (DLS). Complex size measurements were carried out with a Zetasizer 3000 HS from Malvern Instruments, Herrenberg, Germany (10 mW HeNe laser, 633 nm). Scattering light was detected at 90^{o} angle through a 50 micron pin hole at a temperature of 25℃. For data analysis, the viscosity (0.88 mPa•s) and the refractive index (1.33) of distilled water at 25℃ were used. Scattering data (Kilo counts per second, Kcps) were noted during the measurement. The instrument was routinely checked and calibrated using standard reference latex particles (AZ 55 Electrophoresis Standard Kit, Malvern Instruments). Measurements were analysed using the CONTIN algorithm. Particles sizes of PEC are given as mean ± SD (n = 10).

Laser Doppler Anemometry (LDA). The zeta potential measurements of the complexes were carried out in the standard capillary electrophoresis cell of the Zetasizer 3000 HS from Malvern Instruments (Herrenberg, Germany) at 25℃ in 0.01 M Tris buffer pH 7.4. Average values of the zeta potential were calculated with the data from ten runs (± SD).

Insulin loading of PEC. The amount of insulin entrapped in PEC was calculated by measuring the difference between the total amount of insulin added to the solution, and the quantity of non-associated insulin remaining in

the aqueous supernatant after the PEC formation. For this purpose, PECs were centrifuged at 14000 rpm/min for 30 min at room temperature. The quantity of insulin in the supernatant was measured using a Merck HPLC (Hitachi, Darmstadt, Germany) system equipped with a fluorescence detector (F-1050) and a LiChrospher 100 RP- 18e column (5 μm, 4.6×250mm). Samples of 20 μl were injected with an automatic sampler (model As-200A). The mobile phase consisted of eluent A (ultra pure water with 0.1% trifluoroacetic acid (TFA)) and eluent B (acetonitrile: water: TFA 89.9: 10: 0.1) 65: 35. The flow rate was 1.0 ml/min and an emission wavelength of 600 nm, together with an excitation wavelength of 280 nm was employed. Insulin content was quantified by peak integration and insulin association efficiency was calculated as follows:

$$Association\ efficiency = \frac{Total\ amount\ of\ insulin - Free\ insulin}{Total\ amount\ of\ insulin} \times 100\%$$

All samples were measured in triplicate.

Morphology of the complexes. Atomic force microscopy was employed to characterize the morphology of PECs using a Digital Nanoscope IV Bioscope (Veeco Instruments, Santa Barbara, CA, USA). All measurements were performed in tapping mode to avoid damage of the sample surface. Samples were freshly prepared in triplicate before the experiment.

2.4 Turbidimetric Titration

The simplicity and sensitivity of turbidimetric titration method as applied to protein-polyelectrolyte systems is based on the fact that turbidity is proportional to both the molecular weight and the concentration of particles in a system (17). Consequently, the interaction between polymer and insulin was studied with this method in our work. Briefly, insulin solution (1 mg/ml) was added stepwise to 1 ml polymer solutions. Transmittances at 460 nm and pH changes of the mixture were noted throughout (17). Transmittance was monitored with a UV/Vis spectrophotometer (UV-160, Shimadzu, Kyoto, Japan)

connected to a 1 cm path length optical probe and calibrated to 100% transmittance with ultra pure water. The turbidity was reported as 100 - %T, where %T was the average value of triplicate measurements. A pH meter with a combination electrode was used to monitor the solution pH (n = 3).

2.5 Lyophilization

Sucrose (Fluka, Steinheim, Germany) or mannitol (Fluka, Steinheim, Germany) was added to freshly prepared complex solutions. The content of lyoprotectant was expressed as the lyoprotectant / insulin ratio (w/w). Samples (600 μl) were frozen at -80℃ in Eppendorf tubes. Freeze drying was performed using the lyophilizator Beta 1 (Crist, Osterode, Germany). Samples were dried for 48 h at a working pressure of 0.07 mbar corresponding to a condenser temperature of -46℃. Dried samples were resuspended in 600 μl of distilled water and characterized by dynamic light scattering.

2.6 Calculations and statistics

Results are depicted as mean±SD from at least three measurements. Significance between the mean values was calculated using ANOVA one-way analysis (Origin 7.0 SRO, Northampton, MA, USA). Probability values $P < 0.05$ were considered significant.

3. Results and Discussion

3.1 Effect of the pH value of insulin solution

The effects of pH on PEC formation have previously been discussed, with increased pH values promoting the formation of protein-polycation complexes (18). Since complex formation between proteins and polyelectrolytes is primarily driven by coulombic interactions, the pH of the insulin solution will influence properties of the resulting PECs. Insulin solutions (1 mg/ml) of

differing pH values (7.0, 8.0, 8.5, and 9.0, respectively) were added to equal volumes (1 ml) of various concentrations of chitosan 100 kDa solutions at pH 5.5 under gentle magnetic stirring. Figure 1 shows that the particle size of chitosan–insulin PECs is dependent on both the pH of the insulin solution and the chitosan concentration. Soluble insulin-PECs were formed when the final system pH was in the range of 6.5-7.0. By contrast, when the pH of insulin solution was 9.0, then the final system pH was > 7.5. Here, less than 10% of the amino groups of chitosan are positively charged and precipitation occurred. Additionally, extremely large particles were observed at pH 7.0 with increasing chitosan concentration, compared with these prepared at pH 8.0 and 8.5. This effect can be attributed to the increased electrostatic interaction with pH, resulting in PEC compaction. Insulin-PECs with particle sizes in the desired range of 200-500 nm could be formed when the chitosan concentration was in the range of 1.0-2.0 mg/ml and the pH value of insulin solutions was 8.0-8.5.

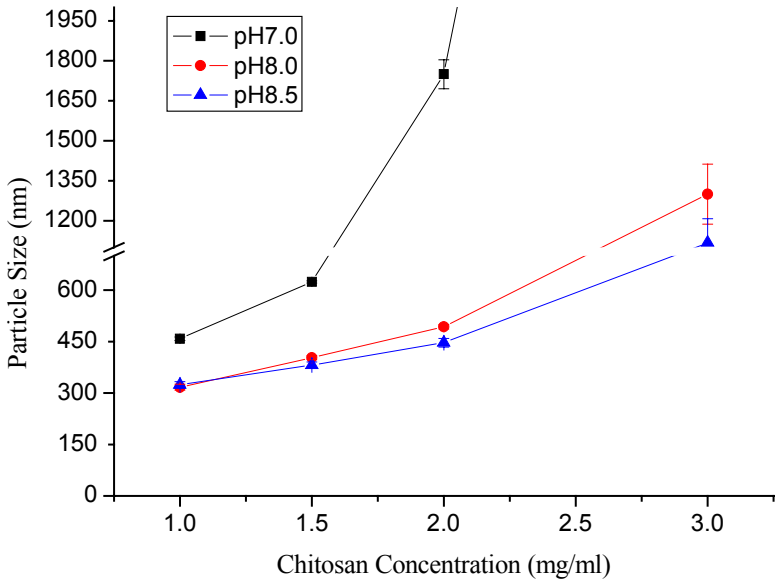

Figure 1. Effect of insulin solution pH and chitosan 100 kDa concentration on the particle size of the PEC. The PEC was prepared by adding 1 ml insulin solution (1 mg/ml) of desired pH into chitosan 100 kDa solution (pH 5.5) dropwise under stirring.

3.2 Stoichiometric ratio of insulin and chitosan derivatives in PEC

It is well known that polymer/insulin ratio influences both the degree of interactions and the properties of PECs. Therefore, the stoichiometry was investigated in greater detail using turbidimetry and dynamic light scattering. Polymer solutions were titrated against insulin solutions, and the resulting particle size and Kcps values were measured. The points at which particle size began to increase dramatically, and the Kcps values reached a plateau were denoted as the endpoint of the titration, and the optimal [polymer]/ [insulin] charge ratio was calculated. Differently structured polymers, namely chitosan 100 kDa, TMC 100 kDa, PEG(5k)$_{40}$-g-TMC(100) and PEG(550)$_{228}$-g-TMC(100) were investigated under identical conditions. Figure 2 presents titration data of the chitosan 100 kDa insulin complex.

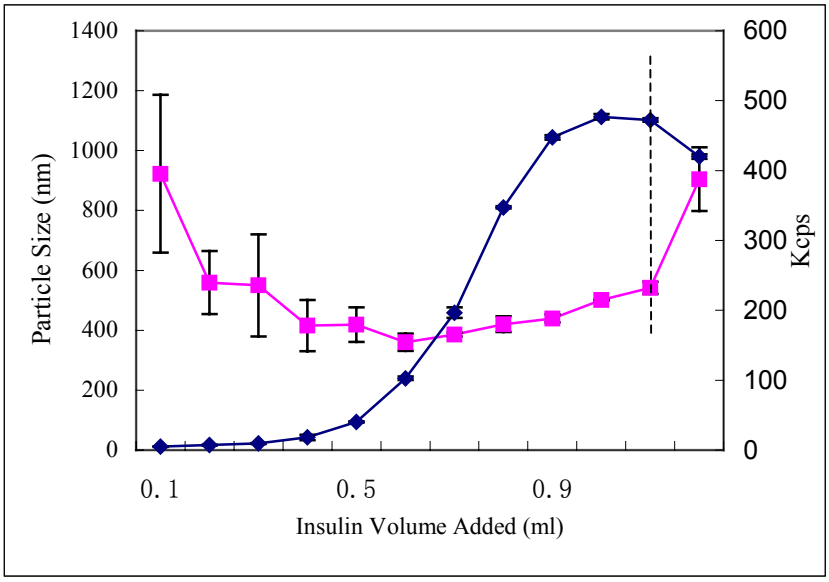

Figure 2. Evolution of particle size and Kcps value of chitosan 100 kDa-insulin complex versus insulin volume. (■) Size; (◆) Kcps. Chitosan 100 kDa solution (2 mg/ml) was titrated with insulin solution (1 mg/ml). Particle size and Kcps values of the PEC were monitored by dynamic light scattering.

During the initial stages of titration, the system pH was below the isoelectric point of insulin. Hence, it was weakly negatively charged and

therefore only large aggregates were observed. They condensed to a more defined and compact structure with increasing insulin concentration until a critical point was reached, from where the particle size increased abruptly. This increase was accompanied by a slight Kcps decrease, implying either the redistribution of insulin in the polymer, or binding on the surface of the polymer. Therefore, this critical point was selected to calculate the optimal ratio between insulin and chitosan. After this critical point, aggregation occurred in one hour due to the significantly increased particle size.

As reported previously (19), at the physiological pH of 7.4 human insulin carries two negative charges per molecule. As for chitosan, the protonation of the molecule's amino groups can be represented by (20):

$$Glc\text{-}NH_3^+ + H_2O \leftrightarrow Glc\text{-}NH_2 + H_3O^+$$

$$(1\text{-}\alpha) \qquad\qquad \alpha \qquad\quad \alpha$$

$$pKa = pH + \log (1\text{-}\alpha)/ \alpha$$

where α is the fraction of unprotonated free amino-groups NH_2. Since the pKa of chitosan is approximately 6.5, we can calculate the proportion of amino groups that are not positively charged based on the final system pH. Making the assumption that 24% of the primary amino groups of chitosan (calculation based on a final system pH 6.8) and all primary and quaternized amino groups of TMC are protonated at neutral pH, the polymer/insulin charge ratio (+/-) was calculated according to the mass of the components at critical points. It was found to be polymer structure dependent and was approximately 7:1, 3:1, 5:1, 5:1 for chitosan 100 kDa, TMC 100 kDa, $PEG(5k)_{40}$-g-TMC(100) and $PEG(550)_{228}$-g-TMC(100) respectively. These results suggest that the stoichiometry of the complexes are primarily determined by the charge density of the polymers.

It is also noteworthy that the size of the PECs was inversely proportional to the quantity of polymer added. Smaller PECs were formed at $\geqslant$ optimal polymer/insulin ratio, whereas larger complexes were obtained below this ratio

and flocculation occurred in a short period of time. Similarly, several groups found that for chitosan and other cationic polymers, an optimal charge ratio of polymer/DNA 5:1 was essential for the protection of nanocomplexes of appropriate size (21,22). This is in agreement with the theory of PEC formation (23). Generally, only highly charged polyelectrolytes with strong ionic groups favor a 1:1 stoichiometry of PEC (24), and this is not the case for chitosan and insulin. The stoichiometric ratios observed for different combinations of components may be understood on the basis of a mass action law, assuming a different degree of dissociation between polyions and counterions. PECs with an excess of polycation are more stable due to the repulsion of charged nanocomplexes in suspension.

3.3 Effect of polymer concentration

Taking chitosan 100 kDa as an example, the effect of polymer concentration on complex formation was investigated. Figure 3a shows that the transmittance of the mixture increased with insulin volume until equilibrium was achieved. Three phases can clearly be observed in Figure 3a. At insulin volumes < 0.3 ml (critical volume, V_c, the precise value depends on polymer concentration), fewer complexes were formed. Turbidity increased rather abruptly after V_c and a plateau was reached at a specific insulin volume, which can be denoted as V_p and considered as the end point of the titration. When considering chitosan 100 kDa, the endpoint is polymer concentration dependent and is approximately 0.8 ml and 1.1 ml for 1 mg/ml (aggregation in 5 minutes) and 2 mg/ml solutions, respectively. Additionally, it is supposed that polymer-insulin binding can alter the local electrostatic environment of ionizable amino acid residues and therefore, the pH change was also monitored throughout. Figure 3b shows the evolution of pH versus polymer concentration. Compared to the control group (acetate buffer pH 5.5), a large number of protons were released during the complex formation process and the proton

number was a function of polymer concentration. More protons were released at a higher concentration, as indicated by a lower pH value. Consequently, fewer complexes were formed due to decreased negative charge density of insulin at low pH. Another possibility explaination for the decreased complex concentration is that a proportion of the charged segments are shielded at high concentration due to the strong intermolecular interactions, as chitosan normally takes the shape of an extended random coil in solution.

(a) (b)

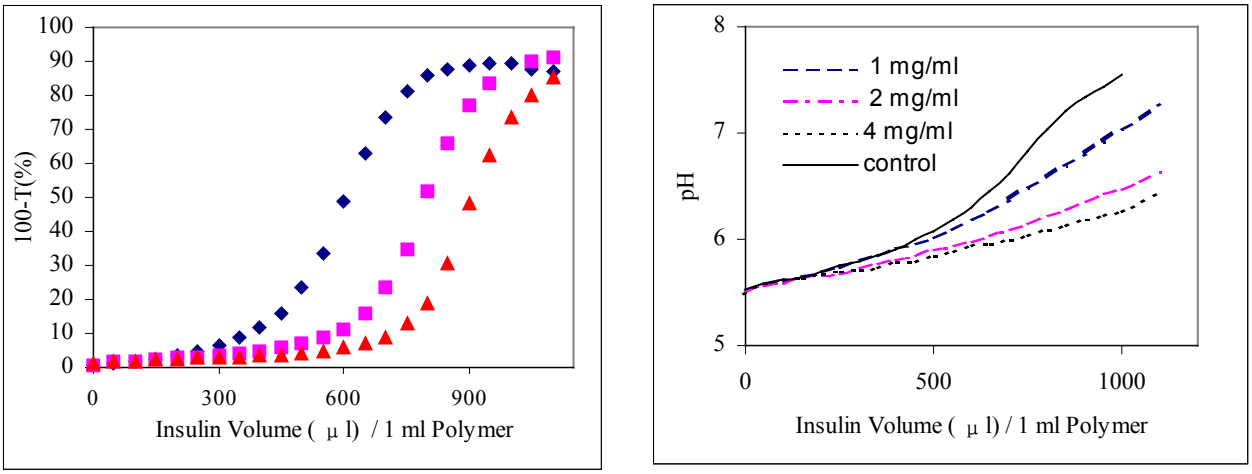

Figure 3 (a) Turbidity evolution profiles as a function of insulin volume using different concentration of chitosan 100 kDa solutions. (◆) 1 mg/ml; (■) 2 mg/ml; (▲) 4 mg/ml.

(b) pH evolution profiles as a function of insulin volume using different concentrated chitosan 100 kDa solutions.

The PEC was prepared by the stepwise addition of insulin solution (1 mg/ml, pH 8.5, 50 μl) stepwise into 1 ml of various concentrated polymer solutions (pH 5.5). The transmittance of the mixture was measured at 460 nm and denoted as T. The pH of the mixture was measured simultaneously.

3.4 Effect of system pH

Since the most important factor that must be controlled during PEC formation process is pH, the relationship between pH value and transmittance was studied with chitosan and TMC, as depicted in Figure 4. An extremely good

correlation between pH and transmittance could be observed. Three regions can be defined in Figure 4. In region 1, columbic repulsive forces present between the positively charged polymer and the mainly positively charged insulin prohibited the complex formation. A sharp increase in turbidity was observed in region 2. In region 3, a saturation plateau appeared, which can be regarded as the endpoint of the titration. These regions can be considered as separate phases, with pHc representing the critical pH value for transition from region 1 to region 2 and pHe representing the equivalent pH value. For both chitosan and TMC, virtually no PEC was obtained at pH < 6.0.

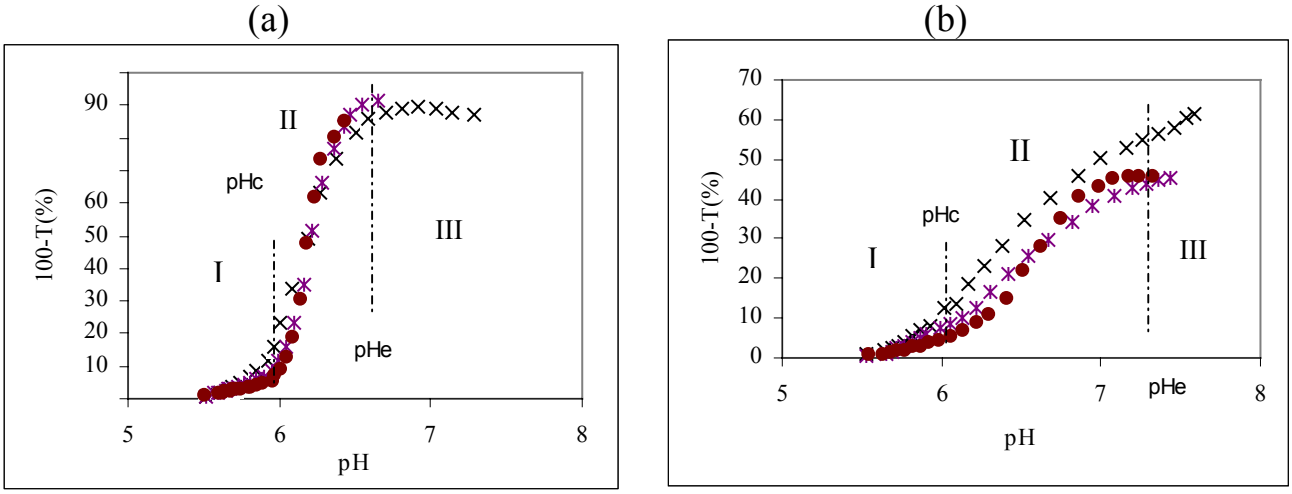

Figure 4. Relationship between pH value and transmittance.

(a) chitosan 100 kDa (×) 1 mg/ml; (*) 2 mg/ml; (●) 4 mg/ml

(b) TMC 100 kDa (×) 1mg/ml; (*) 2mg/ml; (●) 4 mg/ml

This is due to the fact that in order to form a PEC, both polymers have to be ionized and bear opposite charges. In the case presented here, the reaction can only proceed at pH values in the vicinity of the pKa interval of the two polymers (the pKa of chitosan is approximately 6.5, whilst the apparent pI of insulin is 6.4). It is also noted that the pHc value is polymer concentration independent, an observation that has previously been reported (25). In contrast, the pHe value varied with polymer structure. It was measured to be

approximately 6.5 for chitosan and 7.3 for TMC, which can be explained by the different charge properties of the polymers.

However, as suggested by Kabanov (23), soluble PEC species in which the host polyelectrolyte component is a weak polyacid or a weak polybase can be compacted and precipitated by a pH change, i.e. suppressing ionization of single-stranded blocks. As chitosan is a weak polybase, the precipitation pH for chitosan-insulin complex and TMC-insulin complex was investigated. The values were approximately 7.5 and 10.0 for chitosan and TMC respectively. In this case, the system pH should be below the precipitation pH value to obtain soluble PEC. Additionally, at pH values < 5 or > 8, insulin degrades relatively rapidly (26). Consequently, the pH of the system should be controlled in the range of 6.5-8.0 depending on the polymer structure.

3.5 Effect of polymer molecular weight and structure

Since all interpolymer interactions are known to be critically dependent on the chain lengths of the interacting macromolecules (27), the complex formation process was studied with different MW chitosans and evolutions of transmittance (Figure 5a) and system pH (Figure 5b) were observed simultaneously. The critical insulin volume (V_c) for complex formation increased with chitosan MW, from approximately 300 µl for chitosan 50 kDa and 25 kDa to 500 µl for chitosan 400 kDa and 100 kDa. Slopes of the profiles in Figure 5a were calculated using data in the linear range, which were 0.071, 0.084, 0.145, 0.141 for chitosan 400 kDa, 100 kDa, 50 kDa and 25 kDa, respectively. This data is regarded as binding constants between polymers and insulin. It is clear that the formation of chitosan-insulin soluble complexes was chitosan MW dependent, with chitosans exhibiting shorter chains being preferable for complexation. These findings can probably be explained by the fact that complex formation was mainly governed by kinetics which led to preferential binding with the shorter chains due to their greater flexibility.

However, no statistic differences were observed regarding the slope of chitosan 50 kDa and chitosan 25 kDa ($P > 0.05$) or chitosan 400 kDa and chitosan 100 kDa ($P > 0.05$).

(a) (b)

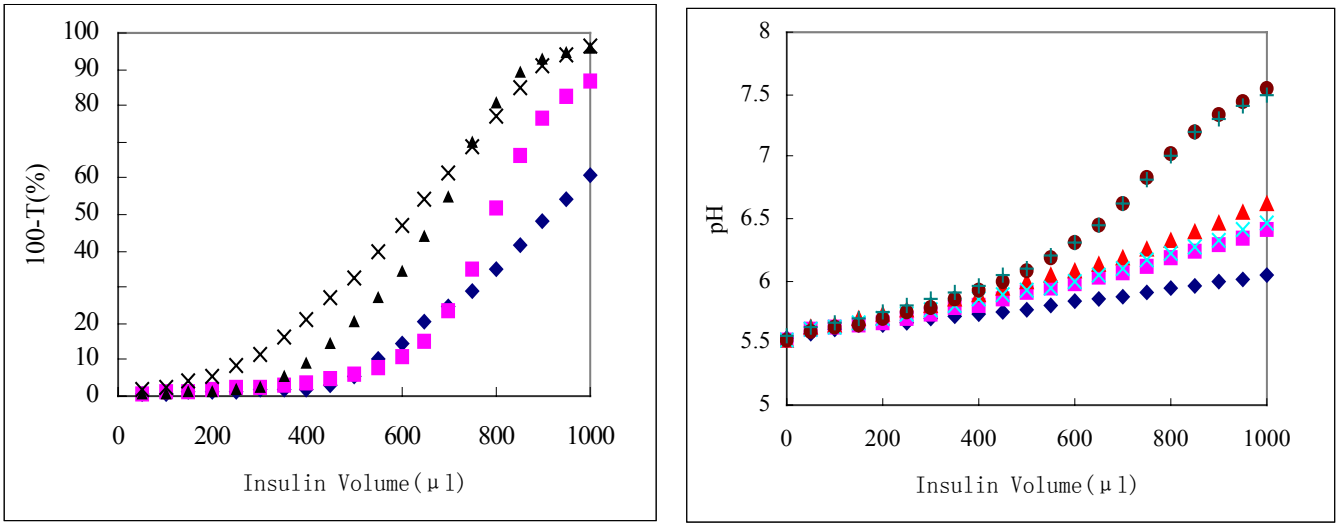

Figure 5. (a) Effect of chitosan molecular weight on the formation of insulin complexes.
(b) pH profiles as a function of insulin solution volume.
(◆)chitosan 400 kDa, (■)chitosan 100 kDa, (▲) chitosan 50 kDa,
(×) chitosan 25 kDa, (●) medium, (+) medium +insulin.

When compared to the control, binding between chitosan and insulin led to proton release by enhancing the dissolution constant, Ka, of the ionizable groups, with this process being chitosan MW dependent (Figure 5b). The particle sizes of the PECs decreased with decreasing molecular weight (376.4±10.3 nm for chitosan 400 kDa compared to 182.3±2.9 nm for chitosan 25 kDa). A considerably decreased particle sizes were obtained from the PECs prepared with PEGylated TMC 100 kDa copolymers, compared to the homopolymer TMC 100 kDa (Table 1). This is probably a consequence of the hydrophilic polyethylene glycol forming a shell on the PEC surface, which subsequently promotes complex condensation. Zeta potentials of the PECs at optimal charge ratios were also measured, and have been listed in Table 1. All of the PECs are

positively charged, and the charge values are in the order of TMC > PEG(5k)$_{40}$-g-TMC(100) > PEG(550)$_{228}$-g-TMC(100) > chitosan. This implies that insulin was encapsulated in the polymers projecting their positively charged chains towards the external aqueous medium, which will subsequently increase the interaction with the negatively charged cell surface and facilitate insulin uptake. The use of copolymers PEGylated with different MW PEG allows variation of the positive surface charge density by changing the relative substitution ratio.

Table 1. Properties and characteristics of the polymers and the PECs

Polymer (kDa)	DD[a] (%)	Substitution (%)[b]	Molecular weight (kDa)[c]	Mass ratio Pol./Ins.[d]	PCS size (nm)	AFM size (nm)	Zeta-potential (mv)	Drug loading (%)	Charge ratio(Pol./Ins.)[d]
Chitosan 400	85.1			2:1	376.4±10.3		13.6±0.3	89.7±2.1	7:1
Chitosan 100	85.4			2:1	308.2±8.5	284.2 ± 37.5	8.8±0.4	87.3±2.4	7:1
Chitosan 50	89.9			2:1	226.8±6.3		7.4±0.3	93.2±1.3	7:1
Chitosan 25	86.2			2:1	182.3±2.9		6.4±1.2	94.2±1.1	7:1
TMC 100		39.3[b1]	100	0.3:1	273.3±4.6	245.5 ± 26.4	22.9±1.8	81.4±2.1	3:1
PEG(5k)$_{40}$-g-TMC(100)		6.44	300	1:1	186.4±8.3	136.0 ± 14.1	21.0±2.2	94.8±1.1	5:1
PEG(550)$_{228}$-g-TMC(100)		36.7	225	1:1	224.6±2.3	215.5 ± 12.3	12.7±2.3	94.2±1.7	5:1

[a] DD degree of deacetylation, calculated by ^{1}H NMR analysis.

[b] Calculation based on the primary amino group content in chitosan, [b1] Degree of quaternization.

[c] Calculation based on the composition of the copolymer.

[d] Calculation based on the stoichiometric ratio optimized in Section 3.2.

When compared with the labile insulin association of 10-85 % observed for chitosan nanoparticles prepared by ionic gelation (28,29), the insulin association efficiencies of the self-assembled nanocomplexes prepared here were high and stable, at approximately 90%. Additionally the complexes displayed a significantly decreased surface charge, with a zeta potential value of

8.8 ± 0.4 versus 27.1 ± 2.6 for chitosan 100 kDa self-assembled insulin nanocomplexes and chitosan 70 kDa insulin nanoparticles, respectively. The difference in particle size was marginal. However, the particle size distribution narrowed for the nanocomplexes (28,29).

3.6 Complex stability

3.6.1 Effect of polymer MW

Maintaining the physico-chemical stability of the delivery vehicles is thought to be one of the essential requirements for obtaining in vivo activity. We began by investigating the influence of chitosan MW on complex stability. When the MW of chitosan was as high as 25 kDa, soluble PECs were obtained and kept stable for at least 8 hours. In contrast, large particle sizes (μm) were observed for the PECs prepared with chitosan 10 kDa and 5 kDa, with precipitation occurring within 1 h. This phenomenon is consistent with the theoretical prediction that suggests the stability of interpolymer complexes are critically dependent on the chain length, and for each system matrix an " upper critical length" of oligomer chains exists, above which the complexes are found to be stable (30). Kabanov also reported that the solubility of PEC in aqueous media is determined by the relative length of oppositely charged polyions (23). A similar MW limitations were observed when different MW PEIs (polyethylenimine) were employed to complex DNA (31). Complexes of LMW PEI were not stable, even in the presence of extreme excesses of polycation (N/P 50). Huang et al. reported the same problem when preparing nanoparticles with chitosan 10 kDa by ionotropic gelation (32).

3.6.2 Effect of ionic strength of the medium

Some studies indicated that the addition of salt could affect the stability of the PEC. For example, it was reported that complexes formed by catalase and polyacrylic acid readily precipitated upon increases in NaCl concentration (27).

Reduced protein binding with increasing ionic strength was also observed in the lysozyme-PMAA system (27).

In order to investigate the effect of salt on the chitosan-insulin interaction, the ionic strength of the solution was adjusted by adding sodium chloride. This was achieved by mixing various PECs with a series of concentrated sodium chloride solutions, and monitoring the integrity of the PECs immediately after mixing by dynamic light scattering. Since we found no apparent change in particle size, only the evolution of Kcps values are presented in Figure 6.

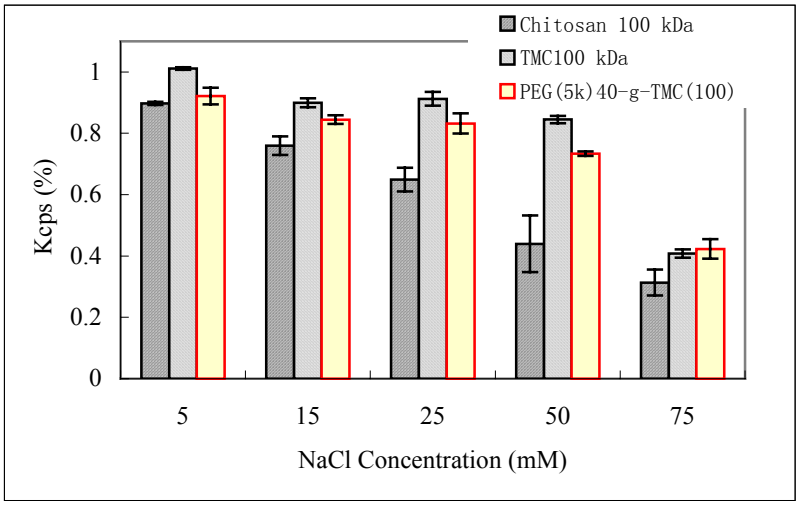

Figure 6. Effect of ionic strength on the dissociation of different structured polymer-insulin complexes.

Dissociation clearly increased with increasing salt concentration, which is probably the result of reduced attraction between the oppositely charged polyelectrolytes by contribution to the counter-ion environment. The degree of influence was polymer structure dependent. This was particularly obvious for chitosan-insulin PECs, with a linear correlation ($R = 0.995$) being observed between the percent of Kcps remained and the ionic strength of the solution. With regard to TMC 100 kDa and PEGylated TMC 100 kDa insulin PECs, the influence appeared to be marginal when the ionic strength was < 50 mM,

probably as a consequence of the steric effect of methyl groups and polyethylene glycol segments. However, severe complex dissociation was observed at an ionic strength of 75 mM, irrespective of the PEC structure. This can be defined as a critical ionic strength (Ic) concerning the complex stability.

3.6.3 Effect of temperature

A number of different PECs were incubated at 20, 37, 50, 65℃ for 6 h, and were subsequently characterized at predetermined time intervals at room temperature. At elevated temperatures, more complexes were formed as indicated by the increased Kcps values. This increase was accompanied by a slight decrease in particle size (10-20%), independent of polymer structure. Figure 7 illustrates the influence of temperature on the properties of chitosan 100 kDa insulin complexes. After 6 h incubation, Kcps values increased by 100% at 65℃ (compared with the value at 20℃), and the particle size decreased by 20%. Thus, increases in temperature facilitate complex formation and compaction. This suggests that the reaction may be entropy driven in the same way polyanion-polycation complexation occurs, where the increase in entropy is associated with the release of small counterions initially bound to the polymers (27). On the other hand, high temperatures may have a profound influence on the kinetics of complex formation.

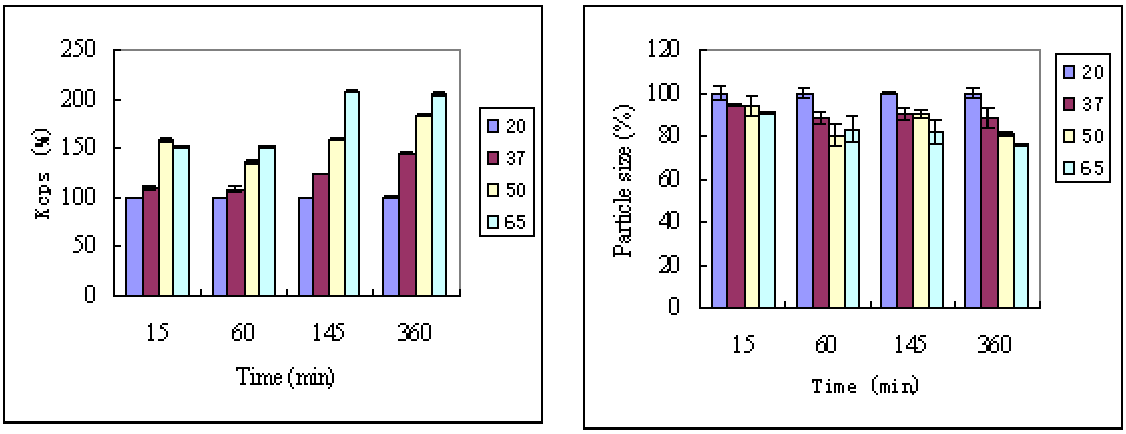

Figure 7. Effect of temperature on the properties of chitosan100 kDa insulin complexes.

3.6.4 Properties of the complexes after lyophylization

Chitosan-insulin complexes were susceptible to aggregation when stored at room temperature or at 4℃ over two days. In contrast, TMC and PEGylated TMC insulin complexes showed no indication of aggregation within one month at room temperature. This improvement in stability probably stems from the higher hydrophilicity of the modified polymer surface. We hypothesize that the surface coupling of PEG increases the hydrophilicity of the complexes and lowers their surface free energy, thereby enhancing their physical stability in aqueous media. The feasibility of preparing PECs by lyophylization was also investigated.

Using sucrose and mannitol as lyoprotectants, properties of the complexes after lyophylization were investigated by dynamic light scattering. It was demonstrated that sucrose could protect the complexes from aggregation effectively at an appropriate sucrose/insulin ratio. On the contrary, aggregation could not be avoided even when the mannitol/insulin ratio was as high as 100:1 (data not shown). The optimal sucrose/insulin ratio was polymer composition dependent. With regard to chitosan 100 kDa and $PEG(550)_{228}$-g-TMC(100), aggregation was prevented when the ratio was above 10:1 with the optimal state occurring at 40:1. This ratio was accompanied by only marginal particle size increases. In contrast, the optimal ratio was approximately 100:1 for both $PEG(5k)_{40}$-g-TMC(100) and $PEG(5k)_{19}$-g-TMC(50) copolymers. The effect of sucrose/insulin ratio on the properties of chitosan 100 kDa insulin complexes and $PEG(5k)_{40}$-g-TMC(100) insulin complexes after lyophylization are depicted in Figure 8.

When considering that all copolymers employed during this study have similar graft ratios, this result implies that the interaction intensity between polymer and insulin is dependent upon polymer structure. Coupled PEG 5 kDa

in the copolymer probably shields a proportion of the positively charged groups on TMC and therefore weakens the interaction with insulin. In contrast, the chain length of PEG 550 Da is possibly too short to have considerable influence.

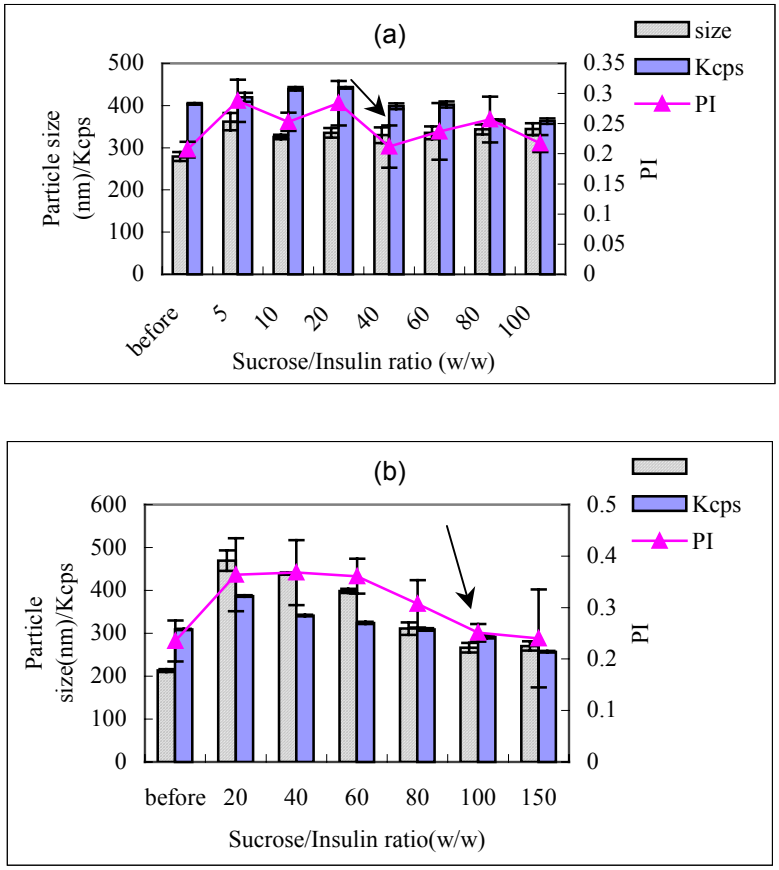

Figure 8. Particle size, Kcps value and polydispersity index of different polymer-insulin complexes as a function of sucrose/insulin ratio (a) chitosan 100 kDa-insulin complexes, (b) PEG(5k)$_{40}$-g-TMC(100)-insulin complexes.

3.7 Visualization of insulin complexes

Compared to electron microscopy, atomic force microscopy (AFM) is a technique that permits the acquisition of images in a liquid environment, without drying or fixation of the sample. Additionally, tapping mode AFM allows the imaging of soft samples at high resolution without damaging the sample surface. AFM can also provide three-dimentional structure and

information of the analysed particles, which is a benefit not available with conventional light-scattering measurements (33). For size determination, all PECs were evaluated individually within a representative scan area (25 × 25 μm). The particle size measurements obtained from AFM images were slight smaller but of the same magnitude as those obtained from dynamic light scattering data (Table 1). Figure 9a-9d shows an overview of different polymer insulin complexes at a scan size of (25 × 25 μm). In Figure 9a, excessive chitosan chains are observed and two subpopulations are found. The smaller fraction had an average diameter of approximately 180 nm, and the larger fraction showed size between 400 and 480 nm. The big particles might consist of two of the small ones. There was also a much smaller fraction of about 40-50 nm. Similar to chitosan complex, also two fractions were found for TMC insulin complex, approximately 380 nm for larger particles and 100-180 nm for smaller ones (Figure 9b). In contrast, smaller particles with low polydispersity were observed for the PECs formed with the copolymers (Figure 9c, 9d). The insert (1x1 μm) of each image allows visualizing the surface morphology of the PECs clearly. It shows that the majority of particles were separated from one other, suggesting that these PECs were possibily stabilized against agglomeration.

A general problem with soft objects such as complexes is to obtain accurate height information. Therefore, topographical images were subsequently captured for generating three-dimentional images of the PECs (Figure 9e,f). From such images it was clear that most of the complexes were spherical or sub spherical with a smooth surface devoid of cracks. Line scan size analysis further demonstrated that the complexes exhibited a good aspect ratio between height and diameter (Figure 9g).

4. Conclusion

Based on the results presented above, it is reasonable to conclude that the

interactions involved in PEC formation are predominantly electrostatic. The PEC formation process is influenced by a varity of parameters, including the

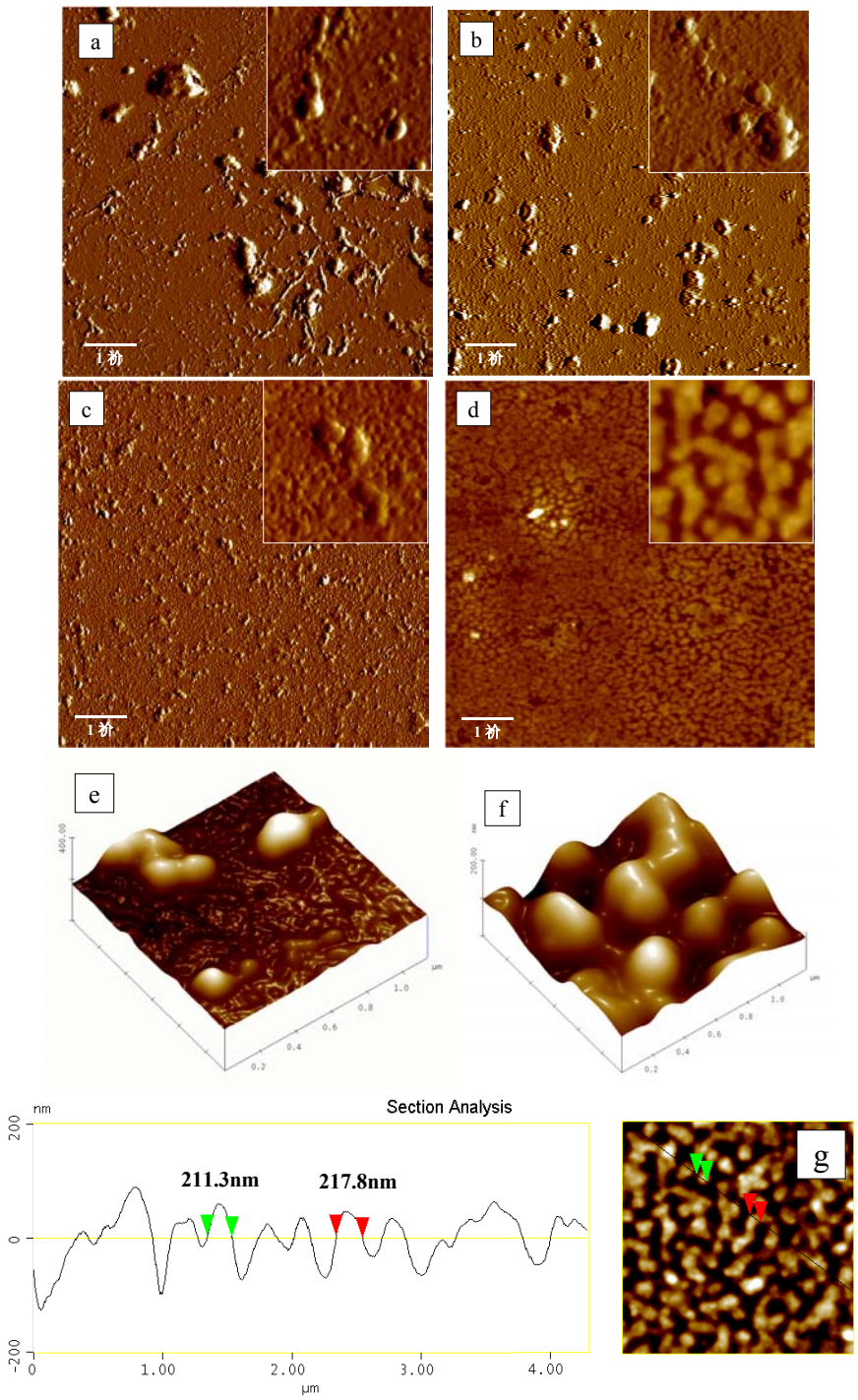

Figure 9. Atomic force microscopy images of polymer-insulin complexes at optimized charge ratio.

(a) Chitosan 100 kDa, (b) Trimethyl chitosan 100 kDa, (c) $PEG(5k)_{40}$-g-TMC(100), (d) $PEG(550)_{228}$-g-TMC(100), (e) Three-dimentional image of chitosan 100 kDa, (f) Three-dimensional image of $PEG(550)_{228}$-g-TMC(100), (g) line scan size analysis of

PEG(550)$_{228}$-g-TMC(100). The inserts are 1x1 μm for each image.

system pH, sequence of mixing, polymer/protein ratio and concentration, polymer molecular weight and structure, ionic strength, etc. Amongst all of these parameters, the most important factor appears to be the system pH. The order of mixing is polymer property dependent. With regard to chitosan, due to its poor solubility at neutral pH, the insulin solution should be added to chitosan solution to avoid precipitation. In contrast, the mixing order appears to have a negligible influence for TMC and PEGylated TMC copolymers. The polymer/protein ratio needs to be optimized individually. When the MW of chitosan and its derivatives were ⩾25 kDa, soluble insulin complexes in the size range of 200-400 nm with spherical or sub-spherical morphology can be readily obtained by simply mixing two components at a specific pH and charge ratio. All of the insulin complexes were successfully freeze-dried without influcing the complex properties, by using sucrose as a lyoprotectant. These studies have contributed much to the understanding of PEC formation and complexation with insulin. This work will be furthered by performing intranasal absorption studies in animal models.

References

1. M. Tobio, A. Gref, A. Sanchez, R. Langer, M. Alonso, Stealth PLA-PEG nanoparticles as protein carriers for nasal administration, Pharm. Res. 15 (1998) 270-275.
2. M.C. Julienne, M.J. Alonso, J.L.G. Amoza, J.P. Benoit, Preparation of poly (D, L-Lactide/Glycolide) nanoparticles of controlled particle size distribution: application of experimental design, Drug Dev. Ind. Pharm. 10 (1992) 1063-1077.
3. H. Ibrahim, C. Bindschaedler, E. Doelker, P. Buri, R. Gurny, Aqueous nanodispersions prepared by a salting-out process, Int. J. Pharm. 87 (1992) 239-246.
4. J.C. Leroux, E. Allemann, E. Doelker, R. Gurny, New approach for the preparation of nanoparticles by an emulsification-diffusion method, Eur. J. Pharm. Biopharm. 41 (1995) 14-18.
5. H. Mao, K. Roy, V.L. Troung-Le, K.A. Janes, K.Y. Lin, Y. Wang, J.T. August, K.W.

Leong, Chitosan-DNA nanoparticles as gene carriers: synthesis, characterization and transfection efficiency, J. Controlled Rel. 70 (2001) 399-421.

6. P. Artursson, T. Lindmark, S.S. Davis, L. Illum, Effect of chitosan on the permeability of monolayers of intestinal epithelial cells (Caco-2), Pharm. Res. 11 (1994) 1358-1361.
7. A.K. Singla, M. Chawla, Chitosan: Some pharmaceutical and biological aspects-an update, J. Pharm. Pharmacol. 53 (2001) 1047-1067.
8. P. Erbacher, Chitosan-based vector/DNA complexes for gene delivery: biophysical characterization and transfection ability, Pharm. Res. 15 (1998) 1332-1339.
9. C.W. Richardson Simon, V.J. Kolbe Hanno, R. Duncan, Potential of low molecular mass chitosan as a DNA delivery system: biocompatibility, body distribution and ability to complexes and protect DNA, Int. J. Pharm. 178 (1999) 231-243.
10. R. Fernandez-Urrusuno, P. Calvo, C. Remunan-Lopez, J.L. Vila-Jato, M.J. Alonso, Enhancement of nasal absorption of insulin using chitosan nanoparticles, Pharm. Res. 16 (1999) 1576-1581.
11. L. Illum, N.F. Farraj, S.S. Davis, Chitosan as a novel nasal delivery system for peptide drugs, Pharm. Res. 11 (1994) 1186-1190.
12. P. Calvo, C. Remunan-Lopez, J.L. Vila-Jato, M.J. Alonso, Novel hydrophilic chitosan-polyethylene oxide nanoparticles as protein carriers, J. Appl. Polym. Sci. 63 (1997) 125-132.
13. A.M. Dyer, M. Hinchcliffe, P. Watts, J. Castile, I. Jabbal-Gill, R. Nankervis, A. Smith, L. Illum, Nasal delivery of insulin using novel chitosan based formulations: A comparative study in two animal models between simple chitosan formulations and chitosan nanoparticles, Pharm. Res. 19 (2002) 998-1008.
14. S. Mao, X. Shuai, F. Unger, M. Simon, D. Bi and T. Kissel, The depolymerization of chitosan: effects on physicochemical and biological properties, Int. J. Pharm. 281 (2004) 45-54.
15. A.B. Sieval, M. Thanou, A.F. Kotze, J.C. Verhoef, J. Brussee, H.E. Junginger, Preparation and NMR characterization of highly substituted N-trimethyl chitosan chloride, Carbohydrate Polymers 36 (1998) 157-165.
16. S. Mao, X. Shuai, M. Wittar and T. Kissel, Poly (ethylene glycol)-graft-trimethyl chitosan block copolymers: synthesis, characterization and potential as water-soluble insulin carriers. (in preparation)
17. A. Tsuboi, T. Izumi, M. Hirata, J. Xia, P.L. Dubin, E. Kokufuta, Complexation of proteins with a strong polyanion in an aqueous salt-free system, Langmuir 12 (1996)

6295-6303.

18. J.M. Park, B.B. Muhoberac, P.L. Dubin, J. Xia, Effects of protein charge heterogeneity in protein-polyelectrolyte complexation, Macromolecules 25 (1992) 290-295.
19. J. Brange, Galenics of insulin: The physio-chemical and pharmaceutical aspects of insulin and insulin preparations, Springer-Verlag, Berlin (1987) 1-103.
20. M.M. Beppu, C.C. Santana, Influence of calcification solution on in vitro chitosan mineralization, Mat. Res. 5 (2002) 47-50.
21. L. Illum, I. Jabbal-Gill, M. Hinchcliffe, A.N. Fisher, and S.S. Davis, Chitosan as a novel nasal delivery system for vaccines, Adv. Drug Deliv. Rev. 51 (2001) 81-96.
22. M. Thanou, B.I. Florea, M.Geldof, H.E. Junginger, G. Borchard, Quaternized chitosan oligomers as novel gene delivery vectors in epithelial cell lines, Biomaterials 23 (2002) 153-159.
23. V.A. Kabanov, Basic properties of soluble interpolyelectrolyte complexes applied to bioengineering and cell transformations, Macromolecular complexes in chemistry and biology, Springer-Verlag Berlin Heidelberg (1994) 151.
24. H. Dautzenberg, J. Koetz, K.J. Linow, B. Philipp and G. Rother, Static light scattering of polyelectrolyte complexes solutions, Macromolecular complexes in chemistry and biology, Springer-Verlag Berlin Heidelberg (1994) 119.
25. K.W. Mattison, I.J. Brittain and P.L. Dubin, Protein-Polyelectrolyte phase boundaries, Biotechnol. Progr. 11 (1995) 632-637.
26. J. Brange, L. Langkjaer, Chemical stability of insulin. 3. Influence of excipients, formulation, and pH, Acta Pharm. Nord. 4 (1992) 149-158.
27. E. Tsuchida and S. Takeoka, Interpolymer complexes and their ion-conduction, Macromolecular complexes in chemistry and biology, Springer-Verlag Berlin Heidelberg (1994) 183.
28. K.A. Janes, M.J. Alonso, Effect of polymer molecular weight on chitosan nanoparticles for peptide delivery, Proc. Int. Symp. Control. Rel. Bioact. Mater. 27 (2000) 8043.
29. Z. Ma, H. Yeoh, L. Lim, Formulation pH modulates the interaction of insulin with chitosan nanoparticles, J. Pharm. Sci. 91 (2002) 1396-1404.
30. N. Karibyants and H. Dautzenberg, Preferential binding with regard to chain length and chemical structure in the reactions of formation of quasi-soluble polyelectrolyte complexes, Langmuir 14 (1998) 4427-4434.
31. H. Petersen, K. Kunach, A.L. Martin, S. Stolnik, C.J. Roberts, M.C. Davies and T. Kissel, Star-Shaped poly (ethylene glycol)-*block*-polyethylenimine copolymers enhance

DNA condensation of low molecular weight polyethylenimines, Biomacromolecules 3 (2002) 926-936.

32. M. Huang, E. Khol, L. Lim, Uptake and cytotoxicity of chitosan molecules and nanoparticles: Effects of the molecular weight and degree of deacetylation, Pharm. Res. 21 (2004) 344-353.

33. H.G. Shi, L. Farber, J.N. Michaels, A. Dickey, K.C. Thompson, S.D. Shelukar, P.N. Hurter, S.D. Reynolds, M.J. Kaufman, Characterization of crystalline drug nanoparticles using atomic force microscopy and complementary techniques, Pharm. Res. 20(2003) 479-484.

Chapter 6

Uptake and transport of PEG-graft-trimethyl chitosan copolymer-insulin nanocomplexes in Caco-2 cell monolayers

Manuscript in preparation

Abstract

Purpose. The objective of this study was to evaluate the influence of chitosan and PEGylated trimethyl chitosan copolymer structure on the uptake and transport of insulin nanocomplexes and delineate the mechanisms.

Methods. Self-assembled insulin nanocomplexes were prepared and characterized. Complex uptake in Caco-2 cells was quantified by measuring the cell-associated fluorescence and localized by confocal laser scanning microscopy using TRITC-labeled insulin. The transport of different insulin complexes through Caco-2 monolayers was then investigated.

Results. All complexes were 200-400 nm in diameter, positively charged and displayed an insulin loading efficiency of approximately 90%. In vitro release of insulin from the complexes was dependent on the medium pH. Insulin uptake was enhanced by nanocomplex formation, and was incubation time, temperature and concentration dependent. Complex uptake in Caco-2 cells was inhibited by 25.2±1.3%, 13.0±1.0% and 16.6±0.7% in the presence of cytochalasin D, sodium azide and 2,4-dinitrophenol respectively. The uptake mechanism was assumed to be adsorptive endocytosis. Additionally, the cell uptake efficiency was shown to be influenced by a combination of polymer molecular weight, viscosity and positive charge density. However, none of the nanocomplexes displayed improved transport properties when compared to insulin transport data after 2 h incubation with Caco-2 monolayers.

Conclusions. Small, stable insulin nanocomplexes were formed using PEGylated trimethyl chitosan copolymers, which significantly enhanced the uptake of insulin in Caco-2 cells by adsorptive endocytosis. However, nanocomplexation did not appear to enhance insulin transport across cell monolayers.

1. INTRODUCTION

In order to maintain blood glucose levels at a near-physiological level and

thereby minimize long-term diabetic complications, the treatment of insulin-dependent diabetes requires up to four subcutaneous injections per day. To circumvent this tedious regimen of therapy, several attempts have been made to exploit mucosal surfaces for the delivery of macromolecular drugs, especially the nasal, pulmonary and oral mucosae (1). The nasal route has been a particular focus of recent research interests due to demonstrations of biologically active peptides, such as desmopressin, salmon calcitonin and corticotrophin, show significant absorption across the nasal mucosa (2).

In fact, the nasal route has been recognized as an attractive alternative for the administration of insulin since 1922 (3). However, despite the promise of intranasal administration for the delivery of peptides, the efficacy of the nasal route for the absorption of large peptides, e.g. insulin, is low (4). Therefore, new nasal delivery systems to facilitate the enhancement of insulin absorption have been studied, including surfactants, protease inhibitors, and solutions of bioadhesive polymers or bioadhesive microspheres (5,6). Unfortunately, most chemical enhancers (surfactants, bile salts, fatty acids, etc.) induce irreversible damage, and irritate the nasal mucosa when used at efficacious concentrations (7). In contrast, nanoparticles and microparticles have been demonstrated to be the most promising macromolecular carriers (8,9).

Unlike other absorption promoters, chitosan, a non-toxic and biocompatible cationic polysaccharide produced by partial deacetylation of chitin derived from naturally occurring crustacean shells, was reported to be able to open the tight junctions without damaging. The issues concerning the use of chitosan as a nasal delivery system have been discussed in the review by Illum et al. (10). Intranasal administration of chitosan insulin nanoparticles formed by a mild ionotropic gelation procedure has reportedly enhanced the nasal absorption of insulin to a greater extent than an aqueous solution of chitosan (11). The mechanism of action of chitosan is suggested to be a combination of bioadhesion and a transient widening of the tight junctions

between epithelial cells (12). However, this absorption enhancing ability was evident only at acidic condition (pH < 6.5), where most of the amino groups are protonated. To solve this problem, PEGylated trimethyl chitosan copolymers were synthesized in our laboratory in an attempt to increase the solubility of chitosan at physiological pH and improve the biocompatibility of trimethyl chitosan (TMC) (13). Insulin nanocomplexes were prepared with the copolymers by electrostatic interaction (14). We anticipate that by combining absorption enhancers, i.e., chitosan derivatives, and nanocomplex systems, intranasal absorption of insulin can be improved significantly.

The goal of this study is to evaluate the influence of chitosan and PEGylated TMC copolymer structure on the uptake and transport of insulin nanocomplexes and elucidate the mechanisms. Since several groups have suggested that Caco-2, a human colon adenocarcinoma cell line, functions as a suitable in vitro model to investigate particle uptake and intestinal permeability of drugs (15,16), in vitro quantification and elucidation of the uptake and transport of polymer-insulin complexes were performed with confluent Caco-2 monolayers. Such monolayers form tight junctions, and exhibit similar properties to those in the intestinal and nasal epithelium.

2. MATERIALS AND METHODS

2.1 Polymers

Chitosan (400 kDa) was purchased from Fluka (Steinheim, Germany) with a degree of deacetylation (DD) of 84.7% and depolymerized according to an oxidative degradation method to obtain chitosan 100 kDa and 50 kDa (17). PEGylated TMC copolymers were synthesized as described elsewhere (13). The following nomenclature was adopted for the copolymers: PEG(X)$_n$-g-TMC(Y), where X denotes the molecular weight (MW) of PEG (polyethylene glycol) in Da, Y denotes the MW of TMC in kDa, and the subscript *n* represents the average number of PEG chains per TMC macromolecule of Y kDa.

2.2 Preparation and characterization of copolymer-insulin self-assembled nanocomplexes

The complexes were prepared via self-aggregation, utilizing the electrostatic interaction between the polymers and insulin (Aventis Pharma AG, Germany) as a driving force. The process parameters were optimised and described in detail elsewhere (14). Briefly, complexes were prepared by mixing equal volumes of insulin and polymer solution at the desired ratio (Table 1) under gentle magnetic stirring, and incubated for a further 20 min at room temperature. Complex sizes and zeta potentials were obtained by using dynamic light scattering and Laser Doppler Anemometry (LDA) measurements as described in the literature (14).

2.3 In vitro release studies

Insulin release was determined by incubating the complexes (100 µl) in 1.5 ml Tris buffer pH 7.4 and acetate buffer pH 4.0 at 37℃. The concentration of the complex in the release media was adjusted in order to access sink conditions for insulin. At appropriate time intervals (30', 45', 1 h, 2 h, 4 h, 6 h) individual samples were centrifuged at 14000 rpm/min for 30 min and the amount of insulin released from the complexes was evaluated by HPLC as described elsewhere (14).

2.4 Labeling of polymers and insulin

Chitosan 100 kDa, PEG(5k)$_{40}$-g-TMC(100) and PEG(5k)$_{19}$-g-TMC(50) were labeled with Oregon Green carboxylic acid succinimidyl ester (Oregon Green 488, Molecular Probes, Eugene, OR, USA) following the previously described method (18). Insulin was labeled with TRITC (tetra-methyl-rhodamine isothiocyanat, Sigma, Taufkirchen, Germany). Briefly, insulin was dissolved at a concentration of 4.5 mg/ml in 0.1 M sodium bicarbonate buffer pH 9.3. A solution of TRITC (1 mg/ml) in dimethyl sulfoxide

(DMSO) was added dropwise under stirring (molar ratio of insulin: TRITC 1:2.9) and the mixture was stirred for 18 h at 4℃ under light exclusion. The reaction was quenched with an excess of ammonium chloride, and stirred for a further 4 h. Purification was performed on a PD-10 desalting column (Amersham Pharmacia Biotech, Freiburg, Germany) with PBS (phosphate buffered salt solution) pH 7.4.

2.5 Cell culture

Mycoplasma-free Caco-2 cells were used at passage numbers 44-50 (HD, DKFZ, German Cancer Research Institute, Heidelberg, Germany) under conditions described previously (19). Cells were seeded at a density of $6*10^4$ cells/cm^2 on 12-well cell culture plates or 6-well uncoated polycarbonate Transwell ^{TM} filter inserts (Costar, Bodenheim, Germany, 0.4 μm pore size, area; 4.71 cm^2) and cultivated over 21 days. The growth medium was changed every second day.

2.6 Uptake Studies

Cell uptake studies were performed with Caco-2 cell monolayers according to the method described in the literature (20). The uptake medium was 0.01 M Tris buffer, supplemented with 100 mM glucose, 1.17 mM $CaCl_2$, 1.03 mM $MgCl_2$, pH 7.4. The cell lysate, obtained by solubilizing the cells with 300 μl/well 2% SDS (pH 8.0), was measured for fluorescence with a LS 50B spectrometer (Perkin Elmer, Ueberlingen, Germany) at an excitation wavelength of 543 nm and an emission wavelength of 560 nm. Protein content was determined by BCA (bicinchoninic acid) assay according to the manufacture's protocol (Promega, Mannheim, Germany). Uptake was expressed as the quantity of insulin associated with 1 mg of cellular protein (mean ± SD, n = 3). To further evaluate the possibility of complex uptake occurring through an

active process, cells were preincubated with the metabolic inhibitors sodium azide (10 mM) and 2,4-dinitrophenol (0.2 mM), endocytosis inhibitors cytochalasin D (0.1 μg/ml) and nocodazole (1 μg/ml) (all from Sigma, Steinheim, Germany) for 30 min prior to complex application and throughout the 2 h uptake experiment.

2.7 Confocal laser scanning microscopy (CLSM)

Confocal laser scanning microscopy was utilized to visualize the internalization of insulin nanocomplexes. Caco-2 cells grown on glass cover slides for 7 days were treated with insulin, the polymers and the complexes (insulin concentration 250 μg/ml). After 2 h incubation at 37℃, cells were washed three times with ice-cold transport buffer, fixed with 3.7% paraformaldehyde in PBS pH 7.4 at room temperature for 30 min and counterstained with DAPI (4,6-diamidino-2-phenylindole, 0.2 μg/ml) for 20 min, both under light exclusion. For the samples without labeled polymer, the cells were counterstained with FITC (fluorescein isothiocyanate)-labeled wheat germ agglutinin (WGA, 0.01 μg/ml) for 30 min. Samples were embedded in FluorSave™ Reagent (Calbiochem, Darmstadt, Germany) and imaged by CLSM (Zeiss Axiovert 100 M Microscope coupled to a Zeiss LSM 510 scanning device, Jena, Germany) which was equipped with a Zeiss Neofluor 40*/1.3 objective. Excitation wavelengths were 364 nm (long pass filter (LP) 385 nm) for DAPI, 488 nm (LP 505 nm) for Oregon Green 488 and FITC, and 543 nm (LP 567 nm) for TRITC (18,20). All images were recorded by using the multitracking mode in which each fluorescence channel was scanned individually. Additionally, trypan blue was post-incubated with cells for 1 min (400 μg/ml in 0.1 M citrate buffer, pH 4.4) after 2 h incubation with the complexes or polymers.

2.8 Transport across Caco-2 cell monolayers

Transport studies were performed 21 days post-seeding. The integrity of the monolayers was checked by measuring the transepithelial electrical resistance (TEER) values in HBSS (Hank's balanced salt solution) buffer pH 7.4 before and after the experiment, as described previously (19,20). Only Cells with TEER value in the range of 250-350 $\Omega \cdot cm^2$ were used for the transport studies. Briefly, filter inserts were rinsed with transport buffer pH 7.4 (the same as the uptake medium) and allowed to equilibrate at 37℃ for 15 min. Experiments were carried out by replacing the apical buffer (1.5 ml) with the samples (insulin 250 μg/ml) and the basolateral buffer with fresh transport buffer (2.5 ml). Every 20 min up to 2 h, 1.0 ml sample was collected from the basolateral chamber and replaced with fresh buffer. Each experiment was performed in triplicate. To study TEER reversibility, monolayers were rinsed with fresh transport buffer directly after the transport experiment and allowed to regenerate in fresh culture medium under culture conditions. After 24 h monolayer integrity was checked in HBSS buffer.

2.9 Calculations and statistics

The apparent permeability coefficient (P_{app}) was calculated from concentration-time profiles using the following equation:

$$P_{app} = dC / dt \times 1 / A \times V / C_0 [cm / s]$$

where dC/dt (μg/s) represents the flux across the monolayer, A (cm^2) the surface area of the monolayer, V (cm^3) the volume of the receiving chamber and C_0 (μg) the initial concentration in the basolaterial compartment. The quantity of all cell-associated insulin was calculated by subtracting the amount transported and remained in the apical compartment from the initial amount. Results were expressed as mean value±SD of three experiments. Significance between the mean values was calculated using one-way ANOVA analysis (Origin 7.0 SRO,

Northampton, MA, USA). Probability values $P < 0.05$ were considered significant.

3. RESULTS

3.1 Physicochemical characteristics of polymers and complexes

The properties of the polymers and the self-assembled insulin nanocomplexes are described in Table 1.

Table 1. Properties and characteristics of the polymers and their complexes with insulin

Polymers (kDa)	DD[a] (%)	Substitution (%)[b]	Graft ratio (%)[c]	Mass ratio[d]	Size (nm)	ξ (mv)	Association efficiency (%)	Charge ratio (Pol./Ins.)
Chitosan 400	85.1			2:1	376.4±10.3	13.6±0.3	89.7±2.1	7:1
Chitosan 100	85.4			2:1	308.2±8.5	8.8±0.4	87.3±2.4	7:1
Chitosan 50	86.2			2:1	226.8±6.3	7.4±0.3	93.2±1.3	7:1
TMC 100		39.3[b1]		0.3:1	273.3±4.6	19.8±1.1	81.4±2.1	3:1
TMC 50		39.6[b1]		0.3:1	236.6±1.3	21.4±0.3	86.3±3.2	3:1
$PEG(5k)_{40}$-g-TMC(100)		6.44	66.1±2.2	1:1	233.3±7.2	18.8±0.3	94.8±1.1	5:1
$PEG(550)_{228}$-g-TMC(100)		36.7	58.5±3.1	1:1	224.6±2.3	13.9±2.9	94.2±1.7	5:1
$PEG(5k)_{19}$-g-TMC(50)		6.13	64.9±1.7	1:1	203.9±7.2	15.0±1.2	90.4±4.4	5:1
$PEG(550)_{132}$-g-TMC(50)		37.4	59.2±3.0	1:1	220.3±5.5	16.4±1.9	94.7±3.3	5:1

[a] DD degree of deacetylation, calculated by ^{1}H NMR analysis.

[b] Calculated based on the primary amino group content in chitosan; [b1] Degree of quaternization.

[c] Calculated based on the composition of the copolymer by ^{1}H NMR analysis.

[d] Optimized polymer/insulin mass ratio for complexes preparation.

All complexes had a size in the range of 200-400 nm, a positive surface charge and an insulin association efficiency (AE) of approximately 90%. The measured particle size of the complexes decreased with chitosan MW. In terms of the copolymer-insulin complexes, the size was comparable to that of small MW chitosan 50 kDa and TMC 50 kDa. The zeta potential of chitosan-insulin

complexes was approximately 2-fold lower than that of TMC and copolymers, and a slightly decreased zeta potential was observed for the copolymers compared to that of TMC. With a similar graft ratio, the zeta potential of PEG(550)$_{228}$-g-TMC(100) copolymer was lower compared to that of PEG(5k)$_{40}$-g-TMC(100) due to the increased substitution ratio. The optimal charge ratio between polymer and insulin was polymer structure dependent, it was 7:1 for chitosan, compared to 3:1 for TMC.

Figure 1 exemplifies the release profiles of insulin from complexes formed with chitosan 100 kDa and PEG(5k)$_{40}$-g-TMC(100). Similar profiles were achieved for the two complexes, showing a pH dependent insulin release. Almost all insulin was released in 30 min at pH 4.0. In contrast, less than 40% insulin was released at pH 7.4 in 6 h.

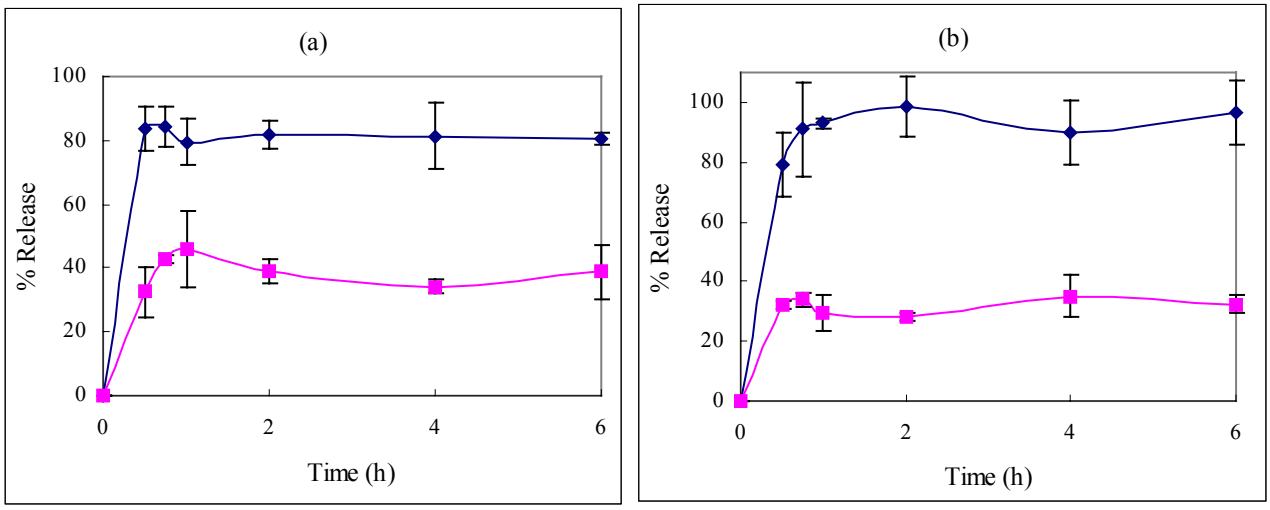

Figure 1. In vitro release of insulin from complexes at different pH.

(a) Chitosan 100 kDa-insulin complexes.

(b) PEG(5k)$_{40}$-g-TMC(100)-insulin complexes. (◆) pH 4.0, (■) pH 7.4.

3.2 Effect of polymer structure on complexes uptake in Caco-2 cells

In order to study particulate uptake in vitro, the most common experimental approach is to use fluorescent-labelled particles. Then, particle uptake can be determined indirectly by quantitative extraction of the markers

from the cells. Moreover, particles labelled with fluorescent marker also provide visual evidence for cellular uptake. Therefore, TRITC-labelled insulin was used in this study.

Based on the stability of the complexes, 0.01 M Tris buffer was selected for uptake studies. Ca^{2+} and Mg^{2+} were added to the buffer since they are essential for the tight junction function of the cells. In preliminary studies the chitosan-insulin complexes were found to be extremely ionic strength-sensitive (14), thus their stability was investigated in the Ca^{2+}/ Mg^{2+} supplemented buffer. This revealed that the influence of Ca^{2+}/ Mg^{2+} on complex dissociation was polymer structure dependent. Regarding chitosan-insulin complexes, dissociation appeared immediately after mixing. In contrast, TMC and PEGylated TMC insulin complexes remained stable for at least 6 h hours (data not shown). Therefore, the cell uptake experiments were performed in buffer without Ca^{2+}/ Mg^{2+} for chitosan-insulin complexes.

To facilitate their direct comparison, all chitosans and copolymers were investigated at 250 μg/ml (constant insulin concentration 125 μg/ml) except TMC (125 μg/ml), which is cytotoxic according to MTT assay. TMC displayed an IC_{50} (the concentration at which cell growth is inhibited by 50%) of approximately 100 μg/ml after 3 h incubation with L929 cells, compared to an IC_{50} > 500 μg/ml for all the copolymers investigated here. The uptake results after 2 h incubation with Caco-2 cells are shown in Figure 2. Compared to free insulin solution, all complexes improved insulin uptake significantly ($P < 0.05$), the extent of which depended on the polymer structure. The highest uptake was observed for TMC despite the lower concentration and comparable result was obtained for the copolymer $PEG(5k)_{40}$-g-TMC(100). With regard to chitosan, insulin uptake efficiency was MW dependent, and two-fold uptake was observed for chitosans 100 kDa and 50 kDa, compared to chitosan 400 kDa. In terms of the other copolymers, similar results were obtained with $PEG(550)_{228}$-g-TMC(100), $PEG(550)_{132}$-g-TMC(50) and $PEG(5k)_{19}$-g-TMC(50)

where uptake quantities were comparable to that of chitosan 50 kDa.

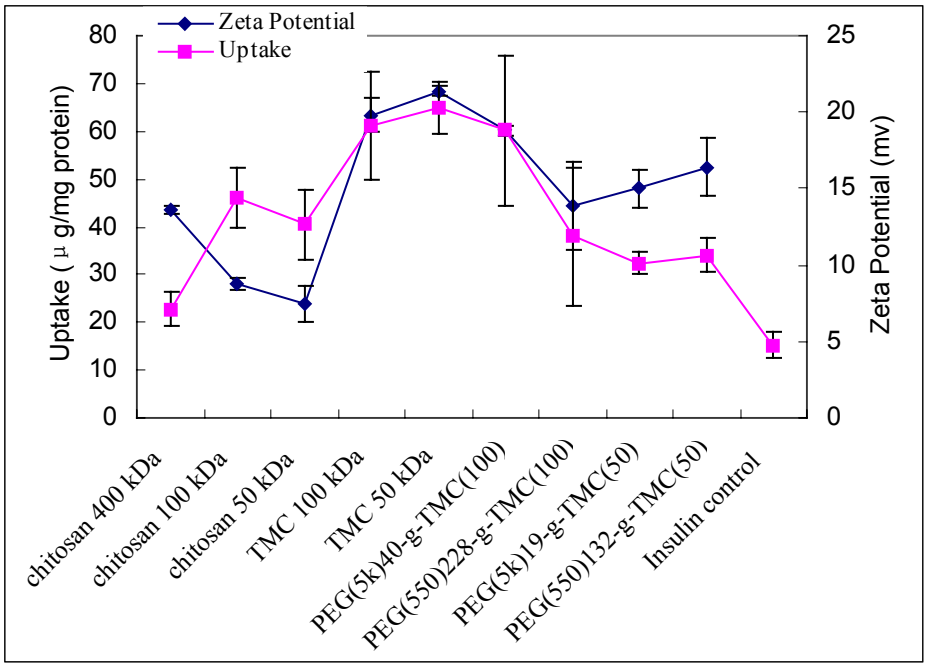

Figure 2. Uptake of polymer-insulin complexes as a function of polymer structure at 37℃ in Caco-2 cell line. Insulin (125 μg/ml) complexes were incubated with cells for 2 h. Error bars represent mean±SD (n = 3).

As can be seen in Figure 2, complexes uptake data correlated with zeta potential values. The observed high uptake efficiency of TMC 100 kDa and TMC 50 kDa were in line with their high positive charge, and negligible statistical difference was observed between each data set ($P > 0.05$). However, cytotoxicity of TMC could possibly be a cause for the high uptake efficiency. With similar graft ratios, the cell uptake efficiency of PEG(5k)$_{40}$-g-TMC(100) insulin complexes, which was comparable to that of pure TMC, was significantly higher than that of PEG(550)$_{228}$-g-TMC(100). This is probably a consequence of its relatively high positive charge, whereas the other copolymers had lower zeta potential and showed lower cellular uptake. Nevertheless, negligible statistical difference was observed between PEG(5k)$_{19}$-g-TMC(50) and PEG(550)$_{132}$-g-TMC(50) insulin complexes ($P > 0.05$). Based on the results

of uptake experiment, the PEG(5k)$_{40}$-g-TMC(100) copolymer insulin complex was selected for following study.

3.3 Mechanism of insulin complexes uptake

3.3.1 Effect of polymer concentration

Keeping the insulin concentration at 125 μg/ml, influence of the PEG(5k)$_{40}$-g-TMC(100) copolymer concentration on complex uptake was studied and is shown in Figure 3(a). The insulin uptake increased with increasing polymer concentration. A 2.5-fold increase was measured when the polymer concentration increased from 125 to 500 μg/ml. Moreover, a linear relationship was established between uptake percentage and polymer concentration in the range studied.

3.3.2 Effect of incubation time

Keeping the PEG(5k)$_{40}$-g-TMC(100) copolymer concentration at 125 μg/ml and insulin 125 μg/ml, the effect of incubation time on the uptake of insulin complexes was investigated and results are shown in Figure 3(b). The insulin uptake increased with incubation time and more than 4-fold uptake was observed by prolonging the incubation time from 0.5 h to 4 h. Additionally, insulin uptake correlated linearly with time for up to 4 h.

3.3.3 Effect of insulin concentration and temperature

Keeping the PEG(5k)$_{40}$-g-TMC(100) copolymer concentration at 125 μg/ml, the effect of insulin concentration was investigated by incubating Caco-2 cells with the complexes for 2 h. Studies were carried out at both 37℃ and 4℃. The rate of uptake increased with insulin concentration and did not exhibit saturation in the range of 62.5-500 μg/ml (Figure 3c). The uptake amount increased 5-fold when the concentration increased from 62.5 to 500 μg/ml. However, the uptake efficiency decreased with increasing insulin concentration

and leveled off at 250 μg/ml at 37℃ (Figure 3d). At 4℃ the uptake efficiency was less than 3% irrespective of insulin concentration.

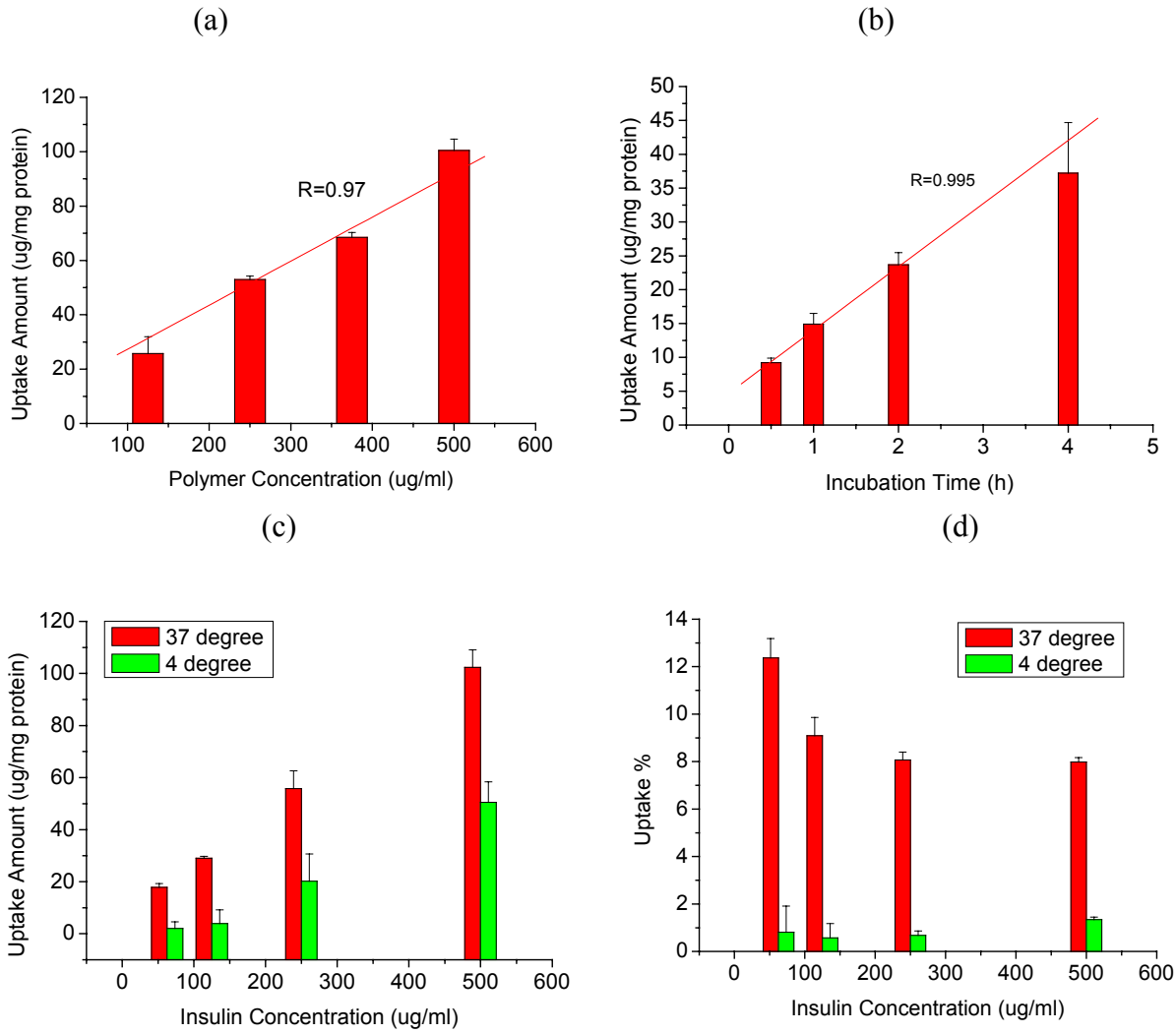

Figure 3. Effect of polymer concentration, insulin concentration, incubation time and temperature on complexes uptake in Caco-2 cell line. Error bars represent mean ± SD (n = 3).

(a) Effect of PEG(5k)$_{40}$-g-TMC(100) copolymer concentration on complexes uptake at 37℃. The concentration of insulin was 125 μg/ml.

(b) Effect of incubation time on complex uptake at 37℃. Both the concentration of insulin and PEG(5k)$_{40}$-g-TMC(100) copolymer used was 125 μg/ml.

(c) Uptake amount versus insulin concentration.

(d) Uptake efficiency versus insulin concentration.

Lowering the temperature from 37℃ to 4℃ abolished uptake of insulin complexes by approximately 70%, indicating that the uptake is temperature dependent. These results suggest that an energy-dependent endocytic process could be responsible for up to 70% of complexes uptake, and the other 30% attribute to physical adhesion or diffusion.

3.3.4 Effect of inhibitors

When the complexes were preincubated with either sodium azide or 2,4-dinitrophenol for 30 min, complexes uptake were reduced by 13.0±1.0 % and 16.6±0.7 %, respectively compared to that of control (Figure 4). This observation suggests that the complex-induced increase in permeability of insulin was to some extent regulated by metabolic energy (cell viability, $P < 0.05$). When the cells were preincubated with 0.1 μg/ml cytochalasin D, an

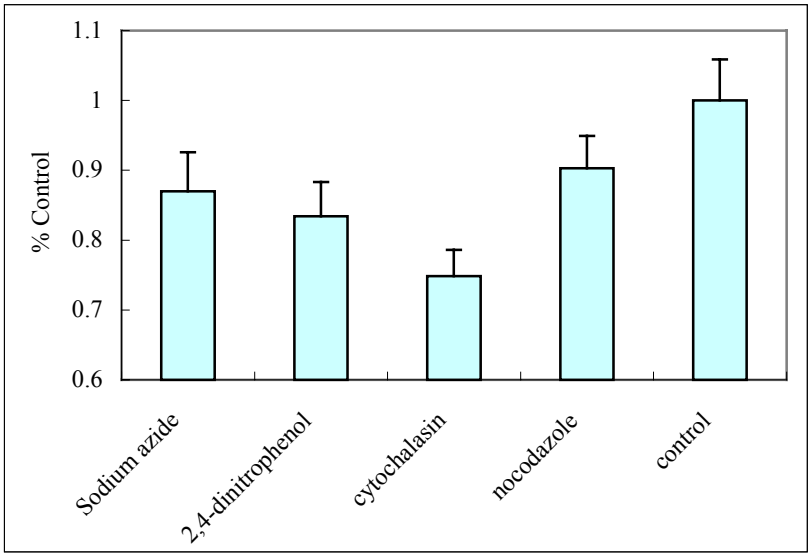

Figure 4. Effect of energy depletion and vesicle transport inhibitors on $PEG(5k)_{40}$-g-TMC(100) copolymer insulin (125 μg/ml) complexes uptake.

actin microfilament inhibitor, uptake was decreased by 25.2 ± 1.3 %, significantly different from that of sodium azide or 2,4-dinitrophenol ($P < 0.05$). In contrast, nocodazole, a microtubule inhibitor, caused only a slight reduction

in complex uptake of 9.7±0.5%. These data suggest that the internalization mechanism triggered by insulin complexes may be associated with the combined effect of microfilaments and microtubules of the cells.

3.4 Visualization by confocal laser scanning microscopy

To confirm the preliminary results indicating an endocytic uptake mechanism, confocal microscopy was employed to provide a direct evidence for complex localization. To distinguish between different cellular structures, cells were double stained with FITC-WGA (membrane, green) and DAPI (blue, nuclei). To investigate the uptake and intracellular localization of the complexes and the copolymers, both complexes and copolymers were fluorescent labeled. With regard to pure insulin solution, only a slight red fluorescence was observed (Figure 5D), probably due to passive diffusion via the transcellular route. Confocal microscopy shows that a small amount of polymers was taken up by the cells (Figure 5C). In contrast, a significantly higher internalization of cell-associated insulin was found for all investigated complexes compared to the insulin control.

To test whether complexes dissociation occurred upon incubation with the cells, the samples were viewed under confocal microscopy after 2 h incubation. An exemplary image of PEG(5k)$_{40}$-g-TMC(100)–insulin complexes is shown in Figure 5(A) by using blue, red and green filters and an overlay of the images showed perfect congruence of red and green dyes. A large amount of yellow color, resulting from the colocalization of green and red, was distributed within the cytoplasm, in small, rounded vesicles localized in the perinuclear area, on the nuclear membrane and on the apical cell membrane, indicating that the complexes were internalized into the cells without dissociation. A similar phenomenon was observed with the other labeled polymers.

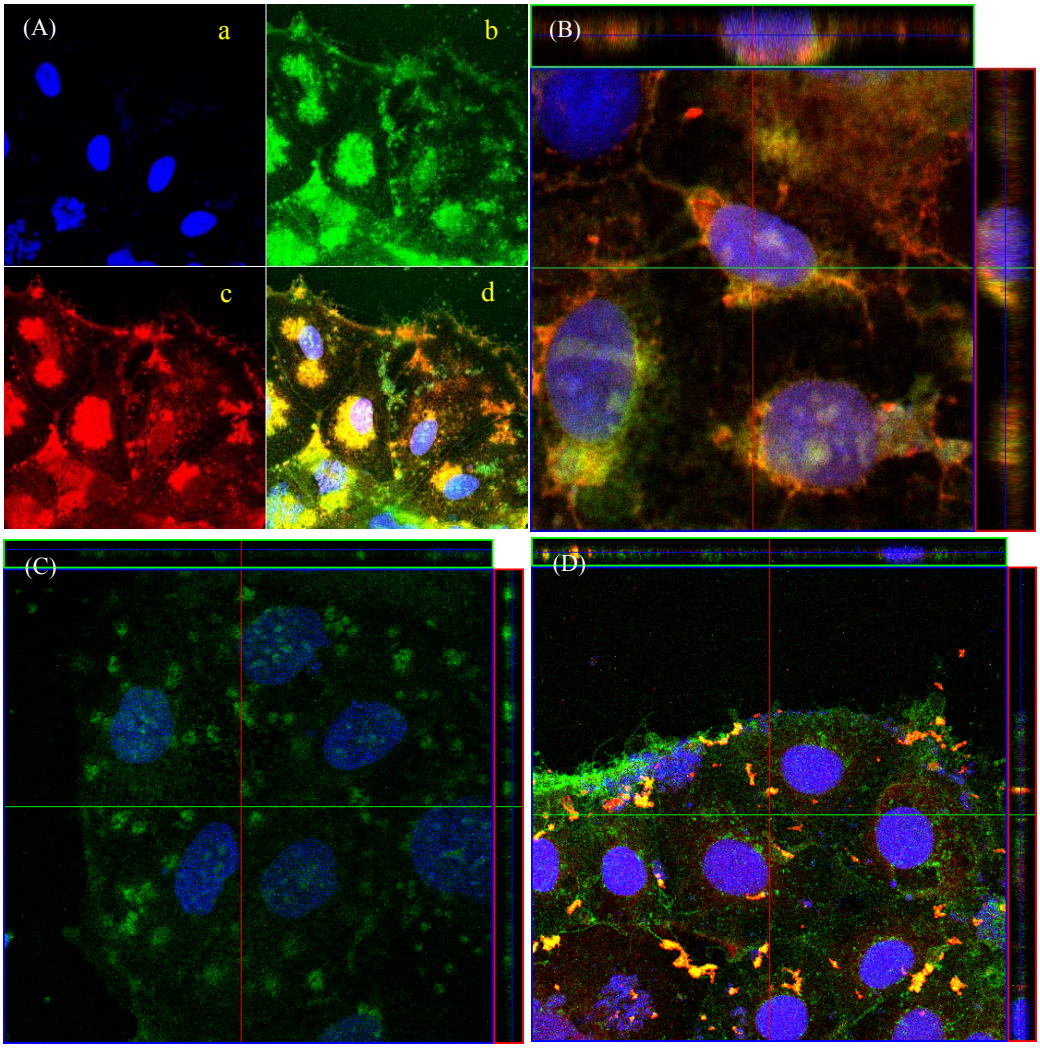

Figure 5. Confocal micrograph images of Caco-2 cell monolayers incubated with complexes, copolymer and insulin for 2 h at 37℃. PEG(5k)$_{40}$-g-TMC(100) copolymer was labeled with Oregon Green 488, insulin was labeled with TRITC and nuclei were labeled with DAPI.

(A) Incubated with PEG(5k)$_{40}$-g-TMC(100) copolymer insulin complexes (a) blue filter, (b) green filter, (c) red filter, (d) overlay of a,b,c.

(B) Incubated with PEG(5k)$_{40}$-g-TMC(100) copolymer insulin complexes for 2 h and post incubated with trypan blue.

(C) Incubated with PEG(5k)$_{40}$-g-TMC(100) copolymer and post incubated with trypan blue.

(D) Incubated with free insulin solution and post incubated with trypan blue. Cell membrane was labeled with FITC-WGA.

It is well known that chitosan and its derivatives are mucoadhesive. They can attach on the cell surface and cannot be washed away completely in some cases. To distinguish between membrane-associated and internalized complexes, trypan blue, a dye that was reported to inhibit extracellular fluorescence (21), was used. An exemplary image is shown in Figure 5(B), which represents vertical scans (XZ images) through the monolayers. Intracellular staining could be observed clearly in the images. Because viable cells excluded trypan blue molecules, the residual fluorescence implied the existence of a substantial amount of intracellular insulin complexes, rather than cell surface adsorption. Interestingly, it was noted that the complexes were mainly localized in the perinuclear region, suggesting endocytic uptake.

Moreover, it was noted that complex uptake was heterogeneous and cell state dependent. For the cells in the stage of division (indicated by the morphology of the nucleus), the complexes uptake was more efficiently compared to non-dividing cells (data not shown). This result could be explained by the fact that, during cell division, the cell membrane opens transiently and the complexes can enter the cytoplasm.

3.5 Transport studies

3.5.1 Effect of calcium and magnesium in the transport buffer

Due to the instability of chitosan-insulin complexes in the existence of Ca^{2+}/ Mg^{2+}, which is essential for the tight junction, uptake and transport of chitosan-insulin complexes were performed in the medium without Ca^{2+}/ Mg^{2+}. To figure out the influence of Ca^{2+}/Mg^{2+}, the transport of $PEG(5k)_{40}$-g-TMC(100) copolymer-insulin complexes, which is stable irrespective of Ca^{2+}/ Mg^{2+}, was investigated in both case and P_{app} values were calculated, as shown in Figure 6(a).

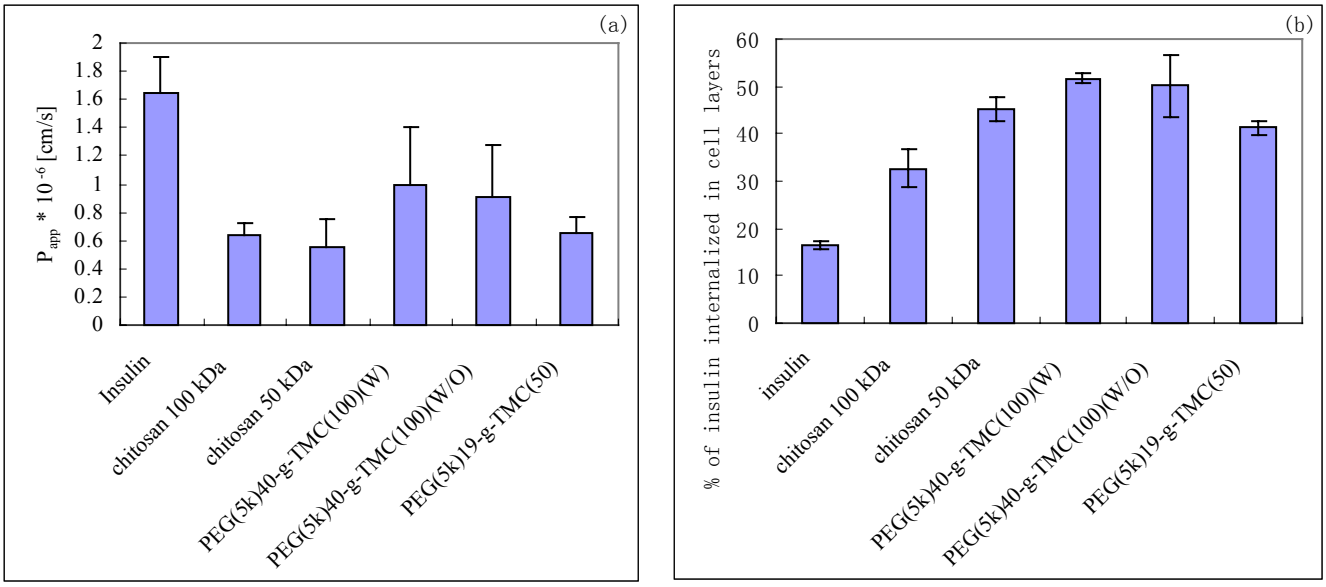

Figure 6. (a) Apparent permeability coefficient (P_{app}) of different polymer-insulin nanocomplexes in Caco-2 cells during 120 min (n = 3). The concentration of insulin was 250 μg/ml.

(b) Percentage of amount of insulin internalized/attached in Caco-2 cell monolayers after 2 h incubation. Each point represents the mean±SD of three experiments.

No significant difference in P_{app} values was found in both cases ($P > 0.05$), implying that the influence of Ca^{2+}/Mg^{2+} on the transport of copolymer PEG(5k)$_{40}$-g-TMC(100) insulin complexes was marginal. In terms of tight junction, after 2 h incubation the TEER values decreased by 60% and 65% with and without Ca^{2+}/Mg^{2+} respectively, compared to the medium. These values were reversible after 24 h. On the other hand, the amount of insulin remained in the apical compartment after 2 h incubation was measured and the amount of internalized or attached insulin was calculated, as shown in Figure 6(b). As we have demonstrated, complexes considerably enhanced insulin uptake in Caco-2 cells, approximately 50% of insulin was attached or internalized in the cells, 3.5 fold higher compared with free insulin, irrespective of Ca^{2+}/Mg^{2+}.

3.5.2 Effect of chitosan MW

Transport of chitosan 100 kDa and 50 kDa insulin complexes was investigated in transport buffer without Ca^{2+}/ Mg^{2+}. Transport amount increased with incubation time and the P_{app} values were calculated and depicted in Figure 6(a). No remarkable difference was found between each other ($P > 0.05$) and both of them were considerably lower compared with that of free insulin, which was transported through the cells two fold faster than these complexes. Instead of transport, large amount of insulin complexes (30-50%) were internalized or attached on cell monolayers (Figure 6b).

3.5.3 Effect of TMC MW in the copolymers

To elucidate the influence of TMC MW in the copolymers on the transport properties of insulin, two copolymers, PEG(5k)$_{40}$-g-TMC(100) and PEG(5k)$_{19}$-g-TMC(50) with similar PEGylation ratio, were employed. The results are depicted in Figure 6. In agreement with the cell uptake results, the P_{app} value of PEG(5k)$_{40}$-g-TMC(100) insulin complexes was higher than that of PEG(5k)$_{19}$-g-TMC(50), however not significantly different due to a high standard deviation ($P > 0.05$). PEG(5k)$_{40}$-g-TMC(100) copolymer is advantageous compared to chitosan concerning transport ($P < 0.05$), but no difference was found between PEG(5k)$_{19}$-g-TMC(50) copolymer and chitosan ($P > 0.05$). Compared to free insulin solution, only at the initial 40 minutes, PEG(5k)$_{40}$-g-TMC(100) copolymer insulin complexes enhanced insulin transport remarkably, and the difference became marginal after 1 h and the P_{app} value was lower than insulin solution but no statistical difference ($P > 0.05$). Similar to chitosan insulin complexes, high internalization or attachment is the advantage of the complexes beyond insulin solution (Figure 6b).

Additionally, TEER values were measured after 2 h incubation with the complexes. Significantly decreased TEER value indicated that the tight junctions between cells were opened. For chitosan 100 kDa and 50 kDa, TEER

decreased approximately 60% and no reversibility occurred after 24 h. In contrast, 60% and 40% TEER decrease was measured for the copolymers PEG(5k)$_{40}$-g-TMC(100) and PEG(5k)$_{19}$-g-TMC(50) and these were reversible.

4. DISCUSSION

In the current study, the cellular uptake and the permeability of chitosan derivatives insulin nanocomplexes were assessed. Despite the remarkably enhanced uptake, the permeation ability of the complex was low.

In vitro release of insulin from the self-assembled nanocomplexes was pH dependent. At pH 4.0, both chitosan and insulin were positively charged, rending complexes dissociation due to electrostatic repulsion and therefore, complete insulin release. This is consistent with a previous report (11). In contrast, insulin release at pH 7.4 (Tris buffer) was slow compared to that from chitosan-insulin nanoparticles (phosphate buffer pH 7.4) (11). The fast release of insulin in pH 7.4 phosphate buffer can be contributed to the strong interaction between phosphoric and ammonium ion of chitosan (22) and insulin was substituted by the phosphoric, rendering a rapid release of insulin. In this case, phosphate buffer is not a proper medium for insulin release investigation from chitosan nanoparticles. Therefore, 0.01 M Tris buffer pH 7.4 was selected in this study based on the stability of the complexes. On the other hand, although copolymer PEG(5k)$_{40}$-g-TMC(100) is completely soluble in the whole pH range, its insulin complexes kept stable at pH 7.4 for at least 6 h, indicated by the Tyndall phenomenon and precipitation at the bottom of the tube after centrifugation, suggesting that the developed insulin complexes may retain insulin on particles until uptake into mucosal membrane. Similar release profiles were observed for the other PEGylated TMC copolymer-insulin complexes, a rapid initial release in the first 30 min accompanied by a plateau after 1 h.

Compared to insulin control, a significantly higher cell-associated insulin

was found for all investigated complexes. Insulin uptake efficiency was chitosan MW dependent, and two-fold uptake for chitosan 100 kDa and 50 kDa compared to chitosan 400 kDa. However, an inverse finding was reported by Huang et al. (23), indicating that higher MW is preferred regarding A549 cellular uptake of chitosan nanoparticles. This discrepancy could be explained by the different cell line and different particle size employed. It is well known that cell uptake efficiency was particle size dependent and smaller size is preferable (24,25). The decreased particle size (226.8±6.3 versus 376.4±0.3 for chitosan 50 kDa and 400 kDa respectively) could probably lead to enhanced uptake. In terms of the copolymers, $PEG(5k)_{40}$-g-TMC(100) was more effective compared to $PEG(5k)_{19}$-g-TMC(50) with the same graft ratio. Considering that they have comparable particle size, we assume that besides zeta potential difference(18.8±0.3 versus 15.0±1.2), polymer molecular weight may play an important role in the permeation ability and high molecular weight is preferred. Ranaldi et al. also observed this phenomenon (26). It was noted that, despite less positively charged at physiological pH, the cell uptake amount of chitosan insulin complexes was still higher than some of the copolymers. This can probably be explained by the mucoadhesive ability of chitosan, which prolonged the contact time with cell membrane. Besides, the absence of calcium and magnesium in the buffer may also be a cause for the high uptake.

In addition, our findings demonstrated that uptake of insulin complexes by Caco-2 cell monolayers was dependent on time, temperature and loading concentration. Lowering the incubation temperature and energy level through the use of metabolic inhibitors reduced complex uptake remarkably, which demonstrates that uptake is an active process. This is in consistent with previously reports by Qaddoumi et al. with the uptake of 6-coumarin PLGA nanoparticles in rabbit conjunctival epithelial cells (27). Energy depletion was also found to reduce the opening of tight junctions in Caco-2 cells (28).

Treatment of Caco-2 cells with cytochalasin D, an actin inhibitor, reduced complexes uptake considerably, implying that uptake may be occurring by endocytosis. Nocodazole, a microtubule inhibitor, caused only slight reduction in complexes uptake. This is quite reasonable while microtubules are involved in vesicle transport but not in endocytosis, and vesicle transport is assumed to be a step after endocytic uptake (29). The reduction in complexes uptake as a result of energy depletion and application of endocytosis inhibitors suggest that adsorptive endocytosis is the main internalization mechanism of insulin complexes in Caco-2 cells. Additionally, the perinuclear localization of the insulin nanocomplexes under confocal microscopy corroborated the endocytosis uptake mechanism. Although there are contradictory reports in the literature concerning the ability of chitosan to be taken up by the cells physically (30), confocal microscopy did indicate that a small amount of polymers was taken up by the cells (Figure 5C). Similarly, Ranalidi et al. suggested the internalization of poly-L-lysine by fluorescent microscopy and assumed that polycations could be internalized by cells (28).

As reported, the mechanism of chitosan to enhance the absorption of drug substance is a combination of mucoadhesion and a transient opening of the tight junctions in the mucosal cell membrane (30). The intactness of tight junction is linked to the presence of Ca^{2+}/ Mg^{2+} ions (31). Reduction of extracellular Ca^{2+} concentration has been reported to result in an opening of tight junctions and consequently increased the paracellular permeability of epithelial cell monolayers (32). Similarly, Ranaldi et al. reported that the presence of calcium ions significantly reduced the permeability of Caco-2 cells by treatment with 0.002% chitosan but no effect for Mg^{2+} (28). On the contrary, the promoting effect of another polycation, poly-l-Arginine, has been demonstrated in a calcium independent manner (33). The influence of Ca^{2+}/Mg^{2+} on the transport was investigated with PEG(5k)$_{40}$-g-TMC(100) copolymer-insulin complexes in both cases. It showed that their influence on the transport properties of

copolymer PEG(5k)$_{40}$-g-TMC(100) insulin complexes was marginal and TEER value decreased to a comparable extent after 2 h incubation, implying that insulin complexes could not pass through the tight junction or at least paracellular transport was not the main pathway despite the ability of chitosan derivatives to open the tight junctions. This is reasonable. Although tight junctions are dynamic structure and can open and close to a certain degree, when needed, the mean size of the channels is in the order of less than 10 A° and the transport of large molecules is considered more limited. Our previous study also demonstrated this point (20). It showed that after the incubation with a solution of FITC-BSA mixed with chitosan, the detected fluorescence was significantly lower as compared to chitosan nanoparticles (20). Similarly, if opening the tight junction is the main mechanism, a large amount of insulin should be measured in the basolaterial compartment, but it is not the case. So far, all the literature reported just demonstrated that chitosan derivatives can open the tight junction on a molecular level. No direct evidence was supplied, which demonstrated transport of drug substance through tight junction. We assume that endocytosis is the main mechanism for insulin complex transport. After taken up into the cytoplasma, the complex will be sorting into endo-lysosome. Due to the acid environment (pH 4.5-5.0) in the endo-lysosome, both the polymer and insulin are positively charged and complex will dissociate. Positively charged polymer will interact with the negatively charged vesicle membrane, leading to insulin release. In this case, endo-lysosome escape is a rate-limiting step for insulin transport.

Similarly, Ma et al. reported that no measurable level of fluorescence was detected in the basolateral compartment after 4 h incubation with chitosan nanoparticles (34). Qaddoumi et al. also observed low transport value through cell monolayers with 6-coumarin-loaded nanoparticles (27). Recently, the pharmacologic responses of an insulin-chitosan (MW 205 kDa, DD 83%) solution formulation were shown to be significantly larger than those produced

by equivalent nanoparticle formulations in the rat and sheep models (35). This is in line with our predication with cell culture results. Therefore, the advantage of complexes or nanoparticles regarding enhancing drug prompt absorption, like insulin, was discredited. It is true that chitosan (CL110, CL210) nanoparticles (300-400 nm) has been shown to be able to increase nasal insulin absorption to a greater extent than chitosan solutions in rabbits (14), but the experiment was performed at pH 4.3 and the nanoparticles were highly positively charged. However, it should be mentioned that in this study, transport buffer was selected based on the stability of the complexes, which, on the other hand, will be a disadvantage for insulin release and transport. Confocal microscopy did demonstrate that there was still a large amount of insulin complexes existing in a intact state within the cells after 2 h incubation. Nevertheless, the efficacy of the insulin complexes needs be proved in vivo.

Besides, for chitosan-insulin complexes, no TEER reversibility occurred ever after 24 h restoration. Ranaldi et al. observed the same phenomenon even with 0.01% chitosan (28). Shortage of calcium and magnesium as a cause could be ruled out, because TEER reversibility was observed after incubation with $PEG(5k)_{40}$-g-TMC(100) copolymer insulin complexes in the same buffer. Probably due to the mucoadhesive properties of chitosan, it cannot be washed away completely and the amount left keeps opening the tight junction.

5. Conclusion

Self-assembled insulin nanocomplexes have been formed between insulin and chitosan derivatives. The complexes exhibit a small particle size and high loading efficiency. In vitro release of insulin was dependent on the medium pH. Encapsulation of insulin into complexes enhanced association with the Caco-2 cell monolayers up to 3-fold when compared to free insulin solution. The cell uptake efficiency has been shown to be a combination of polymer molecular weight, viscosity and charge density. Uptake of insulin complexes was time,

concentration and temperature dependent and it increased linearly with time and polymer concentration. Co-incubation with metabolic inhibitors and endocytosis inhibitors prevented complex uptake. Based on the studies of uptake and confocal images, internalization of the complexes appears to occur via adsorptive endocytosis, an energy dependent process that is proceeded by non-specific interactions of the carrier with the cell membrane, electrostatic interactions between the positively charged complexes and negatively charged membrane and the mucoadhesive ability of the polymers. However, nanocomplexes did not appear to enhance insulin transport across cell monolayers at physiological pH.

References

1. A.P. Sayani and Y.W. Chien. Systemic delivery of peptides and proteins across absorptive mucosae. Crit. Rev. Ther. Drug Carrier Syst. 13: 85-184 (1996).
2. L. Illum. Nasal drug delivery-possibilities, problems and solutions. J. Controlled Rel. 87: 187-198 (2003).
3. R.T. Woodyatt. The clinical use of insulin. J. Metab. Res. 2: 793 (1922).
4. C. McMartin, L.E. Hutchinson, R. Hyde, G.E. Peters. Analysis of structural requirements for the absorption of drugs and macromolecules from the nasal cavity. J. Pharm. Sci. 76: 535-540 (1987).
5. V.H.L. Lee. Protease inhibitors and penetration enhancers as approaches to modify peptide absorption. J. Controlled Rel. 13: 213-223 (1990).
6. N.F. Farraj, B.R. Johansen, S.S. Davis, and L. Illum. Nasal administration of insulin using bioadhesive microspheres as a delivery system. J. Controlled Rel. 13: 253-261 (1990).
7. F.M.H.M. Merkus, N.G.M. Schipper, W.A.J.J. Hermens, V.S.G. Romeijin, and J.C. Verhoef. Absorption enhancers in nasal drug delivery: efficacy and safety. J. Controlled Rel. 24:201-208 (1993).
8. L. Illum, H. Jorgensen, H. Bisgaard, O. Krogsgaard, N. Rossing, Bioadhesive microspheres as a potential nasal drug delivery system. Int. J. Pharm. 39: 189-199 (1987).
9. K.A. Janes, P. Calvo, M.J. Alonso. Polysaccharide colloidal particles as delivery

systems for macromolecules. Adv. Drug Deliv. Rev. 47: 83-97 (2001).

10. L. Illum, I. Jabbal-Gill, M. Hinchcliffe, A.N. Fisher, and S.S. Davis. Chitosan as a novel nasal delivery system for vaccines. Adv. Drug Deliv. Rev. 51: 81-96 (2001).
11. R. Fernández-Urrusuno, P. Calvo, C. Remuñán-López, J. Vila-Jato, M. Alonso. Enhancement of nasal absorption of insulin using chitosan nanoparticles. Pharm. Res. 16:1576-1581 (1999).
12. P. Artursson, T. Lindmark, S.S. Davis, and L. Illum. Effect of chitosan on the permeability of monolayers of intestinal epithelial cells (Caco-2 cells). Pharm. Res. 11: 1358-1361 (1994).
13. S. Mao, X. Shuai, M. Wittmar and T. Kissel. Synthesis, characterization and cytotoxicity of poly (ethylene glycol)-graft-trimethyl chitosan block copolymers. Biomaterials (in preparation)
14. S. Mao, U. Bakowsky, and T. Kissel. Nanocomplex formation between chitosan derivatives and insulin: The effect of system pH, polymer structure and molecular weight (in preparation).
15. F. Delie. Evaluation of nano- and microparticle uptake by the gastrointestinal tract. Adv. Drug Del. Rev. 34: 221-233 (1998).
16. S. McClean, E. Prosser, E. Meehan, D. O'Malley, N. Clarke, Z. Ramtoola and D. Brayden. Binding and uptake of biodegradable poly- DL -lactide micro- and nanoparticles in intestinal epithelia. Eur. J. Pharm. Sci. 6:153-163 (1998).
17. S. Mao, X. Shuai, F. Unger, M. Simon, D. Bi and T. Kissel. The depolymerization of chitosan: Effects on physicochemical and biological properties. Int. J. Pharm. 281: 45-54 (2004).
18. T. Merdan, K. Kunach, D. Fischer, J. Kopecek, T. Kissel. Intracellular processing of poly (ethylene imine)/ribozyme complexes can be observed in living cells by using confocal laser scanning microscopy and inhibitor experiments. Pharm. Res. 19: 140-146 (2002).
19. E. Walter and T. Kissel. Heterogeneity in the human intestinal cell line Caco-2 leads to differences in transepithelial transport. Eur. J. Pharm. Sci. 3: 215-230 (1995)
20. I. Behrens, A.I.V. Pena, M.J. Alonso, T. Kissel. Comparative uptake studies of bioadhesive and non-bioadhesive nanoparticles in human intestinal cell lines and rats: The effect of mucus on particle adsorption and transport. Pharm. Res. 19: 1185-1193 (2002)
21. C.P. Wan, C.S. Park, B.H. Lau. A rapid and simple microfluorometric phagocytosis

assay. J. Immunol. Methods 162: 1-7 (1993).

22. J.Z. Knaul, S.M. Hudson, K.A.M. Creber. Improved mechanical properties of chitosan fibers. J. Appl. Polym. Sci. 72: 1721-1732 (1999).
23. M. Huang, E. Khor, Lee-Yong Lim. Uptake and cytotoxicity of chitosan molecules and nanoparticles: effects of molecular weight and degree of deacetylation. Pharm. Res. 21: 344-353 (2004).
24. M.P. Desai, V. Labhasetwar, E. Walter, R.J. Levy, G.L. Amidon. The mechanism of uptake of biodegradable microparticles in Caco-2 cells is size dependent. Pharm. Res. 14: 1568-1573 (1997).
25. T. Jung, W. Kamm, A. Bteitenbach, E. Kaiserling, J.X. Xiao, T. Kissel. Biodegradable nanoparticles for oral delivery of peptides: Is there a role for polymers to affect mucosal uptake? Eur. J. Pharm. Biopharm. 50:147-160 (2000).
26. N.G. Schipper, K.M. Varum, P. Artursson. Chitosans as absorption enhancers for poorly absorbable drugs. 1: Influence of molecular weight and degree of acetylation on drug transport across human intestinal epithelial (Caco-2) cells. Pharm. Res. 13: 1686-92 (1996).
27. M.G. Qaddoumi, H. Ueda, J. Yang, J. Davda, V. Labhasetwar, V.H.L. Lee. The characteristics and mechanisms of uptake of PLGA nanoparticles in rabbit conjunctival epithelial cell layers. Pharm. Res. 21: 641-648 (2004).
28. G. Ranaldi, I. Marigliano, I. Vespiignani, G. Perozzi, Y. Sambuy. The effect of chitosan and other polycations on tight junction permeability in the human intestinal Caco-2 cell line. J. Nutr. Biochem. 13: 157-167 (2002).
29. M.M. Zegers, K.J. Zaal, S.C. van IJzendoorn, K. Klappe, and D. Hoekstra. Actin filaments and microtubules are involved in different membrane traffic pathways that transport sphingolipids to the apical surface of polarized HepG2 Cells. Mol. Biol. Cell. 9: 1939 – 1949 (1998).
30. N.G. Schipper, S. Olsson, J.A. Hoogstraate, A.G. deBoer, K.M. Vårum, Per Artursson. Chitosans as absorption enhancers for poorly absorbable drugs 2: Mechanism of absorption enhancement. Pharm. Res. 14: 923-929 (1997).
31. L. Gonzalez-Mariscal, R.G. Contreras, J.J. Bolivar, A. Ponce, B. Chavez de Ramirez and M. Cereijido. Role of calcium in tight junction formation between epithelial cells. Am. J. Physiol. 259: C978-C986 (1990).
32. A.B.J. Noach, Y. Kurosaki, M.C.M. Blom-Rosmalen, A.G. de Boer and D.D. Breimer. Cell-polarity dependent effect of chelation on the paracellular permeability of confluent

Caco-2 cell monolayers. Int. J. Pharm. 90: 229-237 (1993).

33. K. Ohtake, T. Maeno, H. Ueda, M. Ogihara, H. Natsume, Y. Morimoto. Poly-L-Arginine enhances paracellular permeability via serine/rhreonine phosphorylation of ZO-1 and tyrosine dephosphorylation of occludin in rabbit nasal epithelium. Pharm. Res. 20: 1838-1845 (2003).
34. Z. Ma, L. Lim. Uptake of chitosan and associated insulin in Caco-2 cell monolayers: A comparison between chitosan moleculars and chitosan nanoparticles. Pharm. Res. 20: 1812-1819 (2003).
35. A.M. Dyer, M. Hinchcliffe, P. Watts, J. Castile, I. Jabbal-Gill, R. Nankervis, A. Smith, L. Illum. Nasal delivery of insulin using novel chitosan based formulations: A comparative study in two animal models between simple chitosan formulations and chitosan nanoparticles. Pharm. Res. 19: 998-1008 (2002)

Chapter 7

Summary and Outlook

Summary

Recently, chitosan has been extensively investigated as a promising carrier in the field of drug delivery. To overcome its poor solubility at physiological pH and the cytotoxicity of trimethyl chitosan, PEGylated trimethyl chitosan copolymers were synthesized and characterized systemically for the first time and their potential as insulin carriers for intranasal administration were studied.

The use of chitosan as an absorption enhancer and gene delivery vehicle is molecular weight (MW) dependent. Therefore, in **Chapter 2**, we utilized an oxidative depolymerization method to prepare and investigate different MW chitosans. The MW of the depolymerized chitosan was shown to be influenced by the initial concentration and source of chitosan. At constant initial concentrations, the MW decreased linearly with the chitosan/$NaNO_2$ ratio and was found to be a function of the logarithm of the reaction time. Chitosan with larger MW was more sensitive to depolymerization. The physicochemical properties of the resulting polymer fractions were then characterized. Infrared and ^1H NMR experiments were performed, and no structural changes were observed during depolymerization. In addition, the thermal properties of chitosan fragments were studied by thermal gravimetric analysis and it was found that the decomposition temperature was MW dependent. Chitosan with MW of 250-500 kDa showed a maximum degradation temperature of approximately 280℃, with low MW chitosan degrading at lower temperature, at 220℃ and 180℃ for MW 25-100 kDa and MW 2.5-5 kDa respectively. Furthermore, the solubility of different MW chitosans was assayed as a function of pH. pH_{50} and cloud point pH were shown to increase with decreasing MW. As reports from the literature regarding the cytotoxicity of different MW chitosan are rarely in agreement, we performed our own study with MTT assay using L929 cell line recommended by USP 26. It showed that the cytotoxicity of chitosan was concentration dependent, but virtually molecular weight

independent. Chitosan 400 kDa showed an IC_{50} of 4200 μg/ml, whilst chitosan 100-5 kDa displayed a figure of approximately 5000 μg/ml.

In an attempt to improve the solubility of chitosan at physiological pH, we used a two-step method to synthesis a series of trimethyl chitosans (TMC) with substitution degree of 40% using the different MW chitosan obtained in chapter 2 as starting material. However, TMC was demonstrated to be toxic. Therefore, PEGylated TMC copolymers were synthesized in **Chapter 3** to improve the biocompatibility of TMC. Hydroxyl-terminated PEGs were converted to carboxyl-terminated intermediates by esterification with cyclic aliphatic anhydride, and then a series of copolymers with different degrees of substitution were obtained by grafting activated PEGs of different MW onto TMC via primary amino group reactions. The structure of the copolymers was characterized by infrared (FT-IR) and ^{1}H, ^{13}C nuclear magnetic resonance (NMR) spectroscopy. Successful coupling was demonstrated by gel permeation chromatography (GPC). Solubility experiments demonstrated that PEG-g-TMC(400) copolymers were completely water-soluble over the entire pH range (1-14) regardless of the PEG MW, even when the graft density was as low as 10%.

In **Chapter 4,** the in vitro biocompatibility of PEGylated TMC copolymers was studied and compared with that of TMC. Using the MTT assay, the effect of TMC MW, PEGylation ratio, PEG and TMC MW in the copolymers, and complexation with insulin on the cytotoxicity of TMC was examined and the IC_{50} values were calculated accordingly with the L929 cell line. All of the polymers exhibited a time- and dose-dependent cytotoxic response that increased with MW. PEGylation decreased the cytotoxicity of TMC, to a great extent in the case of low MW TMC. According to cytotoxicity results, PEG 5 kDa is preferable for PEGylation compared to PEG 550 Da at similar graft ratio. Complexation with insulin increased cell viability after 24 h incubation. Additionally we performed a LDH assay to measure the membrane damaging

effects of the copolymers on the basis of the results of the MTT assay. After 3 h incubation with 1 mg/ml copolymer solutions, less than 6% LDH release was measured for PEG(5k)$_{40}$-g-TMC(100), PEG(5k)$_{19}$-g-TMC(50) and PEG(550)$_{228}$-g-TMC(100) copolymers, compared to approximately 50% for TMC 100 kDa, which is consistent with the conclusions from MTT assay. Moreover, the safety of the copolymers was corroborated by examining the morphological changes of the cells under inverted phase contrast microscopy.

Since chitosan and its derivatives are positively charged, and insulin is negatively charged at pH > PI, polyelectrolyte-protein complexes (PEC) formation process between chitosan derivatives and insulin were studied and factors influencing the process were investigated systemically. This work is presented in **Chapter 5.** Turbidimetric titration in combination with dynamic light scattering (DLS) and laser doppler anemometry were applied to study the preferential binding between insulin and chitosan derivatives. Morphology of the complexes was observed with atomic force microscopy (AFM). It was demonstrated that the complex formation process was pH dependent. Binding between chitosan derivatives and insulin took place only above critical pH (pHc), which was approximately 6.0 for all chitosan derivatives investigated. Soluble complexes in the size range of 200-500 nm, which displayed a spherical or subspherical shape with smooth surface, could be obtained at optimized polymer/insulin charge ratio when the final system pH was in the range of 6.5-8.0, depending on polymer structure. Stability of the complex was polymer chain length dependent, and only when the MW of the polymer was $\geqslant$25 kDa complex precipitation was avoided. Increasing the ionic strength of the medium accelerated complex dissociation by reducing electrostatic interactions. Conversely, high temperatures facilitated complex formation and compaction. Chitosan trimethylation and PEGylation significantly improved the stability of the complexes. The complexes could be lyophilized using sucrose as a cryoprotector without affecting the complex properties. Moreover, it was

observed that a large number of protons were released during the complex formation process, indicating that the interactions enhanced the dissolution constant Ka of the ionizable groups on polymers. On the basis of these results we suggest that the interaction involved in the PEC formation was mainly electrostatic, involving the positively charged amino groups of chitosan and the negatively charged insulin above its isoelectric point.

In **Chapter 6**, the uptake and transport of chitosan derivatives-insulin complexes in Caco-2 cells was studied and the mechanisms were delineated. All complexes were 200-400 nm in diameter, positively charged and displayed an insulin loading efficiency of approximately 90%. In vitro release of insulin from the complexes was dependent on the medium pH, and burst release occurred in 1 h at pH 4.0. In contrast, less than 40% insulin was released at pH 7.4 in 6 h. Insulin uptake was enhanced by nanocomplex formation, and was incubation time, temperature and concentration dependent. Complex uptake in Caco-2 cells was inhibited significantly by cytochalasin D and marginally inhibited by metabolic inhibitors. The uptake mechanism was assumed to be adsorptive endocytosis. Additionally, the cell uptake efficiency was shown to be influenced by a combination of polymer molecular weight, viscosity and positive charge density. Complex internalization was further demonstrated by confocal microscopy. However, none of the nanocomplexes displayed improved transport properties when compared to insulin transport data after 2 h incubation with Caco-2 monolayers. In contrast, the complexes considerably enhanced insulin uptake or adhesion, with approximately 50% of insulin being attached or internalized in the cells after 2 h incubation, 3.5 fold higher compared with free insulin.

In summary, PEGylated TMC copolymers of different MW were synthesized for the first time, and their cytotoxicity was characterized by MTT and LDH assay. The self-assembled PECs between polymer and insulin were prepared and characterized. Ability of the insulin nanocomplexes to enhance

intranasal delivery of insulin was evaluated with uptake and transport experiments in Caco-2 cells.

Outlook

The transport results of the self-assembled PECs between chitosan copolymers and insulin in Caco-2 monolayers cast doubt on the ability of nanocomplexes to enhance insulin absorption in vivo. The release mechanism of insulin from the complexes in the subcellular compartment requires further investigation. Due to the difference between in vitro and in vivo conditions, the efficacy of the PEC for intranasal administration will be further investigated in vivo. Additionally, as a consequence of the decreased particle size, improved stability of the PEC prepared with the copolymers and the ability to be taken up by Caco-2 cells in an intact state, the bioavailability of the PEC via oral route will be subject to further investigation.

As a consequence of the sustained release characteristics of the complexes, and their enhanced uptake by the cells, we believe they will be promising intranasal delivery carriers for vaccines. They could also be used as carriers for anticancer drugs to target the central nervous system (CNS) by intranasal administration to avoid the blood brain barrier (BBB).

Preliminary experiments with the ethidium bromide assay demonstrated that the copolymers could condense DNA by complexation, with promising transfection capability already reported in cell culture experiments. Other investigations are currently ongoing. The relationship between polymer structure and transfection efficiency will be elucidated, and the promising complexes will be subsequently characterized in detail.

We also believe that the biocompatibility and excellent solubility of the copolymers may make them ideal carriers for other peptides or proteins.

Appendices

Publications

1. **Mao Shirui**, Shuai Xintao, Unger Florian, Simon Michael, Bi Dianzhou, and Kissel Thomas. The depolymerization of chitosan: Effects on physicochemical and biological properties, Int J Pharm 2004, 281, 45-54.
2. **Mao Shirui**, Chen Jianming, Liu Huan, Wei Zhenping, Bi Dianzhou. Intranasal administration of melatonin starch microsphere, Int J Pharm, 2004, 272(1-2), 37-43.
3. **Mao Shirui**, Shuai Xintao, Unger Florian, Wittmar Matthias and Kissel Thomas. Synthesis, characterization and cytotoxicity of poly (ethylene glycol)-graft-trimethyl chitosan block copolymers, Biomaterials. (in preparation)
4. **Mao Shirui**, Bakowsky Udo, Germershaus Oliver, Kissel Thomas. Uptake and transport of self-assembled PEGylated trimethyl chitosan block copolymer-insulin nanocomplexes in Caco-2 cell monolayers, Pharm. Res. (in preparation)
5. **Mao Shirui**, Wang Pu, Bi Dianzhou. Investigations on 5-Fu solid lipid nanoparticles prepared by hot homogenization, Die Pharmazie (accepted).
6. **Mao Shirui**, Liu Huan, Chen Jianming, Wei Zhenping, Bi Dianzhou. Studies on the preparing technique of melatonin starch microspheres for intranasal administration. Journal of Shenyang Pharmaceutical University, 2004 (accepted).
7. **Mao Shirui**, Ji Hongyu, Bi Dianzhou. The preparation of solid lipid nanoparticles by microemulsion method, Acta Pharmaceutics Sinica, 2003, 38(8), 624-626.
8. **Mao Shirui**, Liu Jinwei, Bi Dianzhou. Studies on the preparation of acyclovir infusion. Chinese Journal of Pharmaceutical, 2003, 1(4), 137-141.
9. **Mao Shirui**, Bi Dianzhou. Solid lipid nanoparticles (SLN) as drug delivery system. Journal of Shenyang Pharmaceutical University, 2002,19(6), 455-461.
10. **Mao Shirui**, Bi Yue, Bi Dianzhou. Studies on preparing technique of nicardipine hydrochloride gelatin microsphere for intranasal administration, Journal of Shenyang Pharmaceutical University, 2002,19(2), 79-82.
11. **Mao Shirui**, Wang Lei, Cai Cuifang, Bi Dianzhou. Studies on pefloxacin mesylate gel matrix, Journal of Shenyang Pharmaceutical University, 2002,19(1), 9-13.
12. **Mao Shirui**, Yang Hongtu, Tao Hong, Bi Dianzhou. A study on the stability of the analgin solution, Journal of Shenyang Pharmaceutical University, 2001,17(1), 11-13.
13. **Mao Shirui**, Yang Hongtu, Bi Dianzhou. Ways of improving nasal drug absorption, Chinese Pharmaceutical Journal, 1998, 33 (11), 641-645.
14. **Mao Shirui**, Zhou Hui, Bi Dianzhou. Nasal drug delivery and influence factors, Northwest Pharmaceutical Journal, 1997,12(6), 275-278.
15. **Mao Shirui**, Yang Hongtu, Chen Jianming, Bi Dianzhou. Uses of povidone in pharmaceutics, Journal of Shenyang Pharmaceutical University, 1997,14(3), 224-228.
16. **Mao Shirui**, Shi Zhe, Bi Dianzhou. Analgin nasal absorption, Chinese Pharmaceutical Journal, 1997,32 (2), 87-91.

17. **Mao Shirui**, Bi Dianzhou. Determination of analgin content by HPLC, Chinese Journal of Modern Applied Pharmacy, 1997,14(6), 23-25.
18. Chen Jianming, **Mao Shirui**, Bi Dianzhou. Studies on melatonin gelatin microspheres for intranasal administration, Acta Pharmaceutics Sinica, 2000, 35(10), 786-789.
19. Chi Zhiqiang, **Mao Shirui**, Bi Yue. Factors influencing in vitro drug release of Xanthan Gum as hydrophilic matrix, Journal of Shenyang Pharmaceutical University, 2001,17(1), 8-12.
20. Wei Zhenping, **Mao Shirui**, Bi Dianzhou. Comparison between colorimetry and HPLC on the stability test of roxithromycin, Acta Pharmaceutics Sinica, 2000, 35(11), 871-873.
21. Chi Zhiqiang, Bi Yue. **Mao Shirui**, Bi Dianzhou. A study on in vitro drug release pattern of the multi-layered controlled-release matrix tablets containing tramadol hydrochloride, Journal of Shenyang Pharmaceutical University, 2001,18(2), 88-90.
22. Chang Cui, Yang Hongtu, **Mao Shirui**, Bi Dianzhou. Review on the development of dissolution testing method for sustained or controlled release oral dosage forms and correlation with in vivo data, Chinese Pharmaceutical Journal, 1999, 34(12),641.
23. Cai Cuifang, Bi Dianzhou, **Mao Shirui**. Preparation of dextromethorphan hydrobromide sustained-release matrix pellets by extrusion-spheronisation. Journal of Shenyang Pharmaceutical University, 2003, 20, 313-316.
24. Zheng Hangsheng, Pan Wei, Wang Yan, **Mao Shirui**, Bi Dianzhou.Determination of Ondansetron Hydrochloride in Human Plasma by HPLC, Chinese Journal of Pharmaceutics, 2002, 33(12), 603-605.
25. Chen Jianming, Zheng Hangsheng, Zhan Jie, **Mao Shirui**, Bi Dianzhou. Studies on melatonin ethylcellulose microspheres for intranasal administration, Chinese Pharmaceutical Journal, 2002, 37(5), 354-357.
26. Chen Jianming, Gao Shen, Ye Lika, **Mao Shirui**, Bi Dianzhou. Study on melatonin nasal absorption. Academic Journal of Second Military Medical University, 2001, 22(12), 1157-1159.
27. Chen Jianming, Ye Lika, Gao shen, **Mao Shirui**, Bi Dianzhou. Comparison of the differences between melatonin gelatin microspheres and solution in nasal delivery system. The Journal of Pharmaceutical Practice, 2001,19(5),280-281.
28. **Mao Shirui**, Kissel Thomas. Nanocomplex formation between chitosan derivatives and insulin: Effect of pH, polymer structure and molecular weight. CRS Meeting in Heidelberg, April 2004, Germany.
29. **Mao Shirui**, Chen Jianming, Bi Dianzhou. Studies on melatonin starch microspheres for intranasal administration, The nation-wide pharmaceutics and academic exchange meeting, 2001, Beijing China.
30. **Mao Shirui**, Yang Hongtu, Bi Dianzhou. Studies on nefopam coating pellets and its release characteristics, First Asian Particle Technology Symposium (APT2000), December 2000,Bangkok, Thailand.
31. **Mao Shirui**, Wang Shijiu, Bi Dianzhou. Studies on analgin pharmacology and toxicity for

intranasal administration, The nation-wide pharmaceutics and academic exchange meeting, 1998, Guiyang, China.

32. Wei Zhenping, **Mao Shirui**, Bi Dianzhou. Evaluation on the floating kinetics and in vitro drug release of a two layer tablet for gastric retention with cisapride as model drug, International Symposium on Pharmaceutical Science, 2000, Shenyang, China.
33. Yang Hongtu, **Mao Shirui**, Bi Dianzhou. Preparation of controlled-release pellet and research on its release mechanism, The seventh nation-wide pharmaceutics and academic exchange meeting, 1997, Shenyang, China.
34. Bi Dianzhou, **Mao Shirui**, Chen Jianming. Advance of mucosal drug delivery system, National-wide symposium on the development of pharmaceutics subject, 1995, Shenyang, China.

Book Chapters:

1.《Pharmaceutics experiment》, join (the second), Shenyang Pharmaceutical University, 2000.8
2. 《Pharmaceutics》, facing the twenty-first century teaching book, join (70 thousand words), the people sanitation publishing company, Beijing, 2002.8
3. Book Translation: " Pharmaceutical Powder Compaction Technology" Volume 71, edited by Goran Alderborn and Christer Nystrom. Chapter 16 and 17.

Curriculum Vitae

Name: Mao Shirui

Date and place of birth: July 2,1969 Tianjin

Nationality: Chinese

Marital status: Married

Fundamental Education;

1976.9-1981.7 Tianjin Tuhe junior school

1981.9-1984.7 Tianjin Tuhe junior high school

1984.9-1987.7 Tianjin Jinghai No.1 senior high school

Higher Education:

1987.9-1991.7	Shenyang Pharmaceutical University	Bachelor Degree
1991.9-1994.7	Shenyang Pharmaceutical University	Master Degree
2002.10-present	Philipps University of Marburg	Ph. D Candidate

Other Education:

2001.9-2002.6	Tongji University	learn German
2002.8-2002.9	DID institute Frankfurt	learn German

Teaching Experience:

1994.8-2001.8 Pharmaceutics (for undergraduate students)
Pharmaceutics experiments (for undergraduate students)

1991-1994 Pharmacy laws and regulations (for adults and correspondence students)

Working Experience:

1994.8-2001.8 Department of Pharmacy, Shenyang Pharmaceutical University, lecturer